Structural Analysis of the Øygarden Fault Complex, on the northern North Sea Horda Platform

Joseph Gubbi

Master Thesis in Geosciences

Structural Geology and Tectonics

Department of Geosciences

Faculty of Mathematics and Natural Sciences

UNIVERSITETET I OSLO

Preface

As a requirement to attaining the masters degree in Structural Geology and Tectonics, a 60 ECTs thesis forms part of the course outline.

This thesis, therefore is sumbitted to the University of Oslo as fulfilment for the award of the degree.

The following Supervised this work;

Dr. Sian Evans, main supervisor

Dr. Wu Long Co-supervisor

Dr. Mark. J. Mulrooney Co-supervisor, (left)
Prof. Alvar Braathen co-supervisor

Acknowledgment

I am highly indebted, and extend my sincere thanks to Dr. Sian Evans and Dr. Mark Mulrooney (partly) for undertaking the tasks of supervising this project.

Dr. Mark Mulrooney, Dr. Long Wu (Equinor), and Prof. Alvaar Braathen are thanked, as they were instrumental in formulating the project at its inception.

Dr. Sian has been instrumental during the tedious phases of processing, interpretations, and write-up, including various discussions and proof-reading my raw drafts.

Osmon Jonathan is thanked for introducing me to Petrel and Move.

Norah is thanked for her time guiding me during the interpretations.

Schlumberger is thanked for providing the academic licenses to Petrel, and Petex for Move software.

Abstract

With the continued need to reduce CO2 emissions in the atmosphere, the Carbon Capture and Storage (CCS) project is viewed as a critical part of the solution. The search for and identification of suitable CO2 storage sites has been ongoing for sometime. In the northern North Sea, the Beta prospect located on the Smeahea Fault block, has been considered a possible reservoir to store CO2. The Beta is located in the hanging-wall of the N-S trending Øygarden Fault. The Øygarden has large displacement, and juxtaposes the basement. Therefore, structural risks may arise that are related to along and across fault CO2 migration.

As a contribution to the derisking of the Beta prospect as a possible CO2 storage site, a Structural analysis study of Øygarden Fualt Complex, starting in Stord Basin, in the South, extending into the Måloy Slope in the North has been carried. The overall study aim is to try and map new CO2 reservoir sites and assess the risks that may be associated with along and across the Øygarden Faults.

Using regional 2D seismic lines and well data, mapping of the Øygarden and associated Faults in the hanging-wall have been caried-out to assess geometry, lateral and vertical propagation of the fault using throw-distance and Depth-throw plots respectively. Reservoir and seal units have been mapped to try and screen for new sites, and the surfaces used to create thickness maps. Using thickness maps, identification of Øygarden fault activities has also been posible. Damage zones between relay zones have been assessed to predict risks.

In the study, two main rifting phases have been determined; during the Permian-Triassic, as rifting phase one (RP1), and during the Late Jurassic-Early Cretaceous, the second phase (RP2). Two phases of post-rifting have been mapped i.e. post-rift phase 1 in the middle Jurrasic following RP1, and post-rift phase 2 following rifting phase 2 (RP2). The observed approaching tip/linking damage zones between the relay zones are possible fluid/CO2 flow sites. The Øygarden being a large displacement fault, we speculate that it is associated with wide damage zones along and across each of the three curved Øygarden Fault segments (ØFS1-3). These, however may need groundtruthing or advanced seismic attributes to map the damage zones (e.g., Torabi et al., 2017).

The Øygarden Fault Complex, therefore posesses additional risks associated with damage and relay zones. These, combined with juxtaposition risks (e.g., Wu et al., 2021) and the fractured basement, the Beta prospect may rank quite low.

Table of Contents

Chapter one

1.0 Introduction

The search for CO_2 storage sites as a large part of the Carbon Capture and Storage (CCS) project have been ongoing on globally. Approximately 26 large-scale CCS facilities with an estimated 40Mt CO2/yr capture capacity have been reported globally (e.g., Ringrose and Meckle 2019; LIoyd et al., 2021). In northwest Europe, North Sea subsurface contains over two thirds of CO2 storage potential (Lioyd et al., 2021 and references therein).

To develop low carbon solutions to reduce CO2 emissions, the Norwegian CCS Research Centre has been undertaking investigations into injection and storage of CO2 into the subsufarce. With decades of successfully utilized CO2 storage both in the Snøhvit field, Barents Sea (Madal and Tappel, 2004; Eiken et al., 2011; Pham et al., 2013) and the Sleipner field, North Sea (Torp and Gale, 2004; Arts et al., 2008; Ringrose and Meckle 2019; LIoyd et al., 2021), exploration for new sites has since accelerated.

The Aurora and Smeaheia (Fig 1) (Skurtveit et al., 2015; Dupuy et al., 2018; Lauritsen et al., 2018; Mulrooney et al., 2020; Wu et al., 2020; Sundal et al., 2015; Sundal et al., 2016; Wu et al., 2021) prospects in the northern North Sea have been identified as possibly feasible storage sites.

The Smeaheia fault block (Fig 1) is located on the Horda platform bounded by the Vette fault to the west and the thick-skinned (basement involved) Øygarden fault to the east, and is a host to the Alpha and Beta prospects (Skurtveit et al., 2015; Nazarian et al., 2018; Mulrooney et al., 2020). The Alpha is located in the Vette fault zone footwall (approximately 99m CO2 tonnes capacity) and the Beta is located in the Øygarden fault hanging-wall (Mondol et al., 2018; Mulrooney et al., 2018; Mulrooney et al 2020). The presence of a good Upper Jurassic Sognefjord reservoir and the overlying Heather and Draupne formations cap rocks made the Smeaheia prospect highly targeted (e.g., Mulrooney et al., 2020; Wu et al., 2021). This is coupled with sufficient structural storage capacity and the adjacency to the coastline, where there is an already existing subsea infrastructure (Mulrooney et al., 2020; Lauritsen et al., 2018).

The Beta prospect has the potential to store large CO2 amounts, approximately 92.3 Mt (Sacco, 2018) and (100Mt (Gassnova, 2016), but there are risks that need evaluation before big investiments are carried-out. Top seal failure and cross-fault leakage challenges may

arise, and have been assesed. (Mulrooney et al., 2020; Wu et al., 2021). Seal and caprock integrity studies for the Smeaheaia CO2 storage prospect have been assessed, and, it was found that polygonal faults, extend into the reservoir interval (Mulrooney et al., 2020). The Vette fault relay zones and intra-block subsidiary faults were found to exhibit cross-fault self juxtaposition of the reservoir (Mulrooney et al., 2018).

Low to moderate risks of reactivation on faults (more so the N-S trending) and conservative cohesion on the fault surfaces were found to reduce reactivation-related risks significantly (Mulrooney et al., 2018). Simulation, to identify parameters that influence storage capacity and estimate the relative importance of the reservoirs of the smeaheaia was carried out (Lauritsen et al, 2018). The simulation work performed showed that 5-20% of the injected CO2 would elude trapping on Alpha and flow to the Beta structure where it could potentially escape through the Øygarden fault zone (Lauritsen et al, 2018).

Wu et al., (2021) studied containment risks in the Alpha and Beta closures and determined that the Alpha did not exhibit such risks, whereas the Beta structure juxtaposed with the basement across the Øygarden Fault exhibited potentially fault-related containment risks.

Whereas several studies have tried to ensure that challenges regarding CO2 containment are understood, studies detailing the problems involved with possible CO2 migration across the Øygarden Fault Complex to the East where the Beta prospect juxtaposes the fractured basement have been few at present. Moreover, risks of CO2 migration along the fault and the associated deformation in damage zones are at present few. Studies related to Oygarden Fault Evolution and geometry at present are not many either. Much as the prospect has been evaluated for potential and risk, a better understanding of risks related to lateral CO2 migration along the basement-involved Øygarden fault complex is needed.

To evaluate the risk of CO2 migration across the Øygarden, along the Complex, and the associated damage zones of the Øygarden Fault, a detailed ØFC structural analysis needs to be carried out. Lateral (along strike) variations in the hanging-wall (HW) would aid in understanding fault evolution, fault geometry, and the implications for the Neogene-present tectonic history.

Suffice to say, emphasis has been placed on the Beta prospect, however, additional prospects may be found within the Jurassic and potentially in the Triassic formations.

This study, therefore, intends to identify any areas, the Beta inclusive, where prospective CO_2 columns would juxtapose with the Basement across the Øygarden Fault Complex (ØFC) and

assess the lateral risks related to lateral CO2 escape into the basement. Assessing the risks when the beta closure is filled to spill forms, in which case CO2 would be in contact with the basement requires focus. The other aim of the study is to try and identify additional traps that do not directly juxtapose with the basement.

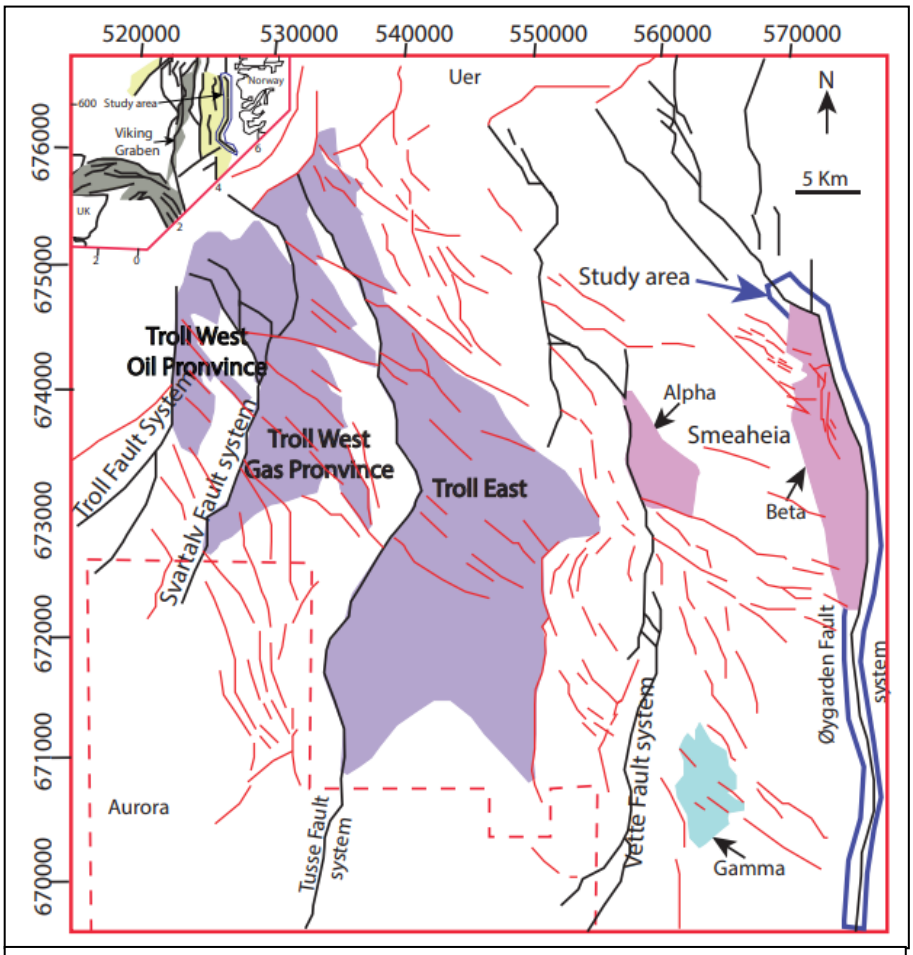

Fig 1: Location of the Øygarden Fault Complex in relation to the Alpha and Beta prospects. The inset map shows the study area in relation to Norway (Map modified from Wu et al., 2021)

1.1 Objectives.

To achieve the set study goals, the main objectives include mapping detailed faults that intersect Triassic units and computing juxtaposition across faults in the Triassic units.

Fault displacement diagrams and attributes are generated to aid in understanding the study area's evolution history. Classification of individual faults based on deformation style, orientation, and geometry will aid in timing tectonic activity and as well the influence the faults have on CO2 migration.

Previous fault reactivation studies on the Smeaheia prospect were carried out on the Vette fault (Skurtveit et al., 2018); Fault seal studies were carried out on the Vette (Wu et al., 2021; Mulrooney et al., 2020); few studies on the Øygarden Fault, whose hanging wall hosts the Beta prospect have been carried out. The study h, therefore,efore aims to make a general assessment of the structural risks associated with CO2 migration through the Øygarden fault complex into the basementhe t, and risks of associated damage zones.

A regional structural analysis, starting from the northern Horda Platform, and extending down to the Stord basin in the South is carried out on the Øygarden Fault Complex. The final goal is to establish along-strike variations in the hanging–wall to discern the present-day geometry, evolution history, and the implications for the Neogene-present tectonic history.

With this study, it is possible additional closures to Beta within the Jurassic and Triassic formations may be identified and characterized. In addition, the study intends to locate prospective CO2 storage areas, including Beta. An assessment of the faults that juxtaposition with the fractured basement, the assessment of damage zones, and relay zones are to be made.

The data utilized in the study include two-dimensional (2D) regional seismic sets and well-log data to constrain mapped horizons. This being a regional study, therefore, it is impossible to confidently map closures with mainly 2D seismic. Once the initial screening of the margin is carried out in this regional study, 3D data seismic will be required where it is lacking so that carry out detailed studies and calculations of volumes.

Petrel E&P and Move/T7 software are the main tools to construct the geological models.

1.2: Theoretical background

1.2.1 Faults and fault evolution

To carry out structural analysis, and eventually, an assessment of lateral CO2 migration across the Øygarden Fault Complex into the basement, and risks involved with Øygarden fault damage zones, it is imperative to understand the general background of what a fault is, fault growth model concepts, and how these impact geological CO2 storage capacity considering CO2 storage is a long term venture (Miocic et al., 2019; Wu et al., 2021).

Faults are structural discontinuities that record displacement in the rock volume. These could be extensional, contraction, and strike-slip, all of which are important when trying to understand subsurface, especially when exploring economic resources. The faults highly affect the distribution and economic occurrence of resources; for example, hydrocarbons,

groundwater, mineral occurrences, and CO2 storage. Faults are ubiquitous in sedimentary basins; which calls for an understanding of lateral and vertical migrations of fluids, which eventually, aids in unraveling risks involved as sealing or non-sealing potential of the faults (Miocic et al., 2019; Bense et al., 2013).

1.2.2 Fault architecture

The occurrence of faults in 3D is naturally complex, contrary to the simplistic view to which they conform (Childs et al 2009, Walsh et al 1999). In 3D (Fig 1.1a) and conceptual model (Fig 1.1b), a fault is observed as a heterogeneous volume or zone of deformed host-rock, consisting of fault core (slip surface) and damage zone/process zone (Caine et al., 1996; Kim et al., 2004; Choi et al., 2016; Mayolle et al., 2019) or the damage zone-fault core transition zone, in the case of carbonate rocks (Fig 1.1b) (Billi et al., 2003) or mixed transition zone (Choi et al., 2012).

1.2.3 Fault core

The fault core (Fig 1.1a, b) is a high-strain zone that accommodates the most displacement and may include single slip surfaces (e.g., Caine et al., 1996, Rotevatn and Bastesen, 2014), unconsolidated clay-rich gouge zones, and brecciated and altered zones, or cataclastic zones (Caine et al., 1996). Whereas the fault core is understood to form a barrier to flow because the fault core materials have low matrix permeability, they do not necessarily act as barriers to flow all the time (e.g., Cain et al., 1996). The variations in thickness dip down and along strike, in combination with composition, control the flow of fluids in core zones. In addition, the role of grain size reduction and mineral precipitation lowers the potential for fault cores to act as conduits for fluid flow.

1.2.4 Fault damage zone

The damage zone (Fig 1.1a, b) is described as a low strain zone composed of a network of secondary structures bounding the fault core. This zone is characterized by fractures, small-scale faults, veins, and folds. These structures cause heterogeneity in the permeability structure of the faults zone. which enhances permeability (e.g., Caine et al., 1996; Kim et al., 2004; Choi et al., 2016; Choi et al., 2012; Rotevatn and Basetesen, 2014). However, in fault evolution, segmentation and fault linkage is the fundamental process.

In the circumstances where displacement is not defined, e.g., seismic data, fault zones are not defined. Quantification of fault zone structure in terms of core and damage zone dimensions is

therefore not relevant to the study of segment linkage or the impact of segmentation on fluid flow within or across fault zones. In segmented faults, therefore, we define fault zones as seen in Fig (1.1C) (Rotevatn and Bastesen, 2014; Childs et al., 2012).

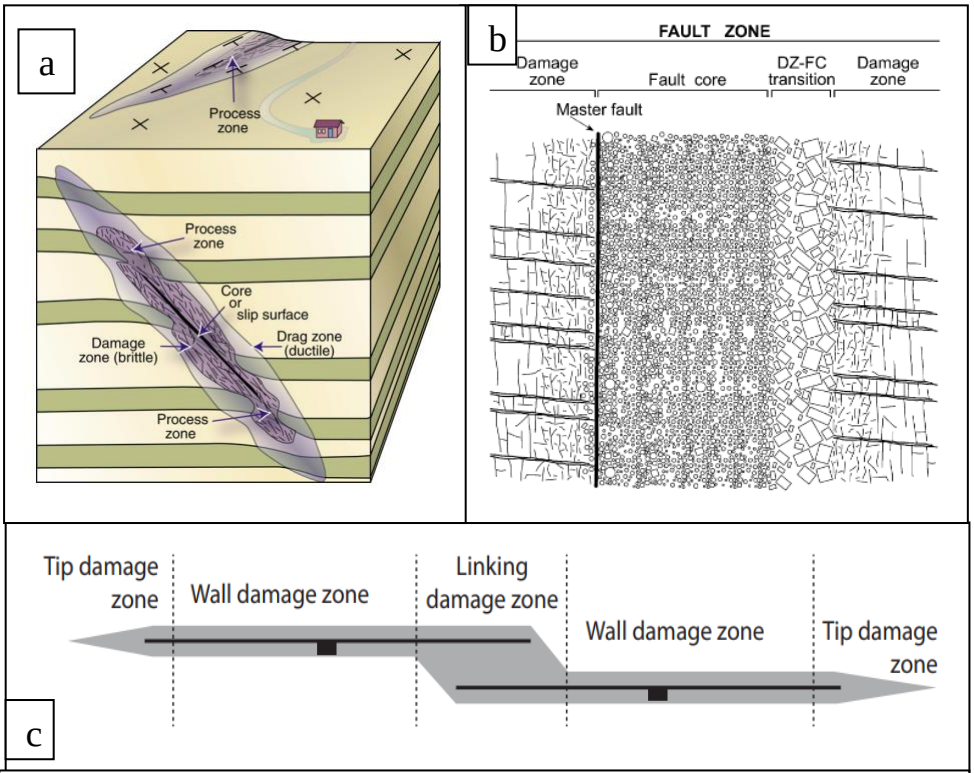

Fig 1.1: Fault zones (a) Fault core/slip surface and damage zone (after Rotevatn and Fossen 2011), (b) Damage zone-fault core transition (after Billi et al., 2003), (c) Fault zone in segmented faults (Peackock et al., 2016, Rotevatn and Bastesen, 2014)

1.2.5 Fault geometry

To assess for, and identify areas of fluid flow, or where possible risks are involved, there is a need to accurately interpret and understand fault geometry within the subsurface. Fault segmentation controls the structural deformation style and strain distribution in faulted strata (Fossen and Rotevatn, 2016; Nicol et al., 2002; Song et al., 2020).

Understanding lateral fault growth and linkage carried both social and economic impacts considering the importance of fault linkage and transfer zones concerning fluid migration (Fossen and Rotevatn, 2016; Song et al., 2020). Fault geometry and growth are intimately linked, and the understanding of the growth of faults is a direct observation of their geometry (Childs et al 2017; Fossen and Rotevatn 2016; Jackson et al., 2017; Rotevatn et al., 2019; Lathrop et al., 2021; Roche et al., 2021).

To understand the geometry and development of fault segments, fault linkage models depend on the physical characteristics of the fault. The two most common models include soft linked, in which case the faults are not physically connected but may be kinematically coherent and strain is transferred between them. The second involves faults that are linked geometrically, in which case, hard-linkage is inferred (Walsh et al., 2003; Jackson et al., 2017; Rotevatn et al., 2019; Song et al., 2020).

During fault evolution and growth, the two most used models to explain the growth process are (I) simple fault tip propagation and linkage of individual small fault segments, termed 'isolated fault growth model' (sensu Walsh et al., 2003) or 'segment growth and linkage' (sensu Trudgill and Cartwright, 1994) or fault propagation model (Fig 1.2 A) (Rotevatn et al 2019; Jackson et al., 2017; Roche et al., 2021; Lathrop et al., 2021).

The second model (II) is the Constant length fault growth (Fig 1.2 B), in which faults rapidly establish lengths, and eventually accrue displacement, but do not propagate (Childs et al., 1995; Rotevatn et al., 2019; Fossen and Rotevatn 2016; Roche et al., 2021; Lathrop et al., 2021). The second model (II) was termed coherent fault growth model by Walsh et al., (2003).

However, a third (III) model (Fig 1.2 C), referred to as the 'hybrid' has also been suggested (Jackson et al., 2017; Rotevatn et al., 2019; Lathrop et al., 2021), in which case, the propagation and constant models are not mutually exclusive. In the hybrid model, the fault initially grows in form of discrete kinematic phases i.e., the initial lengthening (propagation stage) and eventually displacement accumulation (constant length stage) (Jackson et al., 2017; Rotevatn et al., 2019). Fault displacement-lengths studies have been carried out to help understand fault growths (Rotevatn et al., 2019; Jackson et al., 2017).

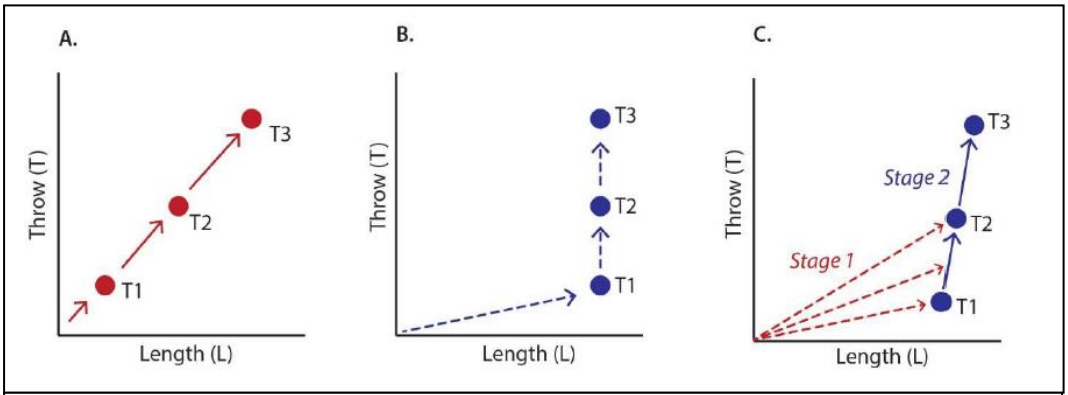

Fig 1.2: Displacement (D)-Length (L) Relations and Fault growth models. (a) Fault propagation model; (b) constant length model, (c) Hybrid Fault model (after Rotevatn et al., 2019)

Displacement (D) and length (L) and are related by the $D \propto L^n$ equation, and are applicable to simple isolated cracks (e.g., Cowie et al., 1992a, 1992b) and complex fault-linked models (e.g., Dawers and Anders, 1994). The D-L scaling relation therefore can be used to infer fault growth for an isolated model, thus giving insight into the propagation, slip history, and the growth and evolution of faults (Kim and Sanderson 2005; Peacock and Sanderson 1991). However, it is also imperative to note that the mechanical behaviour and interaction style of fault segments highly influence the growth of the overall fault in space and time (Crider and Pollard, 1998; Fossen and Rotevatn 2016). Additionally, the arrangement of faults in space, the number of active and inactive faults, density, and distribution of faults, supported with strain are other factors that control fault interaction (Fossen and Rotevatn, 2016).

In 3D seismic, because the horizontal and vertical axes are different, measuring displacement becomes complicated. Therefore, throw, instead of displacement is used when studying the evolution of faults using seismic data (Whipp et al., 2014; Bell et al., 2014; Jackson and Rotevatn 2013; Duffy et al., 2015; Jackson et al., 2017; Deng et al., 2020).

For a typical Isolated fault, in a homogenous medium, the displacement-distance plot nearly exhibits an asymmetrical profile with a maximum throw at the center (stage 1, Fig 1.3a &b). At the fault tips, however, completely isolated faults show a decrease in the throw.

With continued fault propagation, where two en-echelon fault segments are involved, relay zones become breached, forming a through-going fault (stage 2 &3, Fig 1.3a &b). The breached zones manifest as throw minima on a throw-length profile (e.g., Peacock and Sanderson, 1991). We can therefore project fault throw onto the surfaces and use these to understand segmentation history and reactivation events based on the nucleation points (Walsh and Watterson, 1991; Serck et al., 2019).

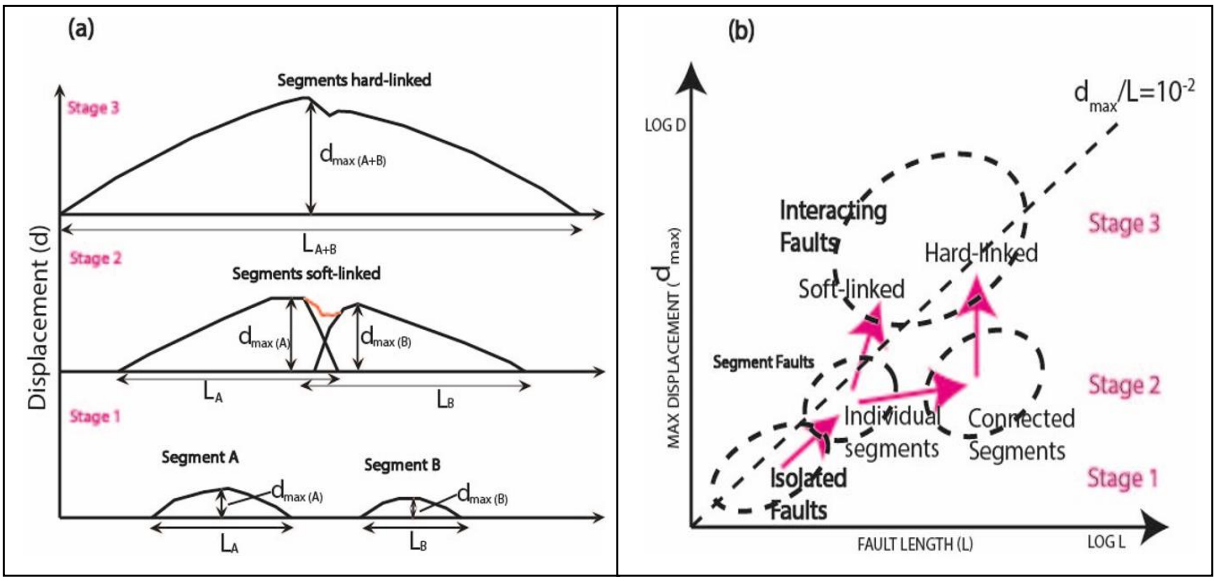

Fig 1.3: Displacement-Length models at the 3 stages fault segmentation and Linkage: stage 1 (a &b) isolated faults with D-L profiles, displaying maxima at centers. Stage 2 (a) displays minima at relay (breached) zone and interaction (b) of individual segments. Stage 3 fully interacted with fault, forming hard-linked segment displaying the sum of the displacement for the individual segments (Modification after Kim and Sanderson 2005).

Chapter two

2.0 The Øygarden Fault Complex

The Horda Platform is bounded by the Øygarden Fault Complex on the eastern part of the northern North Sea, the Viking Graben to the west, and the Stord basin to the south (Fig 1; Fig 2a (marked blue) & 2b). The immediate East, Mainland Sea bedrocks are predominantly Precambrian and lower Palaeozoic, which to the west represent the basement of the North Sea basin (Færseth et al 1995). The Oygarden Fault is a thick-skinned (basement involved) structure, trending north-south (N-S), and extends for about 300Km from Stavanger in the south to Florø in the north. Along strike from the Horda Platform in the North and Stord Basin to the south, the Øygarden Fault Complex exhibits changes in the strike, with northeast-southwest (NE-SW) in the south, where it aligns with Handerngerfjord Shear Zone (Nipen 2019) changing orientation to the North-South (N-S) further North

The North Sea crust was stretched during two main phases of faulting, with the Permian-Triassic phase as the main (also referred to as rift phase 1) and the second phase during the mid-Jurassic-early cretaceous which was a reactivation phase (Christiansen et al 2000; Fossen et al., 2000; Mulroney et al., 2020; Wu et al., 2021). Steep dips of between 55-60^0 are exhibited on the upper part of the Øygarden Fault zone, and flatten downwards into the basement, forming low angles, reminiscent of a simple domino fault model (Burchfiel and Wernicke 1982).

At present, the Øygarden Fault complex is an area of focus mainly because, its hanging wall hosts the Smeaheia CO2 storage prospect, which has received considerable attention for its potential as a possible storage site (e.g., Mulrooney et al., 2020; Osmond et al., 2021; Wu et al., 2021).

2.1 Structural framework of the Northern North Sea.

The North Sea is a rift basin composed of three rift regions, namely, Viking Graben (VG), Central Graben (CG), and Withchground Graben/Moray Firth (WG), all three forming the trilete system (Zegler, 1990a; Burke, 1977).

The northern North Sea region is comprised of the Viking Graben, Sogn, Tampen Spur, the Horda Platform, and the East Shetland Basin further to the west (Fig 2a). The overall basin structure is characterized by tilted fault blocks which were formed due to lithospheric stretching, sedimentary loading, and thermal response. Both planar and listric normal faults are observed.

The northern North Sea was formed from the stretching of a heterogeneous basement composed of structures inherited from Caledonian orogeny, and Devonian post-orogenic extension (**Fossen et al 2017**; Fazlikhan et al 2017). It is characterized by normal faults trending predominantly North-South (N-S), Northeast-southwest (NE-SW), and Northwest-southeast.

The Horda Platform is a 300 km north-south elongated structural high, located on the eastern margin of the northern North Sea. To the east, the Horda platform is bounded by the Øygarden Fault Complex (study area). The Øygarden Fault Complex is one of the five major N-S striking fault zones which dominated the Horda Platform (Fig 2b)**.** The main faults are basement involved and termed first order (Gabrielsen et al 1999).

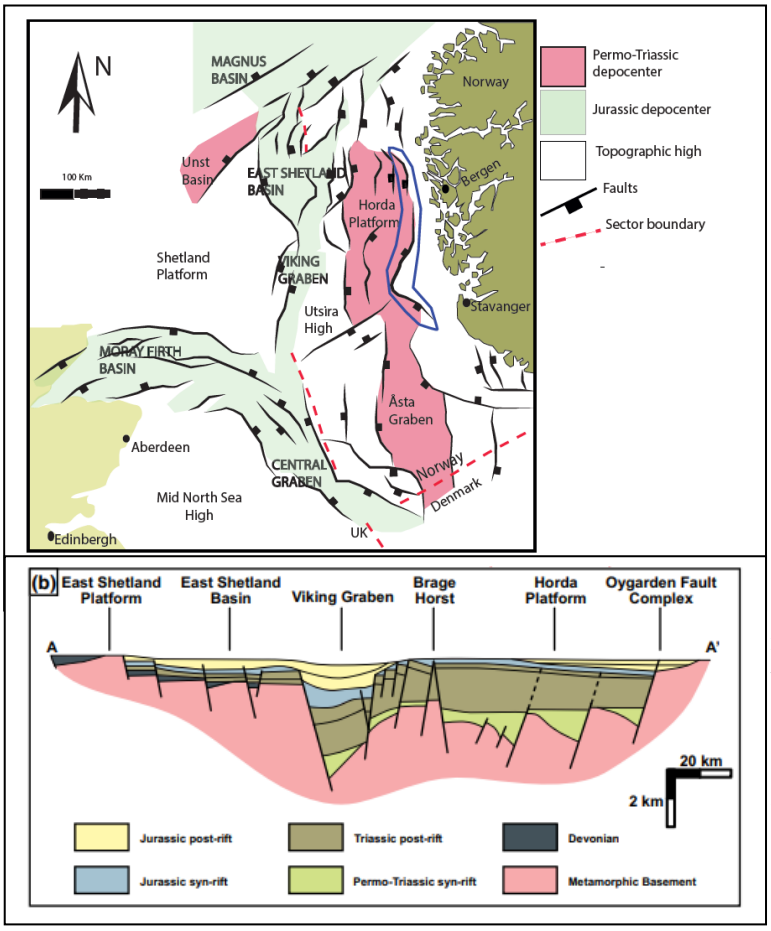

Fig 2: (a) Major structural elements in the northern North Sea; Area marked blue is the area of study (Øygarden Fault). (b) Schematic cross-section across Horda Platform (Fig2 a. modified from Whipp et al., 2014; Mulrooney et al., 2020; (Fig b) from Whipp et al., 2014, after Færseth 1996

2.2 The Northern North Sea tectonic and structural evolution

The northern North Sea tectonic evolution can be summarised by a Pre-Permian phase of several deformation events, followed by two main rifting phases; (a) Permian-Early Triassic (RP I) and (b) Middle Jurassic-Early Cretaceous extension (RP II) (see chronostratigraphic

chart summarising main tectonic events, Fig 2.1). Each of the main rift phases was followed by a thermal cooling stage which was characterized by regional basin subsidence (Christiansson et al., 2000).

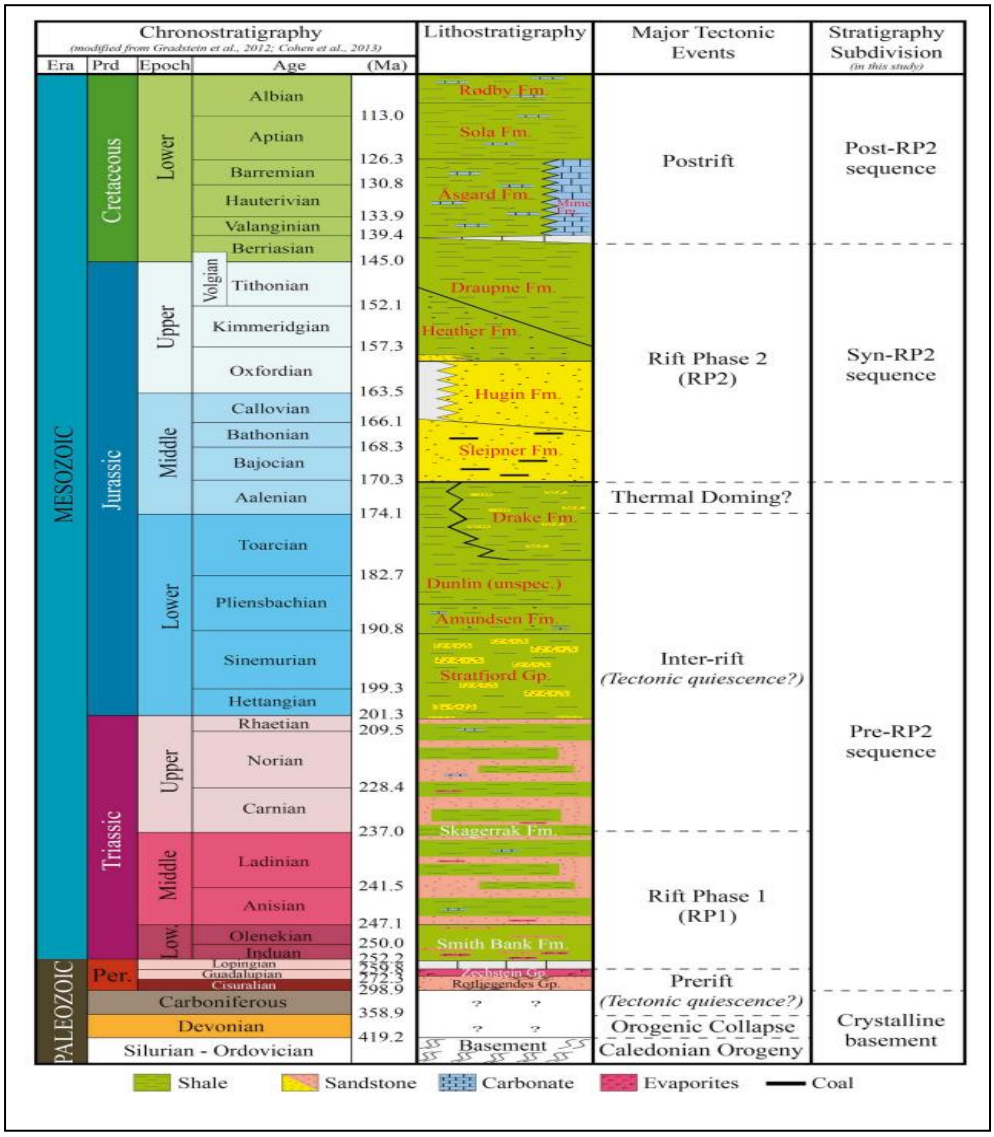

FIG 2.2: MAIN TECTONIC EVENTS AND CORRESPONDING CHRONOSTRATIGRAPHIC UNITS (FROM OSAGIEDE ET AL., 2020; CHRONOSTRATIGRAPHIC CHART MODIFIED AFTER GRADSTEIN ET AL., 2012; COHEN ET AL., 2013)

2.2.1 Pre-Permian period

The Caledonian and Variscan orogenies occurred between 460-400 and 400-300Ma respectively (Roberts, 2003; Gee et al., 2008; Bell et al., 2014). The Caledonian Orogeny commenced during early Ordovician when Iapetus Ocean subduction occurred, resulting in convergence, and eventually Baltica and Laurentia continental Collison during mid-Silurian to

early Devonian (Færseth et al., 1995; Gee et al., 2008; Bell et al., 2014). The Caledonian Orogeny Scandian phase marked the final and main phase that led to the uplift and formation of large mountain chains along with western Scandinavia and Scotland (Faleide et al., 2010; Fossen et al., 2016; Gee et al., 2008; Phillips et al., 2019).

The accreted terrains that formed during the orogenies resulted in a highly heterogeneous crust with a structural imprint in form of lithological layering, shear zones, mylonitic fabric, and thrusts (Fossen et al., 2016). These heterogeneities influenced the subsequent rifting and extension, giving rise to rift segmentation and the formation of transfer zones (e.g., Bell et al., 2014; Fossen et al., 2016; Fazil-Khan et al., 2017).

2.2.2 Devonian extension

Post Orogenic gravitational collapse of the accreted terrains led to extensional deformation following the Caledonian shortening. In the Southern part of the Orogeny, the transition from contraction to extension is believed to have occurred just shortly before 400Ma (Fossen and Dunlap, 1998), whereas, in the north, an overlap between contractional and extensional activity occurred (Tucker et al., 2004).

During the Early Devonian, the extension was oriented E-W to NW-SE, and reactivation of pre-existing Caledonian thrust decollement structures initially accommodated the extension (Fossen 1992; Gee et al 2008; Corfu et al., 2014; Bell et al., 2014; Osagiede et al., 2020; Phillips et al., 2019). With time, however, the Caledonian structures became locked at low angles and could not accommodate the further extension.

Large-through going shear zones such as the low-angle Nordfjord-Sogn Detachment (NSDZ), the steeper Bergen Arcs (BASZ)and Hardangerfjord shear zones (HSZ), the Stavanger shear zone (SSZ) and the Kamøy (KSZ) shear zone, therefore, developed, and accommodated deformation (Fazlikhani et al., 2017; Phillips et al., 2016; 2019; Osagiede et al., 2020). Indeed, the low-angle Nordfjord-Sogn Detachment Zone is responsible for accommodating several supradetachment Devonian basins e.g., the onshore Hornelen, Kvamshesten, and Solund basins (Fossen, 2010; Vetti and Fossen, 2012; Osmundsen and Andersen 2001; Braathen et al., 2000). The offshore intra-basement structures in the northern North Sea reveal possible onshore-offshore continuity e.g., HSZ, NSDZ, and SSZ (e.g., Phillips et al., 2019; FazlilKhan et al., 2017) but also reveal a new Stavanger shear zone, which had been restricted offshore (Fazlikhan et al., 2017).

2.2.3 Early to Late Carboniferous

Following the Devonian extension, the North Sea experienced further extension and compression phases during the Palaeozoic and Mesozoic (Ziegler 1992; Coward et al., 2003; Phillips et al., 2019). The southern and central North Sea area formed the clastic and carbonate shelf, flanked to the south by the Rhenohehercynian deep water trough during the Late Devonian and Early Carboniferous (eventually destroyed during Carboniferous Variscan orogeny) (Ziegler, 1992). The Carboniferous rift basins trending northeast are evident in the British Isles and extend into western parts of the northern North Sea, where they are not defined. However, they were partially inverted during the late Westphalian terminal phase of the Variscan orogeny (Ziegler, 1992).

In the Late Carboniferous-early Permian period, modifications in the convergence direction of Gondwana and Laurussia (North America-Europe) led to the development of complex wrench faults systems which transected Northwest Europe. Wrench tectonics-induced extension events such as the Oslo Graben are evident. The Oslo rift, and as well the offshore rift events were characterized by major volcanic activities which continued into the Triassic period in western Norway. Wrench fault and volcanic activity diminished towards the end of early Permian in northwest Europe, and the North and South Permian basins began to subside in response to thermal relaxation of the lithosphere (Ziegler, 1992; Wilson et al., 2004; Phillips et al., 2016). During the Late Carboniferous-early Permian, evaporite-dominated Zechstein Super-group was deposited, and had a profound influence on depocenter distribution (Jackson and Stewart, 2017; Steward et al., 2007).

2.2.4 Permian-early Triassic rifting phase

The Late Permian to Early Triassic event marked the main rifting phase, commonly referred to as rift phase 1 (RP1) of the northern North Sea (Ziegler, 1992; Færseth 1996; Bell et al., 2014; Phillips et al., 2019; Osagiede et al., 2020; Wu et al., 2021; Mulrooney et al., 2020). This phase initiated around 226 Ma, lasting 25-37Myr, coincident with the breakup of the Pangea (Ziegler, 1992; Bell et al., 2014; Osagiede et al., 2020; Wu et al., 2021). Corroborated by N-S oriented Permian-Triassic dykes which crosscut pre-existing NNW-SSE striking fractures observed onshore Norway, the direction of the extension during the Permian-early Triassic event was inferred to be E-W (Færseth et al., 1997; Fossen and Dunlap, 1999; Færseth 1996; Bell et al., 2014; Phillips et al., 2019; Osagiede et al., 2020; Wu et al., 2021).

The observed onshore basement influenced the distribution of faults, resulting in wide deep Permian-Triassic half and full grabens formed with principal fault-controlled depocenters located in the East Shetland and Stord Basins (Fig 2.2a) (Bell et al 2014; Fossen et al 2016). The N-S striking Permian-Triassic faults were observed orthogonal to the inferred extension direction (Færseth et al 1995; Bell et al., 2014; Whipp et al., 2014; Fazlikhan et al., 2017; 2020; Phillips et al., 2019). Most of the extensional strain was accommodated within the Horda Platform-Stord Basin rift axis during RP1 (Færseth et al 1995; Fazlikhan et al., 2017; 2020; Phillips et al.., Bell et al., 2014; Whipp et al., 2014).

Following the RP1 event, a tectonic quiescence period continued until the Jurassic (Ziegler 1992; Osagiede et al., 2020;). During this time, thermal cooling of the lithosphere was the main driving mechanism of subsidence creation. However, some minor activities may have continued during the inter-rift period within the Latest Triassic and Early Jurassic (Råvnas et al., 2000; Claringbould et al 2017; Deng et al 2017).

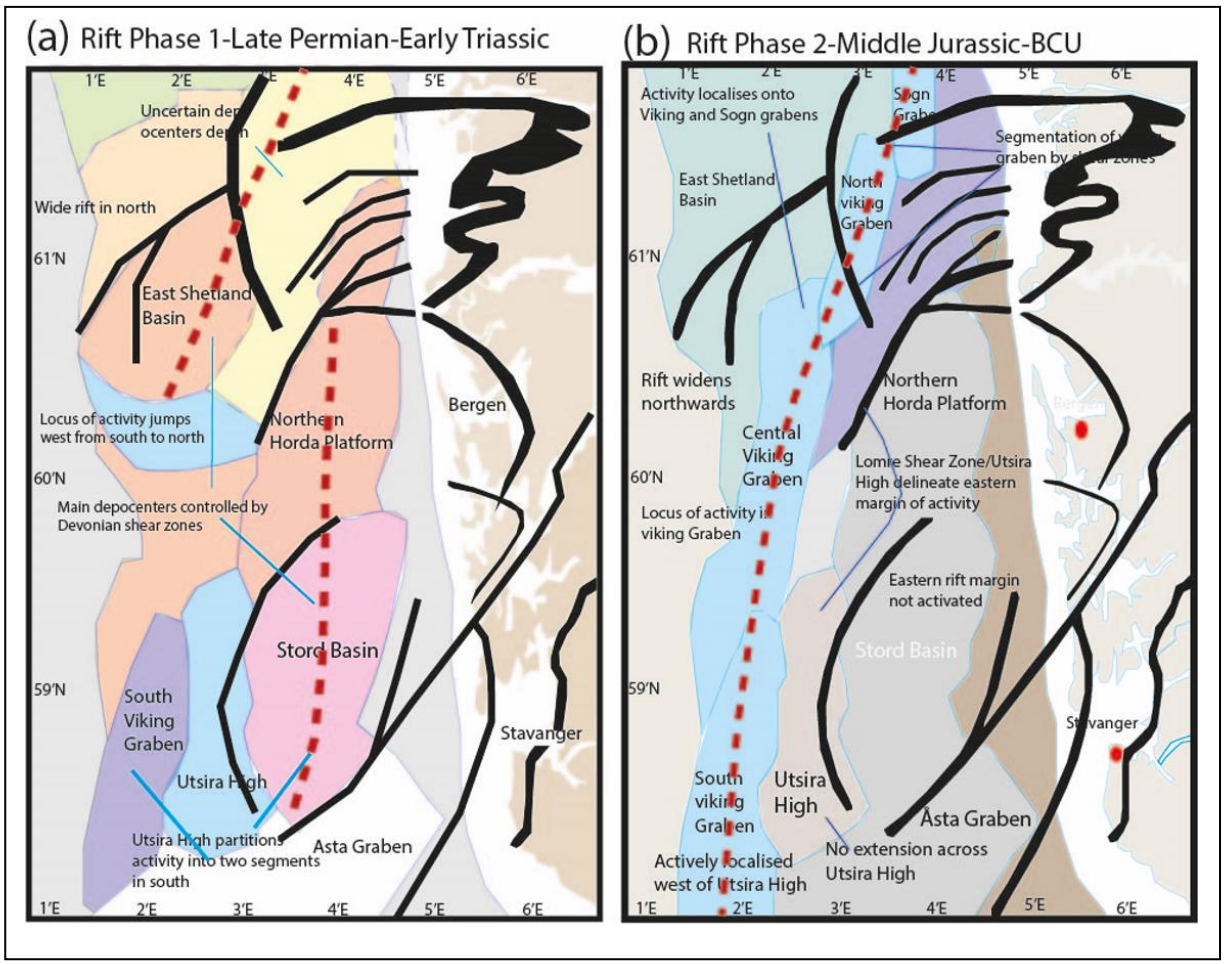

FIG 2.1: SUMMARY OF RIFT ACTIVITIES AND MAIN DEPOCENTERS FORMED DURING THE MAIN RIFT EVENTS (A) EASTLAND BASIN & HORDA PLATFORM/STORD BASIN (DOTTED RED) (B) SHIFT IN RIFT ACTIVITY TO THE WEST (VIKING GRABEN, AS THE HORDA/STORD BASIN, ARE INACTIVE

2.2.5 North Sea Thermal Dome

The North Sea Dome formed because of southward-migrating dome centres (Graversen 2006 and references therein). It was recognised by the near base Middle Jurassic erosional unconformity in central North Sea (Graversen 2006). The North Sea dome is noted to have extended across the entire North Sea (Graversen 2006). Erosion of thick strata across large parts of the North Sea due to the uplift resulted in the redistribution of sediments in the neighbouring areas (Davies et al., 2000; Quirie et al., 2019; Underhill & Partington, 1993). The deltaic sequences in the Brent sandstone group (now Brent Group) in the northern North Sea, for example, formed due to erosion of the Middle Jurassic North Sea Dome (Helland-Hansen et al 1992; Nottvedt et al 2008).

Extensional episodes during the middle-Jurassic occurred near central segment of the northern North Sea, most especially around the Viking Graben and the Sogn Grabens (Bell et al., 2014; Deng et al., 2017; Wu et al., 2021). On the northern margin of the Horda Platform, several faults were active in the Uer Terrace area in the middle Jurassic. On the western margin, on the other hand, minor fault-controlled thicknes changes were experienced on the Brent Group sequences on the hanging-wall side of the Troll Fault system, on the Horda Platform (Whipp et al., 2014). No fault tectonic activity has been reported on the Horda Platform, because, from the Late Triassic to Late Jurassic times Horda Platform was stable (e.g., Wu et al., 2021). The Horda Platform therefore experienced a phase of quietness, referred to as the first post rift phase (PRP-1). Using seismic sections, this has been supported by tabular sedimentary packages across the Horda Platform.

2.2.6 Middle Jurassic to Early Cretaceous (Rift Phase 2)

The collapse of the thermal dome in the Middle to Late Jurassic was followed by a second rift phase (RP2) which lasted until the Early Cretaceous (Ziegler, 1992; Færseth et al 1997; Færseth, 1996; Coward et al 2003; Bell et al 2014; Phillips et al., 2016; 2019; Osagiede et al 2020; Wu et al., 2021; Mulrooney et al., 2020; Osmond et al., 2021).

This phase is thought to have been initiated due to the deflation of the central North Sea thermal dome (Ziegler 1990; Bell et al 2014). Davies et al (2001) and Nottvedt et al (2008) believe that the dome collapse exerted regional tension, which resulted in the development of the trilete North Sea junction (Viking Graben, Moray Firth, and Central Graben).

The second rifting phase was focused on a more western position in the northern section, with an extension more concentrated on the North Viking Graben and Sogn graben (Fig 2.2b) (Bell et al., 2014; Deng et al., 2017; Phillips et al., 2019; Wu et al., 2021).

The thermal dome heated and acted to weaken the lithosphere in the vicinity of the present Viking Graben, which may explain the localization of strain in the Viking Graben during this phase (Bell et al., 2014).

The Timing of Initiation of RP2 has been dated to Bajocian (Ca. 167-170Ma) based on stratigraphic analysis of faults on the Horda Platform and East Shetland (Davies et al., 2000; Cowie et al 2005; Bell et al 2014). The timing of the initiation and cessation of RP2 episodes is diachronous across the basin, with estimates of the duration of individual faults activity ranging between 10 and 40 Myr (e.g., Cowie et al., 2005; Bell et al., 2014; Mulrooney et al., 2020; Wu et al., 2021).

On the Horda Platform, the pre-existing N-S oriented main faults were reactivated, forming several half-graben depocenters (e.g., Bell et al., 2014; Whipp et al., 2014; Wu et al., 2021). During the early phase of RP1, the Draupne Formation was deposited, and minor onlaps have been exhibited. The main phase of fault in the RP1 saw the deposition of the Cromer Knoll group. This formation showed wedge shaped and rotated onlaps on in the half graben (e.g., Whipp et al., 2014; Wu et al., 2021).

Rifting during the Middle Jurassic to Early Cretaceous took place as a series of discrete rift events associated with variations in the regional extension direction (Davies et al 2001; Bell et al 2014; Deng et al., 2017; Wu et al., 2021).

Whereas many large Middle Jurassic to Early Cretaceous faults in the Northern North Sea represented reactivated Permian-Triassic structures, recent 3D Seismic and Well data studies on the East Shetland area reveal crosscutting relations between east-dipping RP2 (Middle-Late Jurassic) and west-dipping RP1 (Permian-Triassic) faults (Færseth 1996; Bell et al., 2014). This implied that during RP2, initiation of new faults was favoured over reactivation of pre-existing ones (Færseth 1996; Bell et al., 2014).

2.2.7 Post rift phase

The second and last main rifting event (RP2) was followed by a major transgression, albeit uplifted areas remained dry and islands for most of the Early Cretaceous (Faleide et al 2010). A well-marked characteristic of the post-rift phase on seismic sections across the North Sea is the major Base Cretaceous unconformity (BCU) between the Cretaceous and the Jurassic, except where sedimentation continued in the deeper parts (Faleide et al., 2010). Fault activity waned during the Cretaceous, and subsidence was due to crustal cooling after Jurassic rifting (Faleide et al 2010). However, tectonic activity has been reported in the northern North Sea, with sequences deposited from Ryazanian to late Turonian exhibiting tectonic activity (Gabrielsen et al 2001). Corroborating this, was the closeness of the Viking and Sogne Graben to Møre Basin (Fig 2.3), which, was part of the deep axial basins of the North Atlantic rift system that experienced tectonism during the Aptian-Albian time.

In the northern North Sea, Gabrielsen et al., (2001) and Faleide et al., (2010) describe the post-rift phase in three stages; (a) Ryazanian–latest Albian incipient post-rift, characterized by varying subsidence and influenced by syn-rift structural features like crests of rotated fault blocks, relay ramps, and sub-platforms; (b) Cenomanian–late Turonian medial stage during which sedimentation rates outcompeted accommodation space creation; (c) The early

Coniacian–early Palaeocene mature post-rift stage during which the basin evolved and became saucer-shaped, more so, where syn-rift features ceased. Since thermal equilibrium was reached at this stage, subsidence ceased, and the pattern of basin filling became, to a larger degree, dependent on extra-basinal processes.

During this post-rift thermal subsidence phase on the Horda Platform, the Shetland group composed of deep-water clastics and Carbonates, the Siliciclastic-dominated Rogaland and Hordaland group were deposited (Fossen et al., 1997). Uplift and erosion of the Horda Platform and the entire took place during the Neogene period. Overlying the eroded deposits were the Nordland Group composed of Quaternary post-glacial deposits.

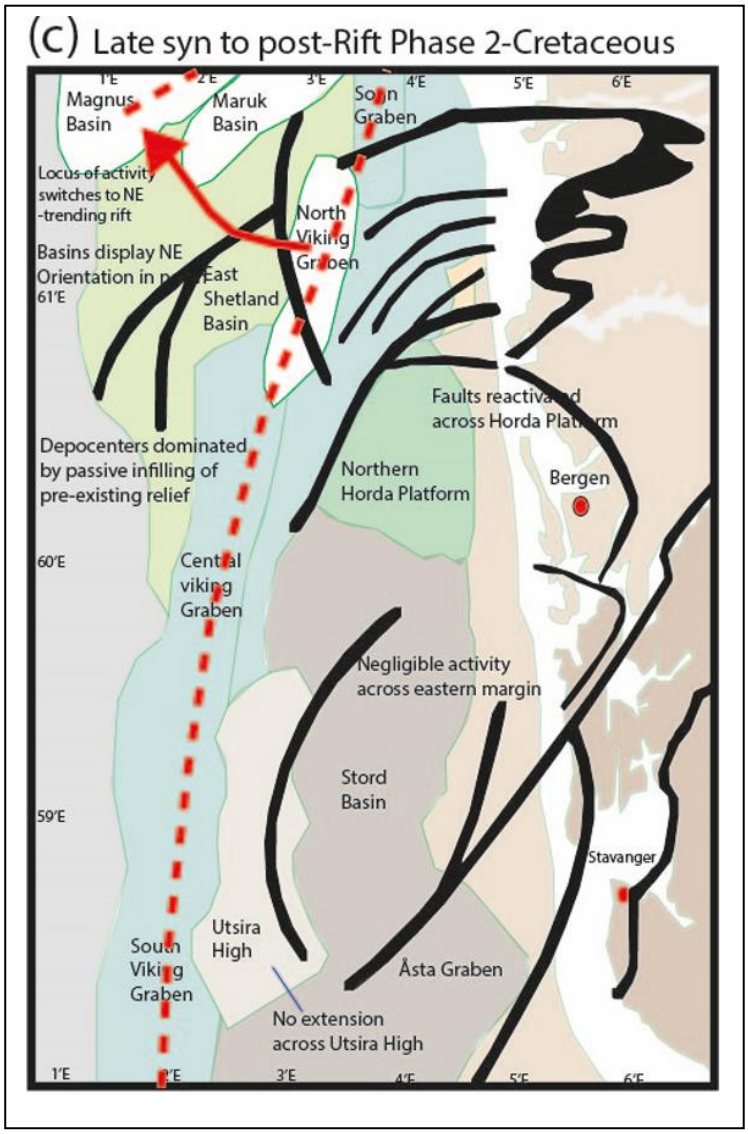

FIG 2.3: LATE SYN TO A POST-RIFT NORTHWARD SHIFT IN RIFTING AS A RESULT OF NORWEGIAN-GREENLAND SEA RIFTING ACTIVITIES (AFTER PHILLIPS ET AL., 2019)

Chapter three

Data set and methods.

3.0 Data

3.1 Seismic Data

In this study, densely spaced 2D seismic lines (Fig 3.0) were used to understand the structural and stratigraphic trends of the basin-bounding Øygarden Fault Complex and its hanging wall. focus. The study has regionally focused, covering a significant length of the Norwegian Continental shelf, approximately, 350 km from the Stord Basin in the south to the Horda Platform in the North, and thus it relies on a good regional 2D seismic data coverage.

The 2D data in form of time migrated seismic lines were acquired from the NPD data Diskos repository. The blue box below shows the extent of the study area, starting from Stord in the south to the Måløy slope, in the North.

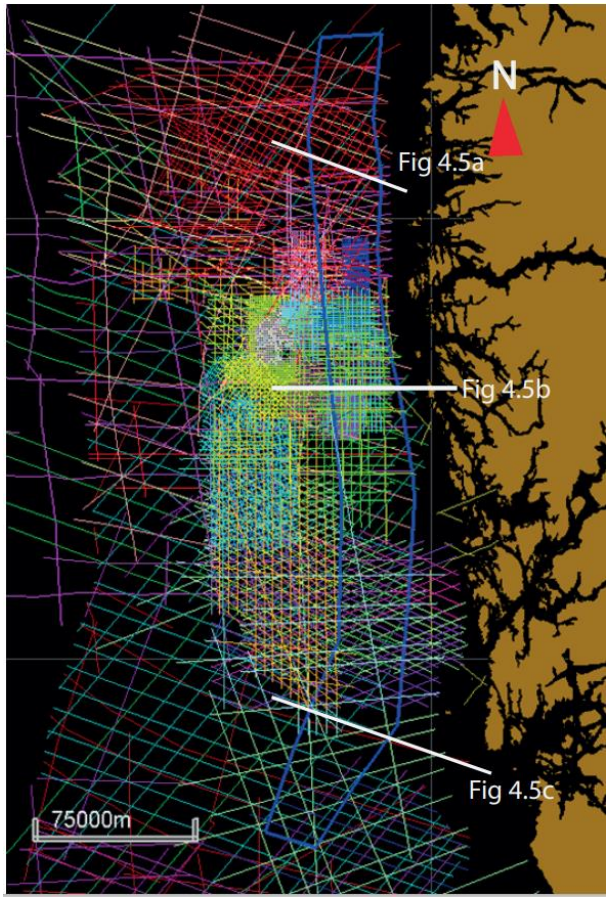

FIG 3.0: SUMMARY OF SEISMIC LINES AS USED IN THE STUDY AREA. FIGS 4.5A-C INDICATE LOCATIONS OF SELECTED FIGURES

3.2 Well Data

Additionally, 2D seismic data were integrated with borehole data, to constrain the stratigraphy, by correlating well tops and seismic horizons.

Most of the wells drilled are located within the central part of the study area (Horda Platform), and quite a few are located to the north and south, and, where present in these locations, the wells are further apart, and scattered, making a correlation quite hard.

The significant number of wells drilled on the Horda Platform was due to the significantly high number of hydrocarbon discoveries made over time. In the south, in the Stord basin, the lack thereof, of hydrocarbon discoveries, presumably due to a lack of play systems, meant increased risks, and thus low hydrocarbon wells were drilled.

In addition, unfavorable structural setup and lack of source rocks, and migration channels for the hydrocarbons, if absent, will not favor drilling activities, resulting in few wells (e.g., Sørensen and Tangen 1995). Among the most used wells in correlation well tops and horizons were wells number 32/-2-1 and 31/3, drilled in the alpha structural high, close to the Øygarden Fault, and within the Tusse Fault on the Western side of the Øygarden. Further to the west side of the Vette Fault, was drilled well number 31/2-1, which was also considered when correlating horizons.

Due to the quality of the 2D seismic data (Table 1 below), which was not good, uncertainty in interpretations, especially of the units in the North and South, where there is a lack of wells to correlate the seismic horizons are expected and were experienced.

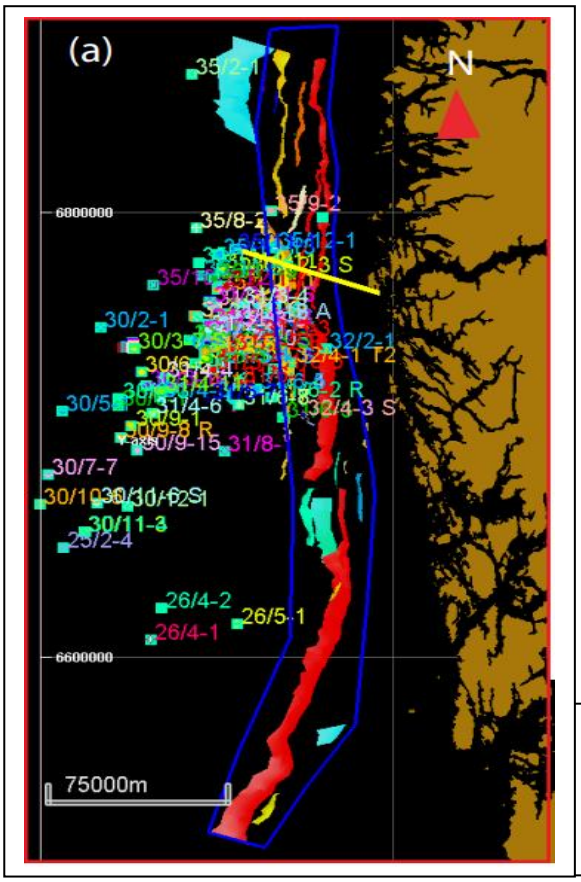

FIG 3 1: DISTRIBUTION OF WELLS IN THE STUDY AREA. THE MOST CONCENTRATION OF THE WELLS IS IN THE CENTRAL AREA, AND MOST SPARSELY DISTRIBUTED IN THE NORTH & SOUTH

Table 1

Survey	Year	type	company	Quality	Survey	Year	type	company	Quality
NVGTI-92					ST8408-REP91		2D		
NVGT-88					ST8116R84		2D		
SG9202	1992	2D	Saga Petroleum ASA		ST8116R08		2D		
NSR +									
NSR06		2D			SG9206		2D		
GNSR-91	1991	2D			SBGS-RE-94		2D		
GSB-85R97	1997	2D			SBGS-87		2D		
MN88-3	1988	2D			TE90		2D		
									Very
MN9101	1991	2D			TE93		2D		good
SH8001	1980	2D			RV0801		2D		
SH8401	1984	2D			NSR-06_A		2D		
ST8201	1982	2D			NSR-06_B		2D		
ST8301	1983	2D			NSR-06_C		2D		
SBGS-87	1987	2D			NSR		2D		
ST8518		2D			NOA-92		2D		
MN88-3		2D			NNST84_B		2D		
MN88-3		2D			NH8202		2D		
MN88-3		2D			MN9104		2D		
GSB-85R97		2D			MN9103		2D		
GNSR-91		2D			MN89-6		2D		

3.3 Methods

Following the successful literature review of most works on the northern North Sea, which gave an understanding of the regional tectonic and stratigraphic evolution of the area, seismic 2D data interpretations were carried out, using the Petrel E&P Software Platform 2021 suite. The focus was centered on the main Øygarden, and the secondary faults associated with it. Stratigraphy (Horizons) was thereafter mapped, and these were constrained using well data as indicated in the previous section.

3.3.1 Horizons interpretation

The Horizons were interpreted manually, and where possible, auto-tracking offers quite good control, in addition to quickening the process. To follow consistently the horizons, well tops were used to augment their picking. However, where wells were absent, the use of stratal terminations, which indicate changes in deposition, and stratigraphic images became important, and were applied. Our focus was mainly on the Permian-Triassic, Jurassic, and Cretaceous main horizons. The reason for the choice of the mentioned surfaces is because, our intention was to understand the evolutionary history of the Øygarden Fault Complex, starting in the oldest stratigraphy (Permian-Triassic), to present (Quaternary). In addition, the Jurassic formations form good reservoirs, and the Cretaceous (Cromer Knoll in particular) form good caprocks, characteristics considered when mapping CO2 reservoir sites (e.g., Mulrooney et al., 2020; Wu et al., 2021; Deng et al., 2017).

During the horizon mapping, uncertainties related to seismic quality limited the interpretations, and greatly affected the interpretations of the Basement surface and Permian-Triassic units.

3.3.2 Fault mapping

By screening through the entire data set, it is possible to make the right decisions before actual fault mapping is carried out. Previous works e.g., (Bell et al., 2014; Whipp et al., 2014; Mulrooney et al., 2020; Wu et al., 2021) were also used to constrain fault populations and as reference works. The fault mapping is focused on the Øygarden fault complex and associated secondary faults. The fault interpretations were mapped by considering the offset between horizons.

With the high density of closely spaced 2D seismic lines, the uncertainties related to lateral extent of faults were suppressed. However, some uncertainties related to seismic resolution, were experienced during the interpretations.

3.3.3 Thickness maps

With the successful mapping of faults and main horizons, it is then possible to create time-structure and time-thickness maps, which both give information about sediment deposition. The time thickness maps show changes in thickness in a time interval. These maps visualize vertical thickness between two surfaces, above and below in a particular time interval. This is the equivalent of stratigraphic thickness for a horizontal layer. In addition, with thickness maps, the shapes, and patterns of sedimentary packages, highly impacted by fault activities are depicted. Therefore, thickness maps can depict fault activity through time i.e., increases in thickness are an indicator of active faults at the time (syn-rift phases), especially augmented with wedge-shaped geometries in seismic sections. Where decrease or constant thickness occurs, this indicates periods of inactive faults (post-depositional faulting) or cessation of fault activities. The justification for this method was to predict fault activities at a particular time.

3.3.4 Throw vs distance and Depth vs Throw plots

Fault throw vs distance and Depth vs throw methods were used to understand both the lateral and vertical propagation, and thus the evolutionary history of the faults and depositional history (e.g., Peacock and Sanderson, 1991). To make the Throw-distance and Depth-throw plots, cutoff points in the hanging wall and footwall on the seismic section were measured in TWT (ms). Acquiring cutoffs in our case has been carried out manually, in combination with the multi-z tool in Petrel, with the latter making it easier when several horizons are considered.

The goal of using throw-distance plots is to understand the spatial evolution of faults. The minima and maxima points in the T-x plots indicate linkage points and initiation/nucleation points respectively (e.g., Peacock and Sanderson, 1991). Where a sudden decrease in throw is observed, this may indicate displacement accommodated by the branching fault. The geometry of faults therefore can easily be deduced from these plots, e.g., where the T-x plot shows asymmetry in the curve, in combination with high displacement at the segment boundary, an echelon fault evolution can be concluded (e.g., Dawers and Underhill, 2000). A summary of the work and interpretation flow are here below given (Fig 3.2 a, b).

The T-z plots record throw of the fault for interpreted horizons, and the captured information helps in understanding vertical fault propagation history (e.g., Deng et al., 2017; Holden 2021).

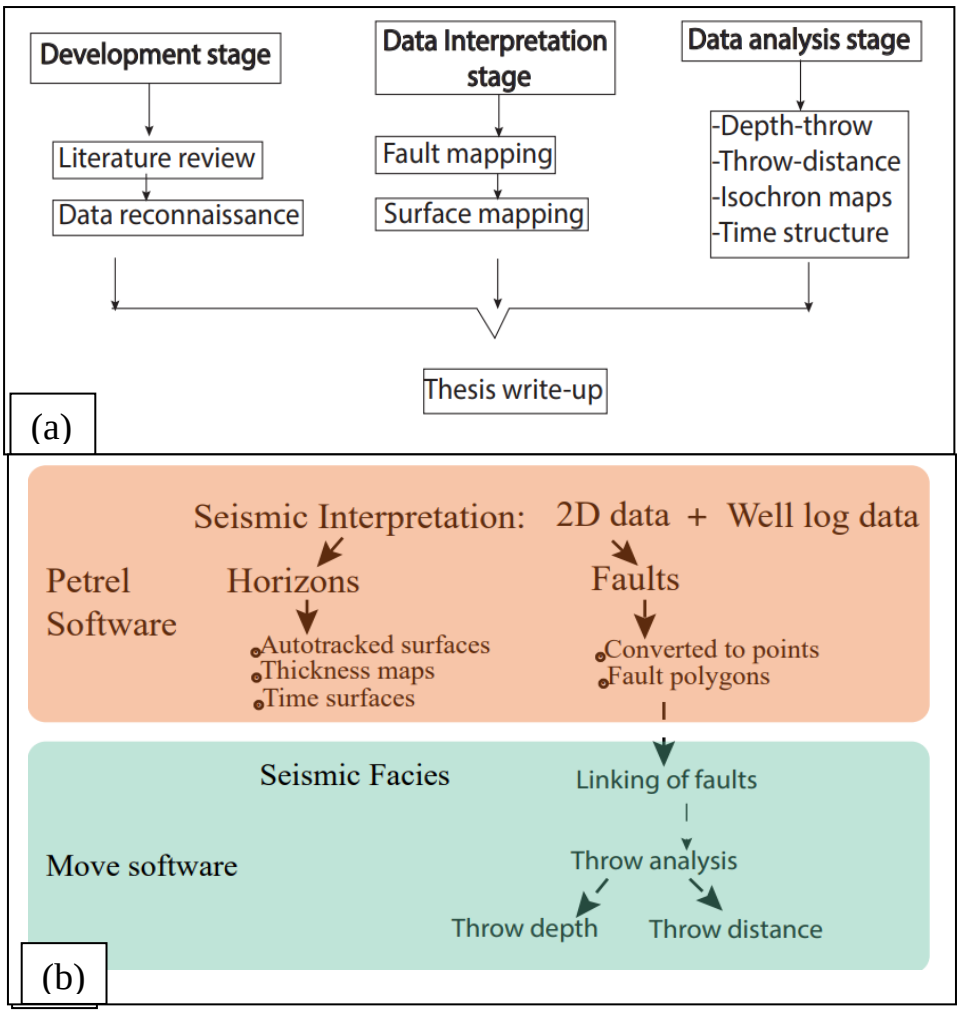

FIG 3.2: SUMMARY OF DIFFERENT STAGES IN THE WORK FLOW

Chapter four

4.0 Results

4.1 Seismic interpretation.

Five horizons were interpreted i.e., Horizon, H1, Base Quaternary unconformity interpreted and assigned formation names by correlating the seismic and well data available. From the youngest, shallowest to the oldest, deepest, these include Base Quaternary unconformity; Top Shetland GP, Top Cromer Knoll Gp, Top Draupne Gp, Top Sognefjord Gp, Top Brent Gp, and Basement. It must also be noted that due to the quality of seismic data, it wasn't possible to follow laterally, the continuity of the basement, and thus, an acoustic basement is inferred.

A detailed figure capturing the main stratigraphic units/and Surfaces mapped in the study area is shown (Fig 4.1 a, uninterpreted and Fig 4.1c Interpreted section). Growth strata are used to identify pre, post, and Syn-rift packages. In terms of age, we divide the formations into the Permian-Triassic group (which may include Statfjord, and Hegre formations, Lunde formation), the Jurassic group, which may include Dunlin/Brent, Sognefjord, Draupne groups, and finally the Cretaceous package which includes Cromer-Knoll GP and the Shetland units.

4.1.1 Permian-Triassic Units

The Permian-Triassic package exhibits a wedge-shaped geometry, thickening towards the Øygarden Fault, and thinning towards the west (Vette) (Fig 4.1C). This package is mainly affected by first-order faulting, which is mostly extended into the basement e.g. the Øygarden in the east and Vette in the west. The reflectors are quite parallel to sub-parallel and somewhat discontinuous (quite hard to follow laterally). Based on the growth strata, therefore, sediment deposition occurred in conjunction with the movement of the N-S trending faults.

4.1.2 Jurassic Units

The Jurassic package in general, on the other hand, maintains a relatively uniform thickness towards the Øygarden Fault, and it is characterized by tabular, high amplitudes reflectors, which are parallel and laterally continuous. Another observation in the Jurassic package is the folding (Fig 4.1) around the Øygarden, in which drilling of well 32/2-1 was carried-out. Folding, therefore, played a role in the evolutionary history of the basins on the Horda Platform. This formation/package is also affected by both first-order and second-order faulting, as evidenced by the N-S oriented large Øygarden Fault and small secondary faults oriented in a similar direction to the major Øygarden (Fig 4.1C). Within these units, in the hanging-wall of the Øygarden Fault, the Beta CO2 prospect is located. Furthermore, these

units juxtapose with the main Øygarden Fault in the east. There is a lack of strata on the eastern side of the Øygarden though. The uniform thickness observed is an indicator of a post-rift phase, where subsidence was influenced by post thermal subsidence upon cessation of rift phase one (RP1) in the Permian-Triassic. During this time, the Horda Platform tilted, when the Brent Group was being deposited.

In some areas, the secondary faults are responsible for the segmentation of the basins, and the observed local small thicknesses depocenters are indicators of secondary tectonic activities within the basin. The Jurassic units, therefore, form the Post rift phase (PRP1).

4.1.3 The Cretaceous package

Bounded by the Tertiary units above and the Jurassic below, the Cretaceous package, and, in particular, the Cromer Knoll unit shows evidence of growth strata, thickening and expanding towards the Øygarden hanging wall, and thinning westwards towards the Vette Fault. In the Cromer Knoll units, seismic reflectors down-lapping onto the Top Draupe surface are evident (Fig 4.1 arrows) in this unit, indicating sediments that were prograding.

However, around the Øygarden Fault, and in areas penetrated by well 32/2-1, evidence of erosion can be deduced (Triangles, in Fig 4.1C), where reflectors top lap onto the eroded, undulating Base Quaternary Unconformity (BQU). An abrupt stoppage of the Øygarden fault in the Cromer Knoll unit is noticeable, overlain by a truncation surface of the Base Quaternary Unconformity. The Øygarden Fault, therefore, was eroded during the Cretaceous period.

The Cretaceous is overlain by the Tertiary package, which itself is overlain, unconformably by the Quaternary package. The Tertiary package shows some evidence of post-rift faulting supported by small faults (Fig 4.1C).

The growth strata and top laps observed are interpreted as indicators of continuous fault-controlled subsidence when the Øyagaden was active. The general thickening towards the west is related to the regional subsidence in the hanging wall that occurred when the N-S trending and west-dipping faults and the Horda Platform on the east, in general, were uplifted and rotated. Uplift of the tilted fault block resulted in erosion above the Cretaceous, thus the observed undulating truncations (Fig 4.1).

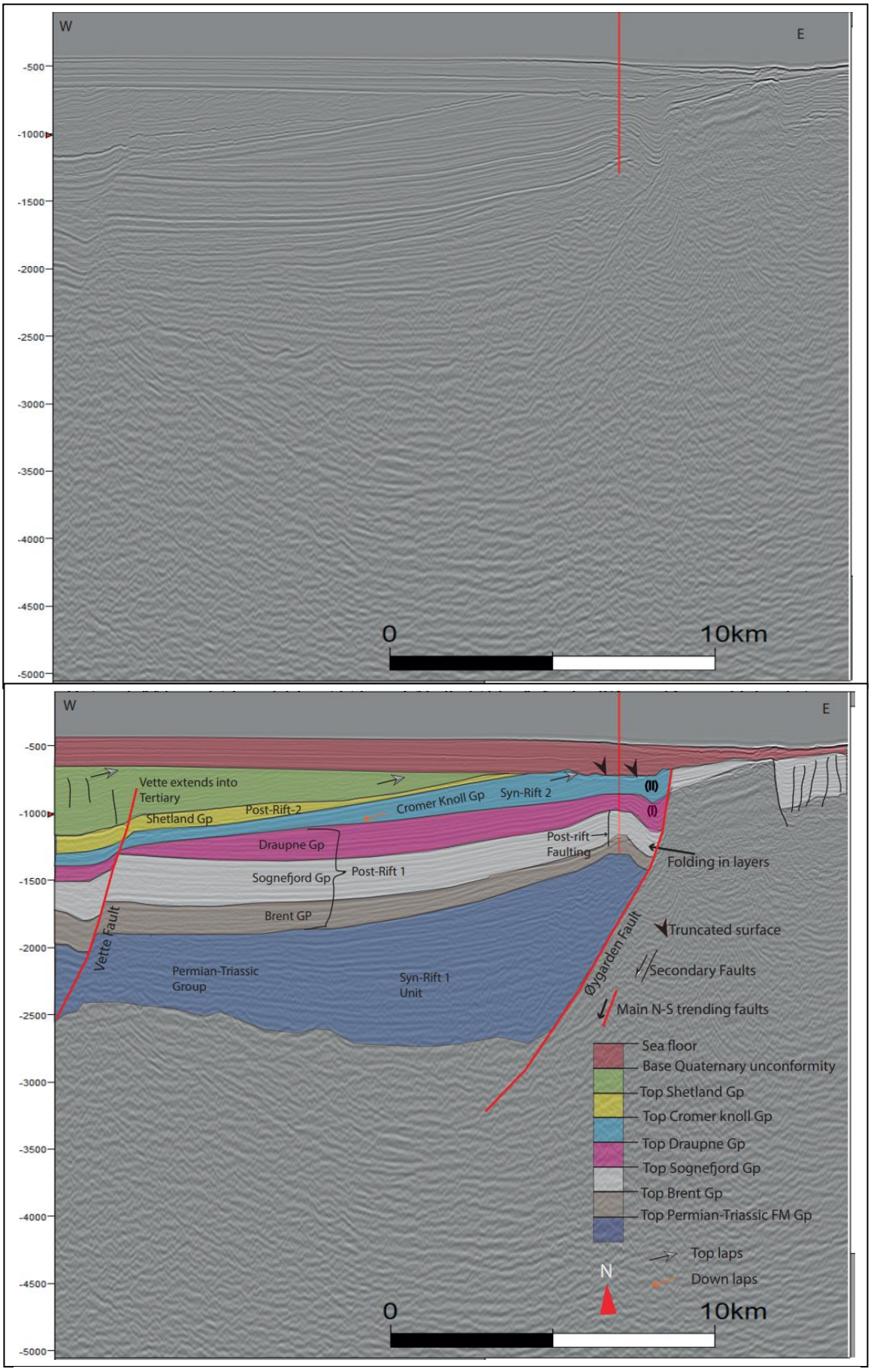

FIG 4.1: (A) UNINTERPRETED SECTION, AND (B) INTERPRETED SECTION SHOWING THE MAIN UNITS AND DESCRIPTION OF SOME STRUCTURAL FEATURES

4.2 Time structure maps

In TWT (ms), the structure maps are a representation of the topography of the interpreted horizons. The time structure maps can give information about the geometry of the basin, sediment deposition, as wells as sediment routing sites.

4.2.1 Base Quaternary Unconformity (BQU)

This surface is interpreted based on seismic terminations and the rugose/undulating nature of the surface. The unconformity surface exhibits relatively shallow relief (up to -90 ms) in the southern part of the study section compared to the northern part, which exhibits lower elevation (Fig 4.2b).

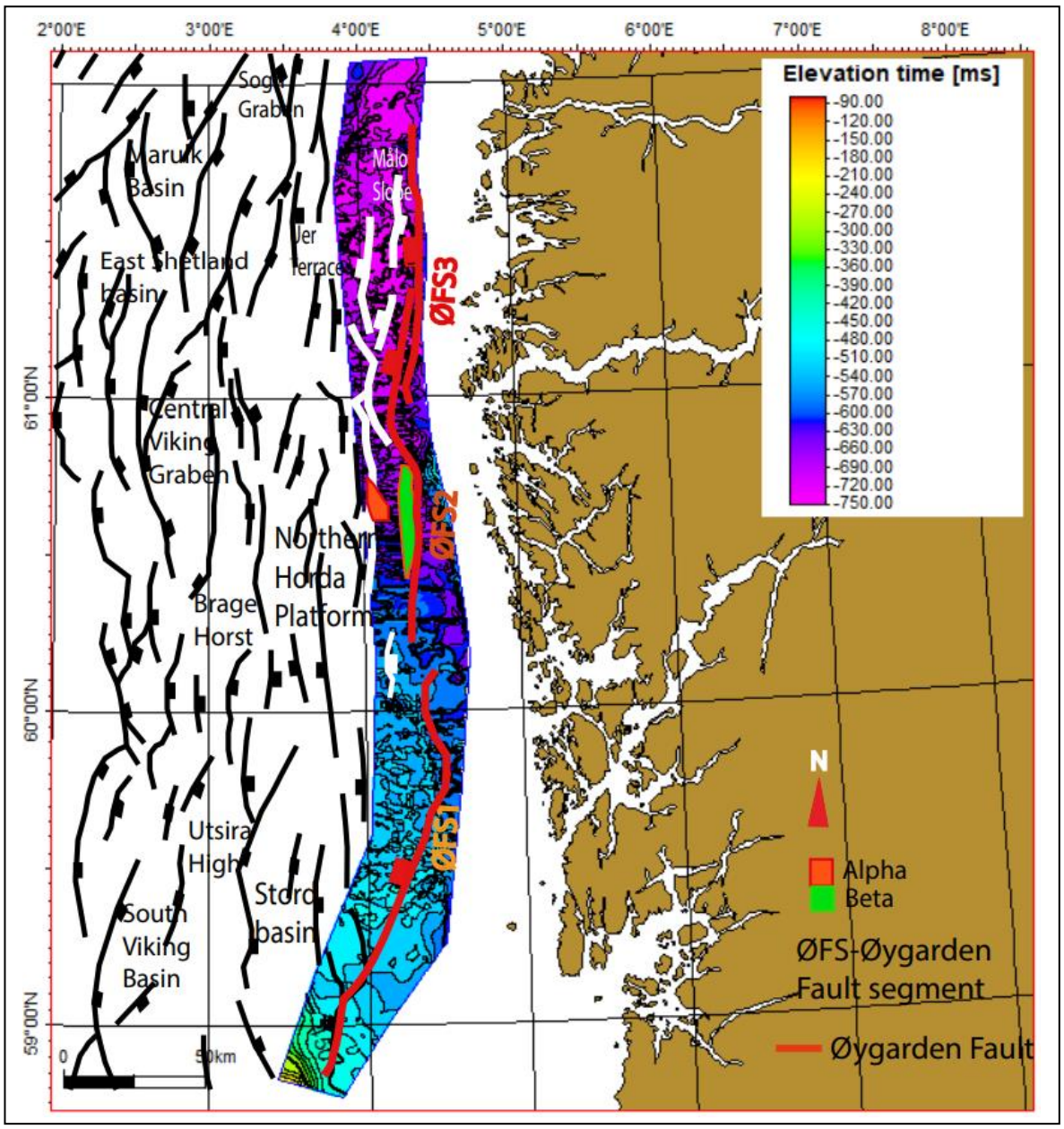

FIG 4.2A: TIME STRUCTURE MAP FOR THE BASE QUATERNARY UNICONFORMITY SHOWING VARIATIONS IN ELEVATION

4.2.2 Top Shetland group

The Top Shetland surface is represented by a strong pick across the area. It shallows towards the coast (in the east) and is particularly elevated in the central area, where values up to -100 ms are exhibited **(Fig 4.2b).** Deeper areas are located mostly offshore (west) and located in the northern and the southern areas.

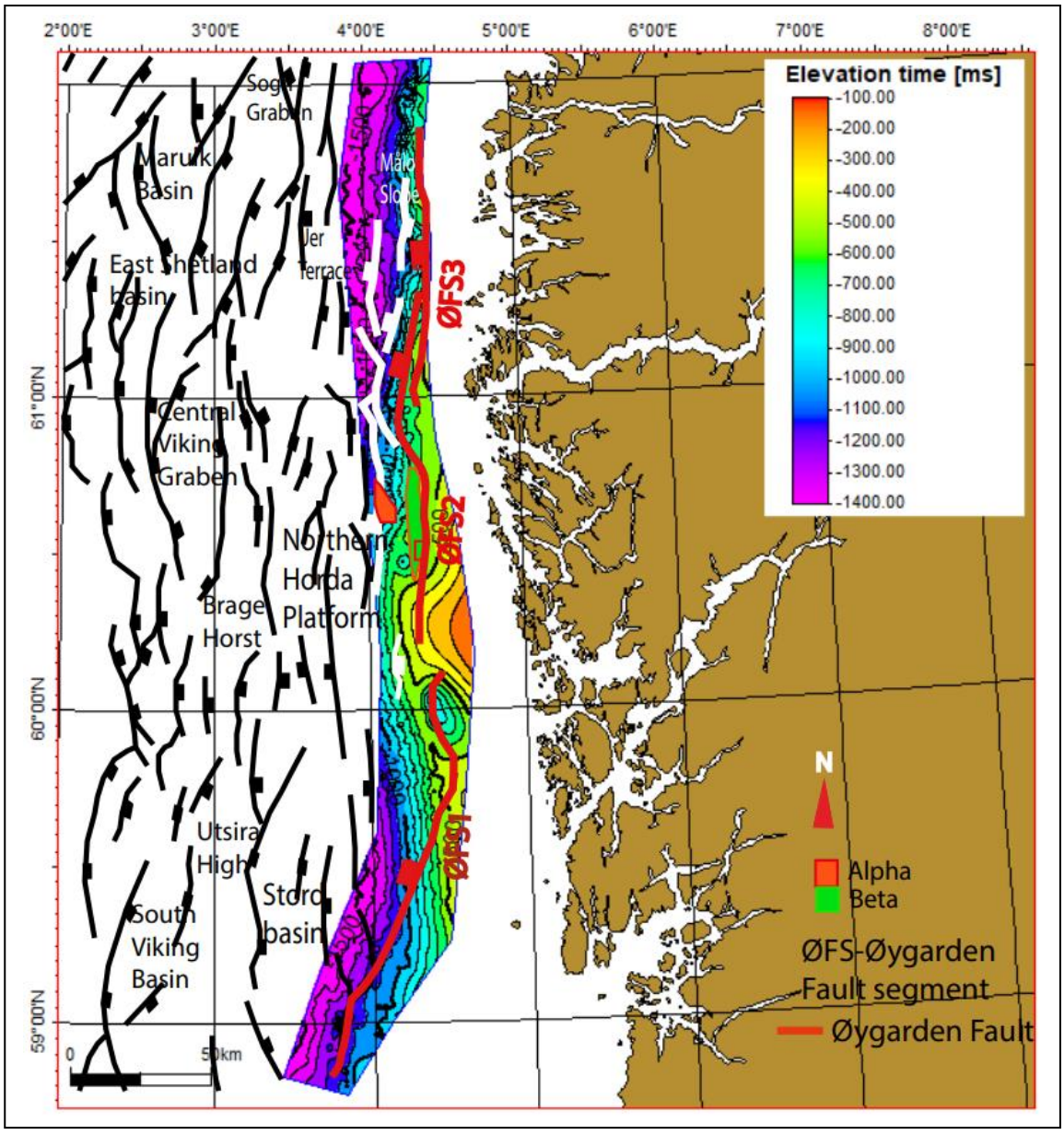

FIG 4.2C: THE SHETLAND GROUP TIME STRUCTURE MAP SHOWING A GENERAL SHALLOWING ALONG THE EAST COAST. MORE SHALLOWING HOWEVER IS OBSERVED IN THE CENTER

4.2.3 Top Cromer knoll Group

Like the Shetland group, the Top Cromer Knoll is picked along a continuous, relatively strong peak. The surface also deepens into the basin (west), where depths up to up to -1600 ms are exhibited i.e., an increase in depths away from the margin. Note the much deeper values in the extreme northern (Måløy slope) and Southern (Stord basin) areas where depths of -1600 ms are observed (Fig 4.2d). consisting of marine sediments and some calcareous material of low energy open environment, the Cromer Knoll surface represents the top of the Lower Cretaceous deposits. This surface is offset by the main Øygarden Fault, but the throw is not that much.

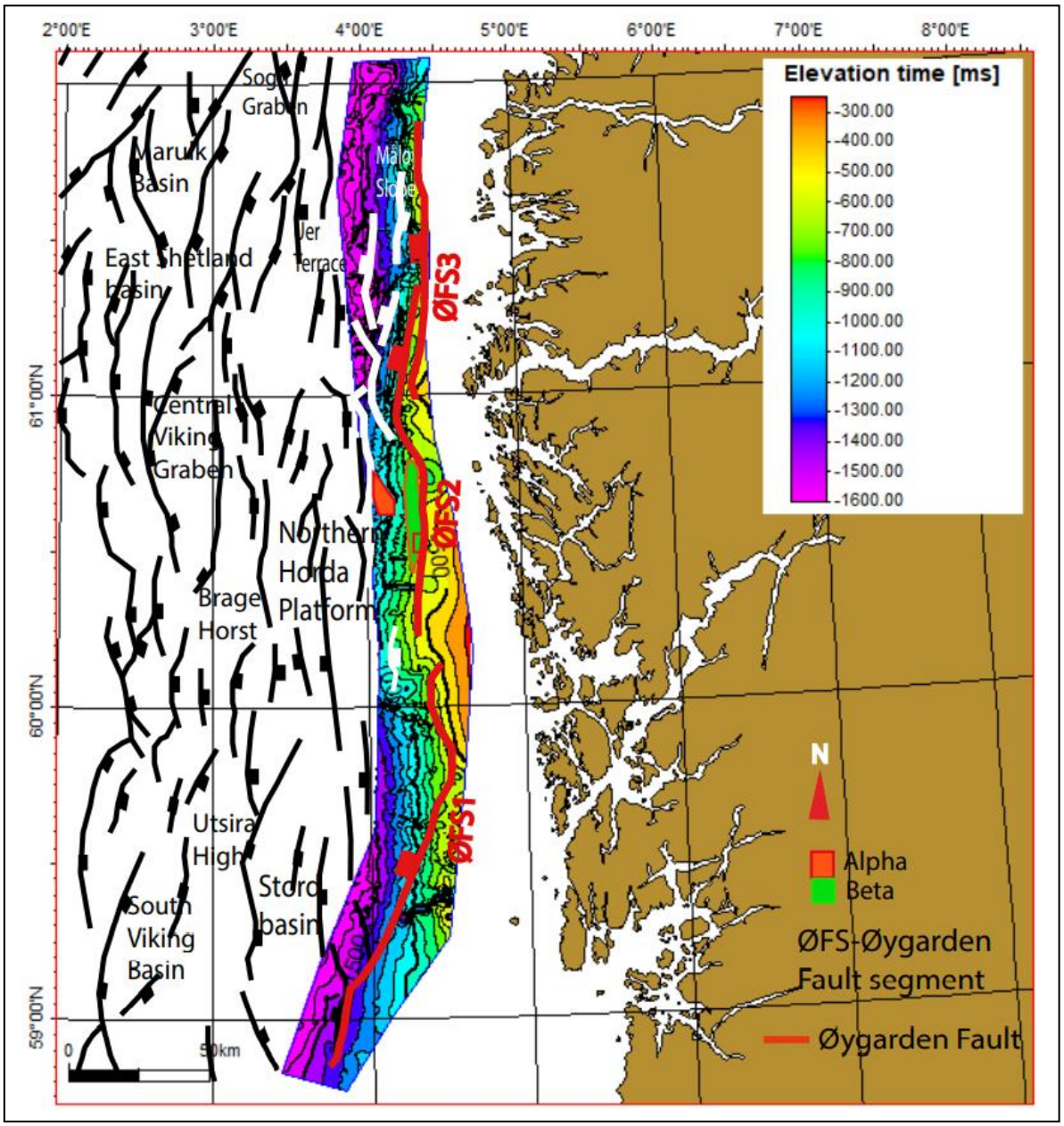

FIG 4.2D: TIME STRUCTURE MAP FOR THE TOP CROMER KNOLL GROUP. NOTE DEEPENING IN THE SOUTH AND NORTHERN BASINS ALONG THE WEST.

4.2.4 Top Draupne Group

In general, the Top Draupne surface is characterized by topographic high on the eastern part (along the coast), and relatively low reliefs on the western side (offshore areas), both in the south (close to Stord basin) and north (Måløy slope). The highest relief is focused on the middle or central areas, with elevation values of -100 ms).

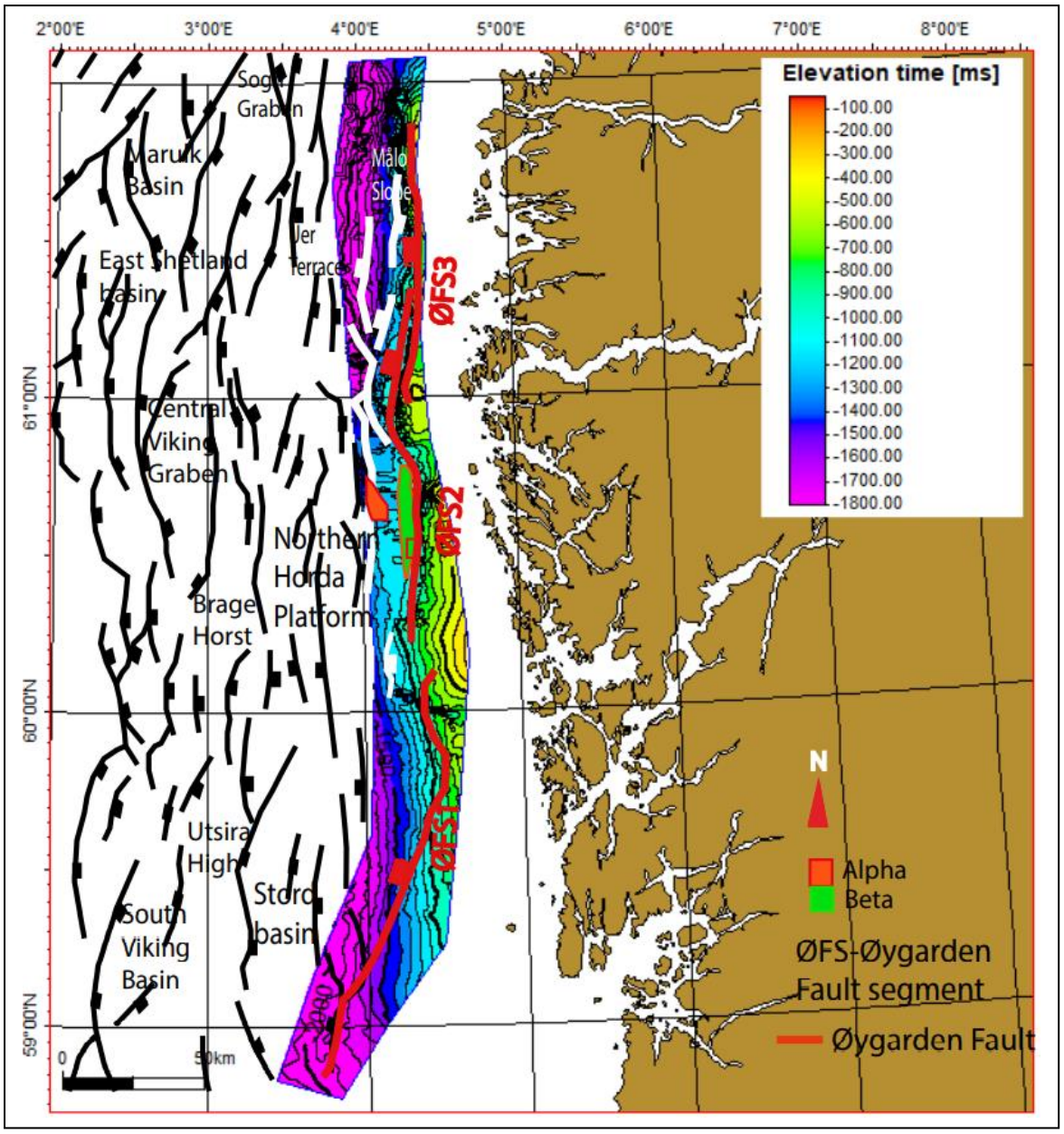

FIG 4.2E: TOP DRAUPNE SURFACE TIME STRUCTURE MAP SHOWS DEEPENING TOWRDS THE WEST, AND MORE DEEPENING OBSERVED IN NORTH AND SOUTH

4.2.5 Top Sognefjord group

To the west (offshore), like the surfaces above, the Top Sognefjord is characterized by low relief areas, both in the south and north. To the east, on the coast, the surface shows shallow values and is the shallowest in the central areas. In general, the surface deepens into the basin (offshore).

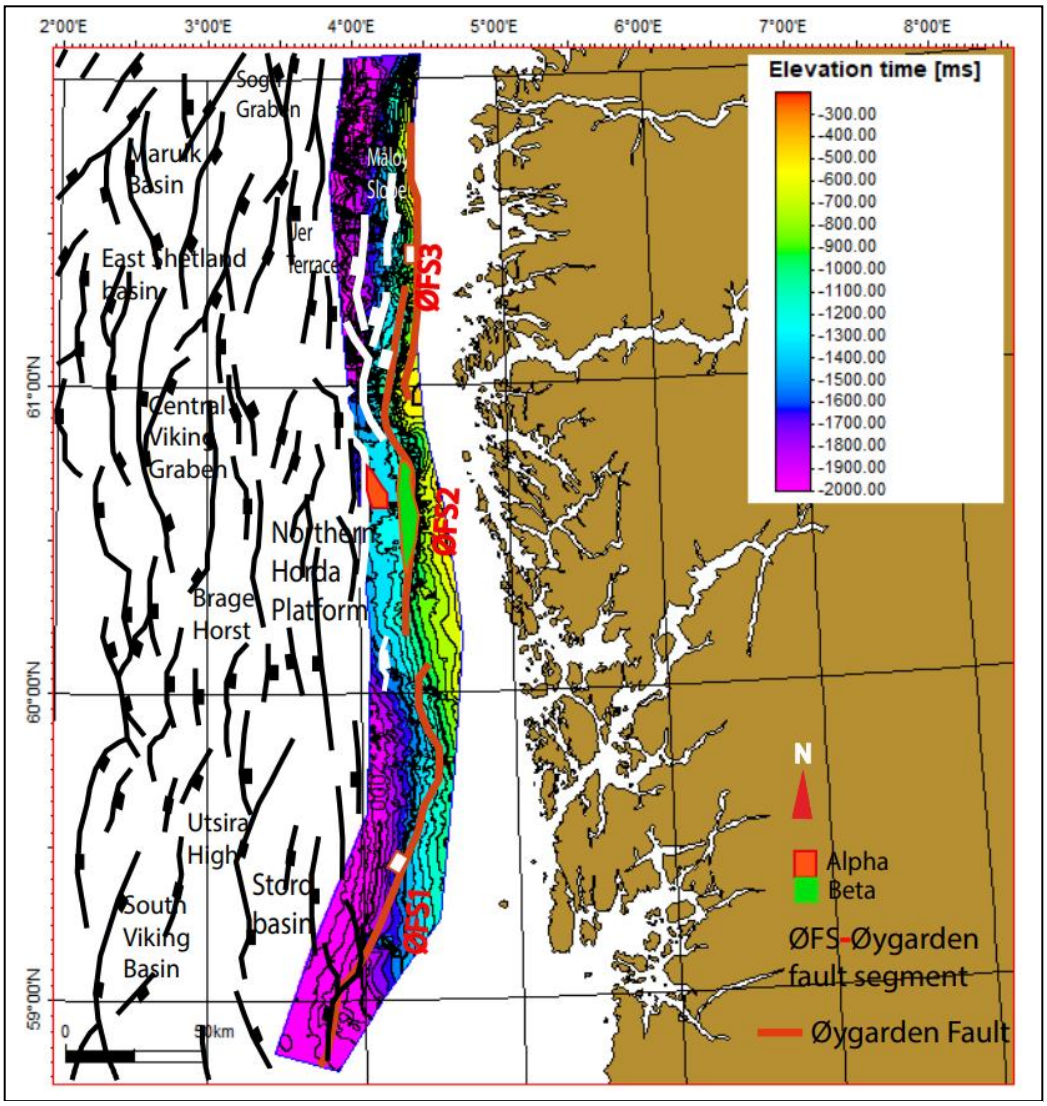

4.2 1 SOGNEFJORD TIME STRUCTURE MAP. NOTE MORE DEEPENING IN NORTH AND SOUTH AREAS

4.2.5 Top Brent surface

The Top Brent is generally characterized by shallow values (-100 ms) on the eastern areas along the coast, which generally deepen towards the west (offshore). Like the previous surfaces, the Northern (Måløy slope) and Southern (Stord basin) areas experienced much

more deepening (-2200 ms) when compared to the central areas (Fig..) with values of -200 ms.

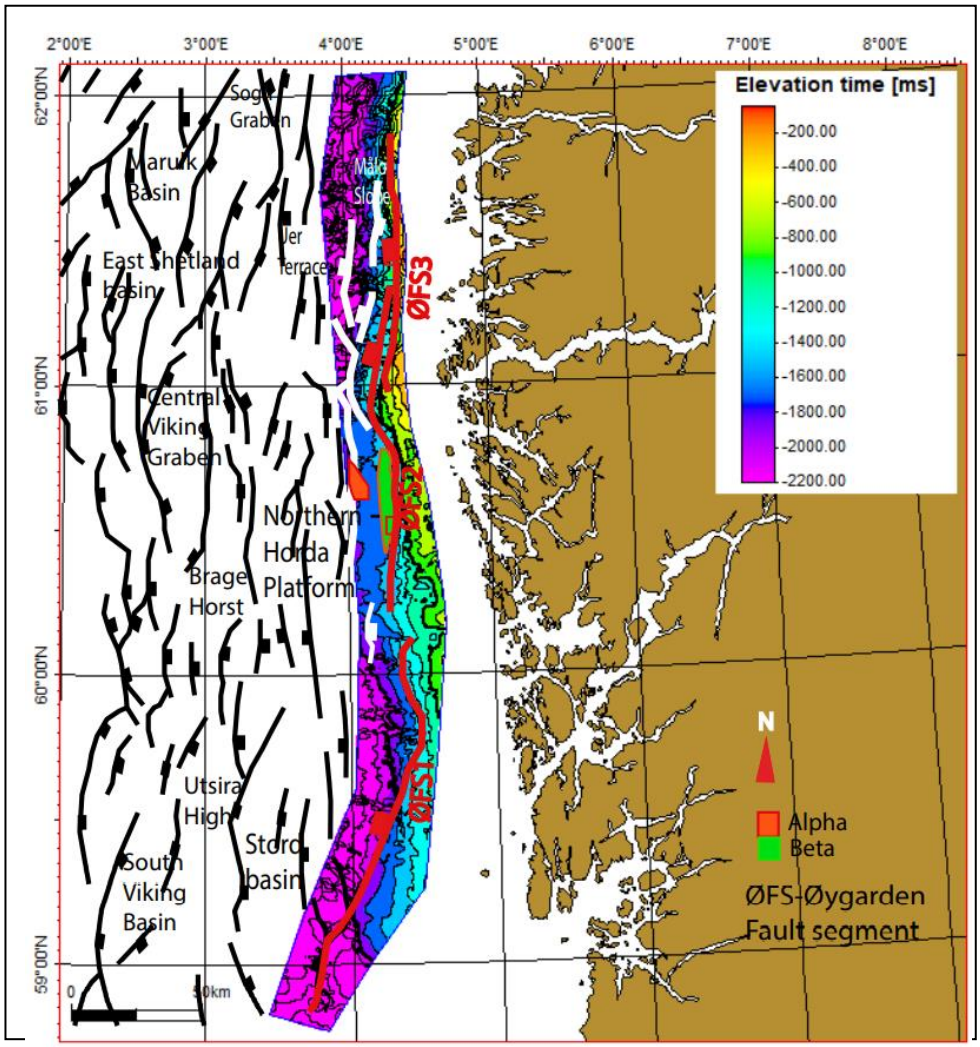

FIG 4.2F: BRENT TIME STRUCTURE MAP INDICATES DEEPENING IN THE NORTH AND SOUTH

4.2.6 Basement surface

The basement is picked on a positive peak reflector, that at times is discontinuous due to the data quality. Depending on the data set used, the reflector can be continuous and strong.

It is characterized by a general shallowness along the coast in the east, starting from the north to the south. On the west, however, a general deepening occurs into the basin (westwards), from north to south, including the central areas which retained high topographic relief in the previous surfaces. The basement surface is offset by the large Øygarden Fault, with quite large throws.

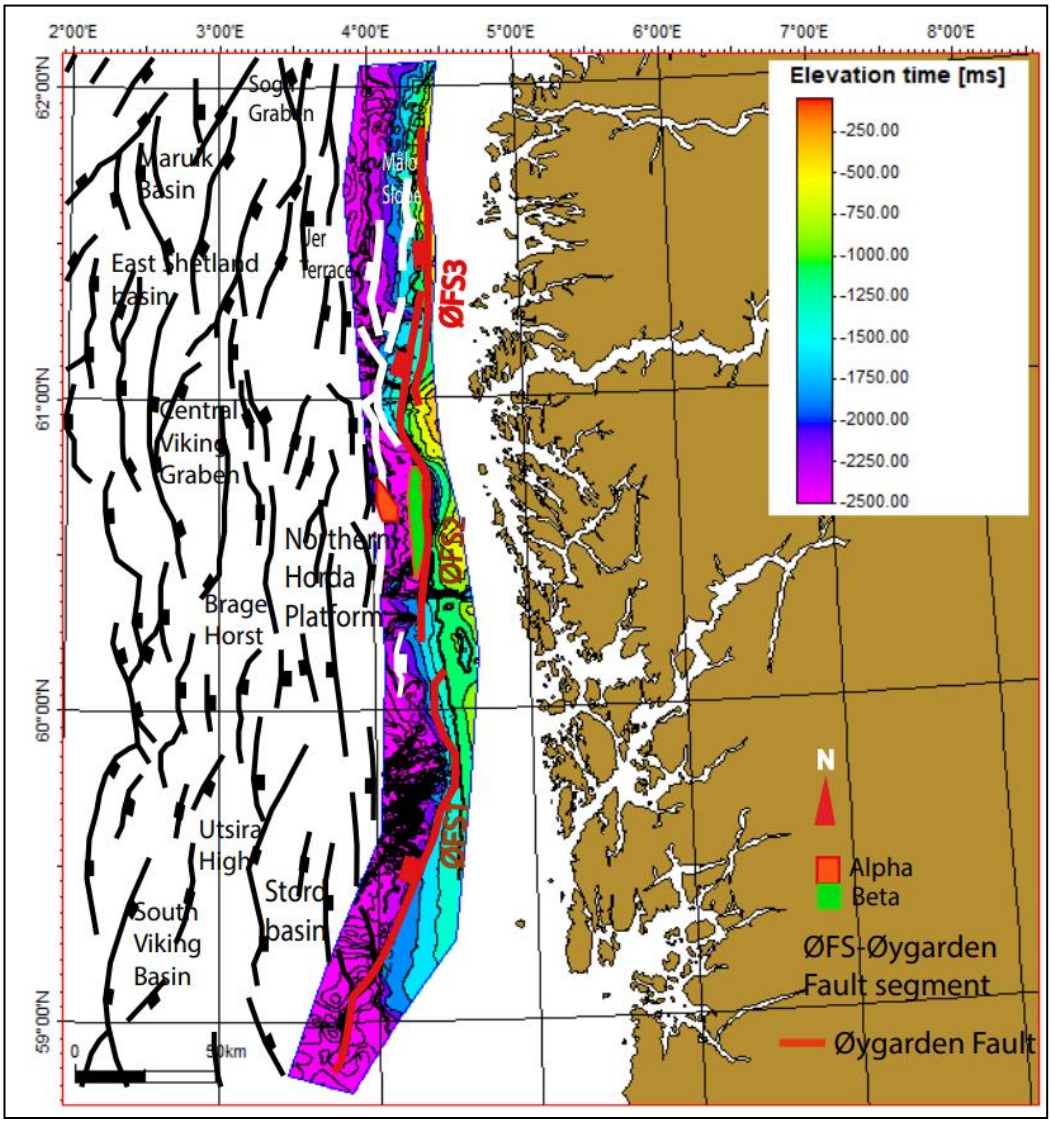

FIG 4.2G: DEEPENING TOWARDS THE WEST OF THE BASEMENT SURFACE

4.3 Thickness surfaces

The creation of thickness maps, for the above surfaces, was carried out. Normally, these maps record the shape, size, and location of fault-controlled depocenters through time. Time-thickness maps, created by calculating the difference in TWT between two horizons to track spatial variations in subsidence, are used to predict fault activity during those time intervals Directly and Quantitatively

Isochron maps is an indirect qualitative method of tracking spatial variations in subsidence, which is related to syn-depositional faulting (e.g., Bell et al., 2014).

4.3.1 Top Brent-Basement thickness

This unit is generally characterized by thinning along the coast in the east, and thickening towards the west i.e., from 200 to 1600 ms, consistent with previous regional studies. The general increased thickness westwards was related to uplift and westward tilting of the Horda Platform, when this group was being deposited. Based on the lack of thickening in the North, no evidence of fault activity is observed within the Måløy slope area.

The thickest depocenters with values up to 1600 ms and located within the central areas on fault segment ØFS2 trend in the N-S direction.

In the south, thick areas are also located on some portions (locally) i.e., lower, and upper sections of segment ØF1, with values of 1200 ms. The thickness variations in the South are sporadic, and not gradual (Fig 4.3a). The thickest depocenter may thus be related to fault activity during the evolution or sediment loading during the progradation build-up. The thinning may be interpreted to be associated with a lack of active faults, and thus no accommodation space was created. Some sporadic small areas of thickness related to minor fault activities are possible.

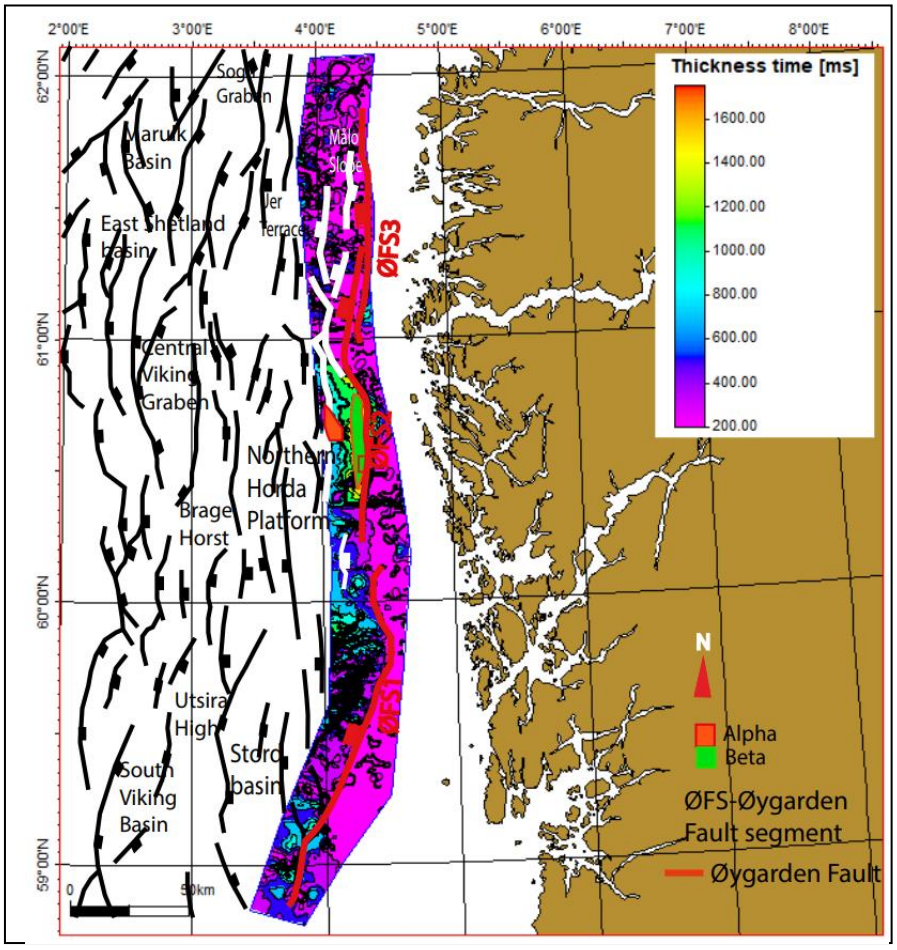

FIG 4.3A: THICKNESS MAP FOR THE BRENT-BASEMENT UNIT SHOWING A GENERAL THICKENING TOWARDS THE WEST. CENTRAL AREAS, WHERE BETA AND ALPHA PROSPECTS ARE LOCATED ARE MORE THICKENED. PORTION OF SEGMENT ØFS1 SHOWS THICKENED

4.3.2 Top Sognefjord-Top Brent thickness surface

The unit generally exhibits thinning, especially on the east, nearby/along the coast, and a relative thickening towards the west. Sporadically, much thickening of small depocenters may be exhibited in the northern areas, nearby the Måløy slope (values up to 900 ms), and somewhat in the central, with values in the range of 400-500 ms (Fig 4.3b).

The thickness is however not as prominent, when compared to the brent-basement units, and does not seem to be dependent on the fault activity.

Thus, this could be interpreted as a unit during which accommodation spaces is related to thermal relation and not faulting/tectonism.

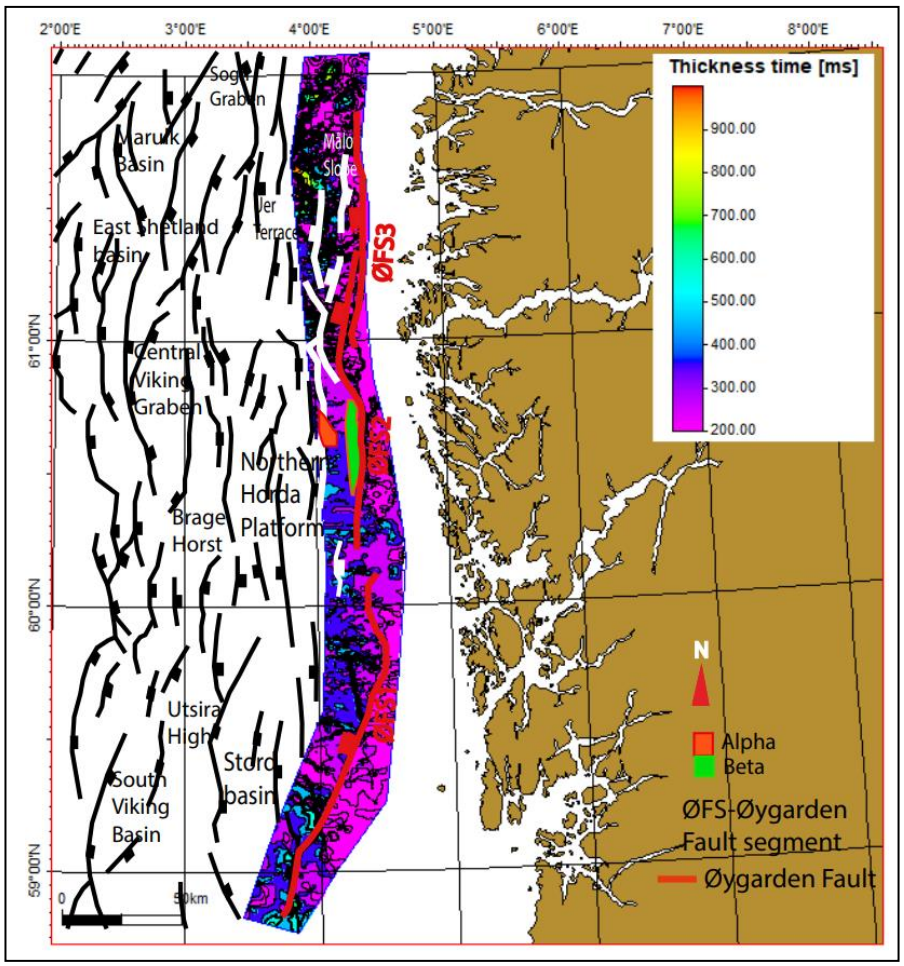

FIG 4.3B: SOGNEFJORD-BRENT THICKNESS MAP SHOWING A THICKENING WESTWARDS. IN TH ENORTH, SPORADIC THICK AREAS ARE NOTED. SAME OBSERVATIONS ARE IN IN THE SOUTH

4.3.3 Top Draupne-Top Sognefjord

The unit is bounded by the Sognefjord below and the Cromer Knoll above.

This unit may be divided into two, an area with extensive thickening in the south and the thinning areas in the north (Fig 4.3c). In the south, the thickness values are maximum at 550 ms, whereas in the North the lowest values are 100 ms.

Considering the observed seismic in which the unit shows no change in strata shape, the unit was deposited during a time when faut activities ceased. The thickening in the south is mostly related to subsidence and sediment loading, and nis ot primarily fault controlled. Moreover, the thickness is extensive, and not localized (Fig 4.3c)

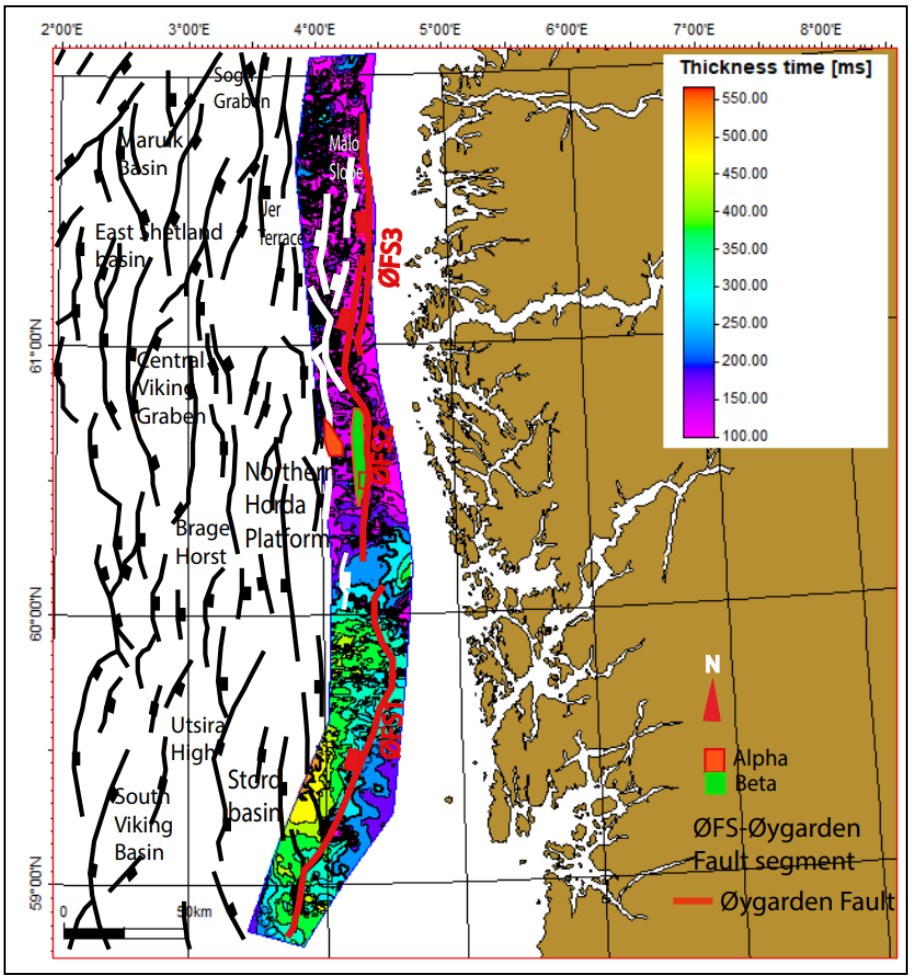

FIG 4.3C: THICKNESS MAP BETWEEN DRAUPNE-SOGNEFJORD UNIT SHOWING MORE THICKENING IN THE SOUTH, ESPECIALLY ALONG FAULT SEGMENT ØFS1, AND RELAY ZONE 1.

4.3.4 Top Cromer Knoll-Top Draupne unit

The cretaceous unit is comprised of Cromer Knoll, which is an early cretaceous unit.
This unit (Fig 4.3d) is characterized by a general thickening towards the west (offshore) and thinning in the east. The unit shows three areas where thickening is observed.
The thickening in the south is extensive and not necessarily localized to an individual fault.

In the central, on the other hand, thickening is localized to the fault segment 2 (ØFS2). Based on this, it is possible that fault activities were migrating, along the strike of the Øygarden. The extensive thickening in the south, however, was possibly caused by regional subsidence which continued through the Jurassic and possibly into the Cretaceous.

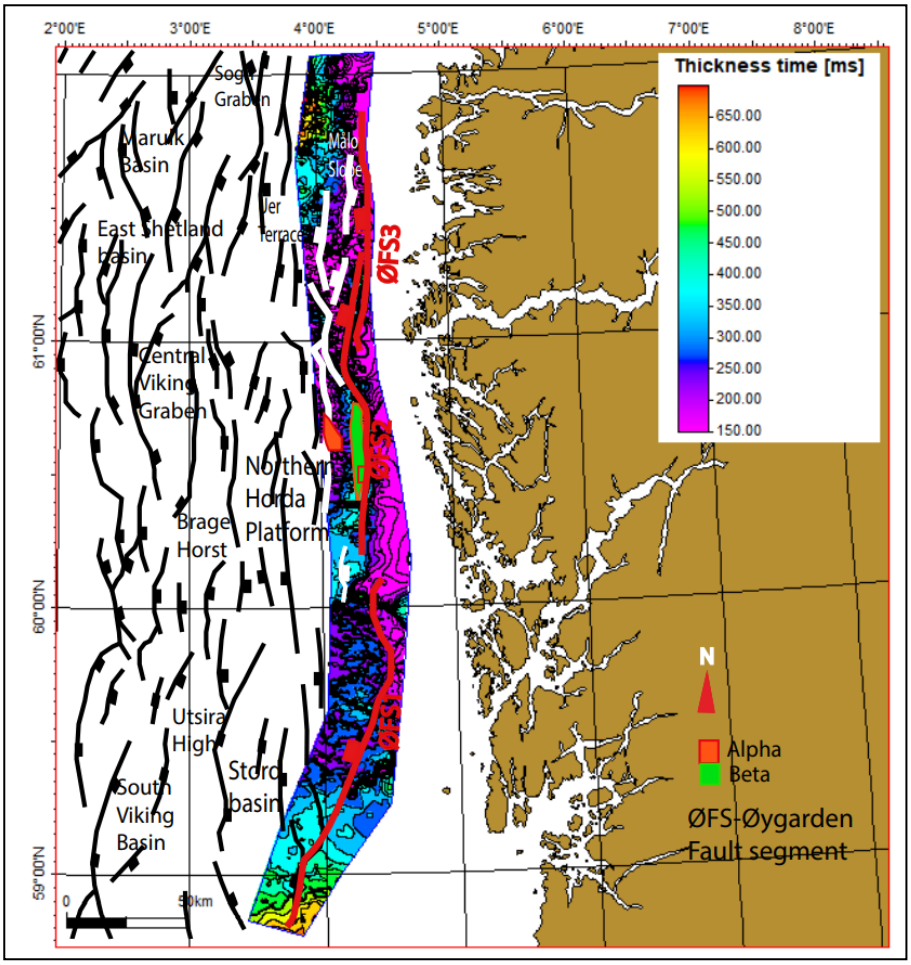

FIG 4.3D: THICKNESS MAP FOR THE UNIT BETWEEN CROMER KNOLL-DRAUPNE UNIT SHOWING MOST THICKENING IN THE NORTH, ON PART OF ØFS2, WITHIN THE CENTRAL AREAS AND FURTHER THICKENING SOUTHWARDS IN THE STORD BASIN.

4.3.5 Top Shetland-Top Crome-Knoll unit

The unit (Fig 4.3e) is generally characterized by thinning on the east, and relative thickening on the west. However, the thickening is not gradual, rather sporadically occurring in the central, and within the relay zones of the Øygarden Fault segments (ØFS1), in the south and ØFS 2 in the central. In the north, thickening occurs further in the west, albeit sporadically, and away from the Øygarden Fault.

In the central, and especially the lower tip of segment ØFS2, and on the upper tip of segment ØFS 1, the thickening is most likely controlled (locally) by the faulting activities. We can therefore infer that during this period, thickening was also much concentrated in the central areas, albeit the lack of growth strata evidence in the seismic to corroborate fault activity.

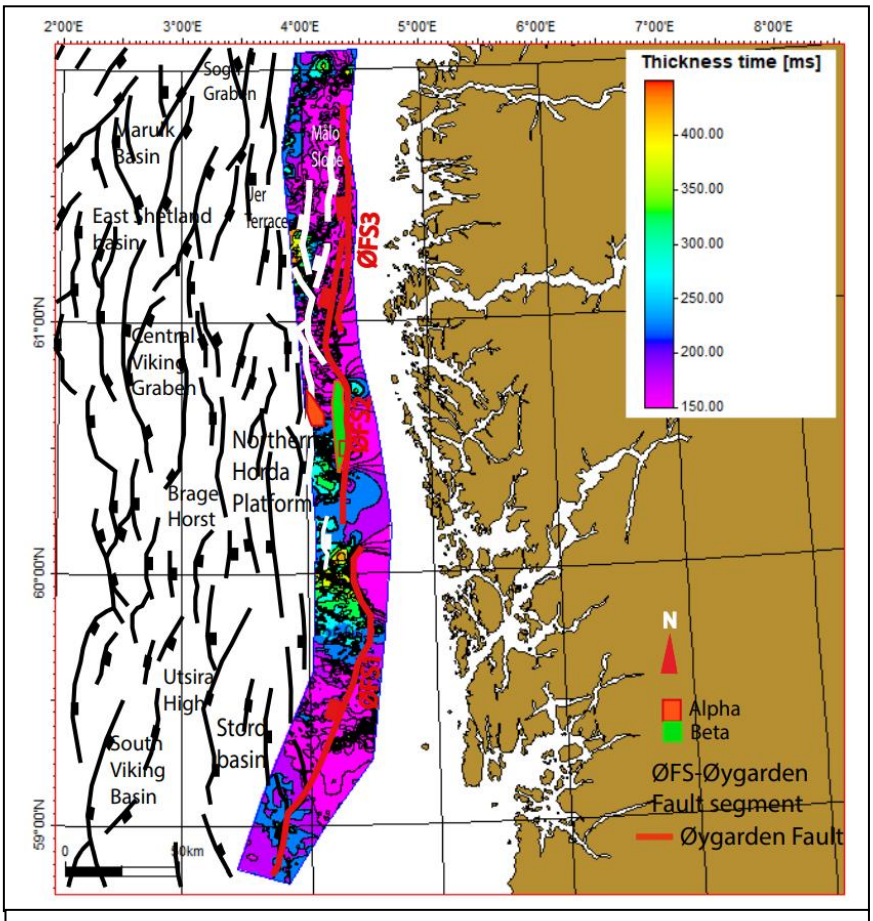

Fig 4.3e: Shetland-Cromer Knoll unit shows sporadic thickening. Note thickening on the topmost tip of segment ØFS1, and partly on lower portion of segment (ØFS 2). Thickening sporadically noted in the Måløy slope

4.4 Structural description

4.4.1 Visualization, Geometry, and orientation of the Øygarden Fault Complex

The Øygarden is a west-dipping major, segmented fault, extending from the stord Basin in the south into the Måløy slope in the north. It bounds the Horda Platform in the east and dips to the west.

The geometry of the fault is planar, appearing straight up dip to almost perpendicular, but may decrease in the dip at depth, forming almost a listric fault. The Øygarden segments are generally curved, with ØFS2 showing a kink geometry.

In general, the Øygarden Fault is made up of 3 main segments, namely ØFS1-ØFS3.
The 3 segments, as observed in (Fig 4.4a, b), and they measure as follows; ØFS1 in the south is approximately 140,7km, ØFS2 (center) measures approximately 138,8km, and, lastly, ØFS3 (extreme north) measures approximately 116,2km.

Fault segment ØFS1 bounds the eastern margin of the Stord basin, it is curved and oriented in the NE-SW direction (Fig 4.4a, b). At the tip end, towards the north, however, the segment ØFS1 curves to almost an N-S direction. In general, the geometry of the fault segment is described as curved.

In the central, the second segment ØFS2 is oriented in the north-south (N-S) direction. However, its tips curve to an almost NW-SE, and then back to an N-S direction, and it eventually tip-off. The nature and curving geometry of this segment (ØFS2) seem to indicate(suggest) two curved fault segments that formed through the linkage process.

The third segment (ØFS3) is oriented in an almost a North-South direction but as well shows curve-like geometry at the tips (Fig 4.4a, b). This segment starts within the central Horda Platform and extends towards the north within the Måløy slope. The fault geometry of the Øygarden Fault complex could give information about the propagation and linkage process during the entire development of the fault.

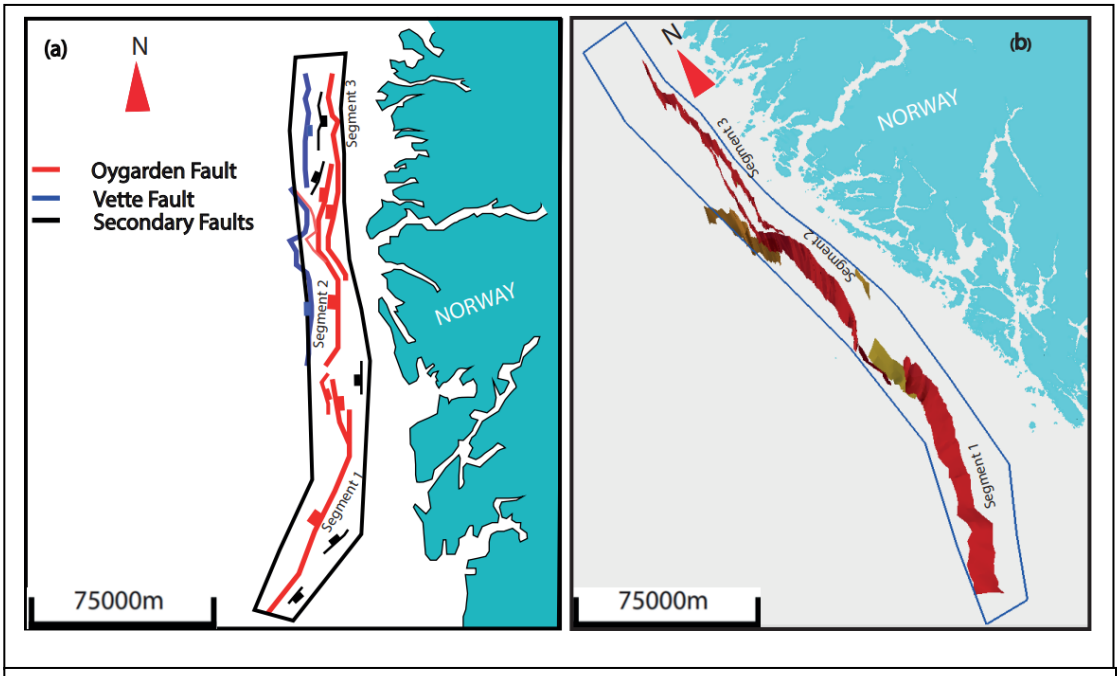

Fig 4.4: 2D (a) and 3D (b) overview of the main Øygarden and associated secondary faults

4.4.2 Variations in fault Geometry along strike

The main cross-sectional geometry exhibited by the Øygarden fault, starting in the south where the fault segment is more listric, with high dips up-section but decreases in dip downwards into the basement.

In the northern part, within the Måloy Slope, a system made of small depocenters is observed. The bounding faults to the depocenters are NW-SE-oriented bounding faults, which do or do not extend into the basement. The depocenters can be described as down-stepping towards the southwest, and mostly oriented in the N-S direction (Fig 4.5a). Additionally, there is absence of large basin bounding faults, which are characteristic of the northern North Sea and Horda Platform.

In the central areas, on the other hand, the Øygarden shows high dips, forming as a planar up-section but decreases in dip down-section as it extends into the basement. In the north, the segments are more planar, and dip towards the east.

In the middle/central Horda Platform area, on the other hand, large basins bounded by the Øygarden main fault on the east, and the main Vette Fault to the west can be observed. The Øygarden and Vette faults exhibit listric nature, extending into the basement, and therefore are a first-order fault (Fig 4.5b).

In the south, near the Stord basin, a horst and graben system are observed, for example **(**Fig 4.5c**),** formed by two main bounding faults, one dipping in the west and another in the east.

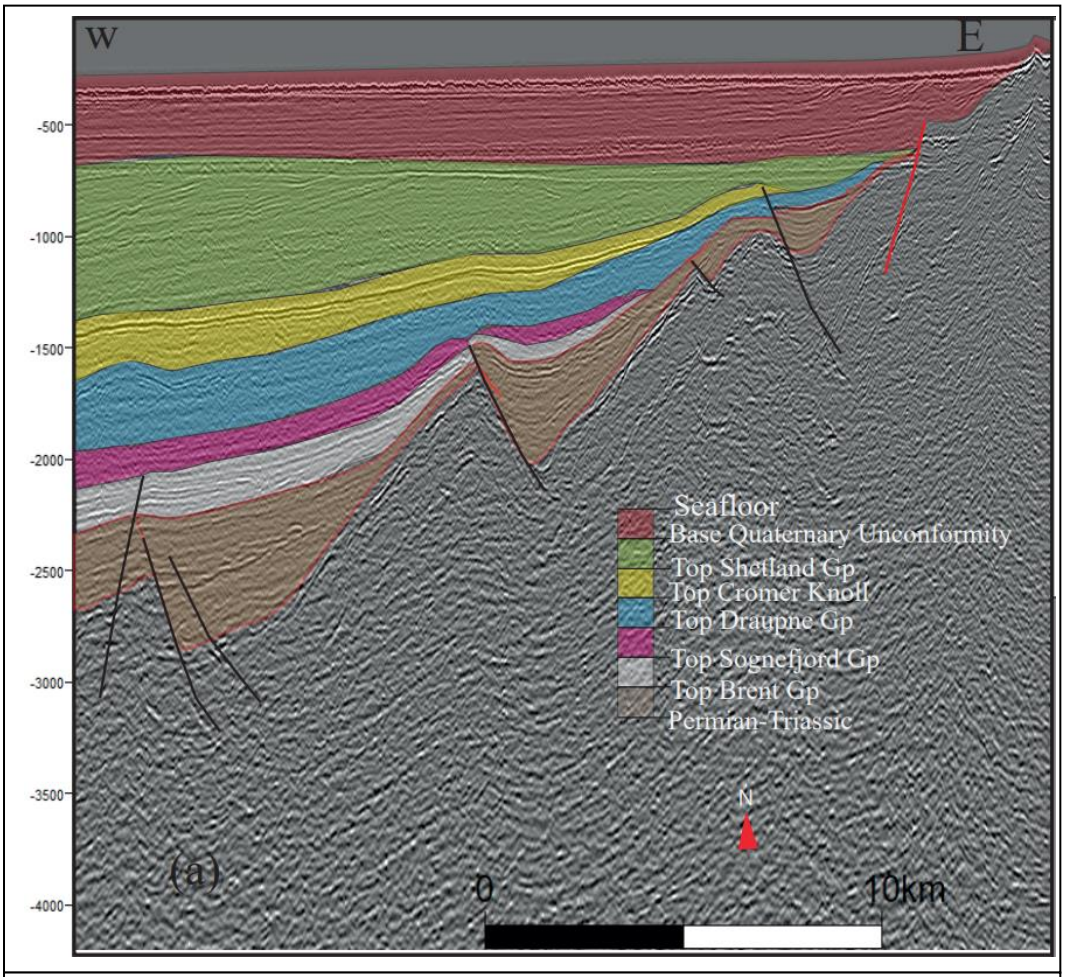

Fig 4.5a

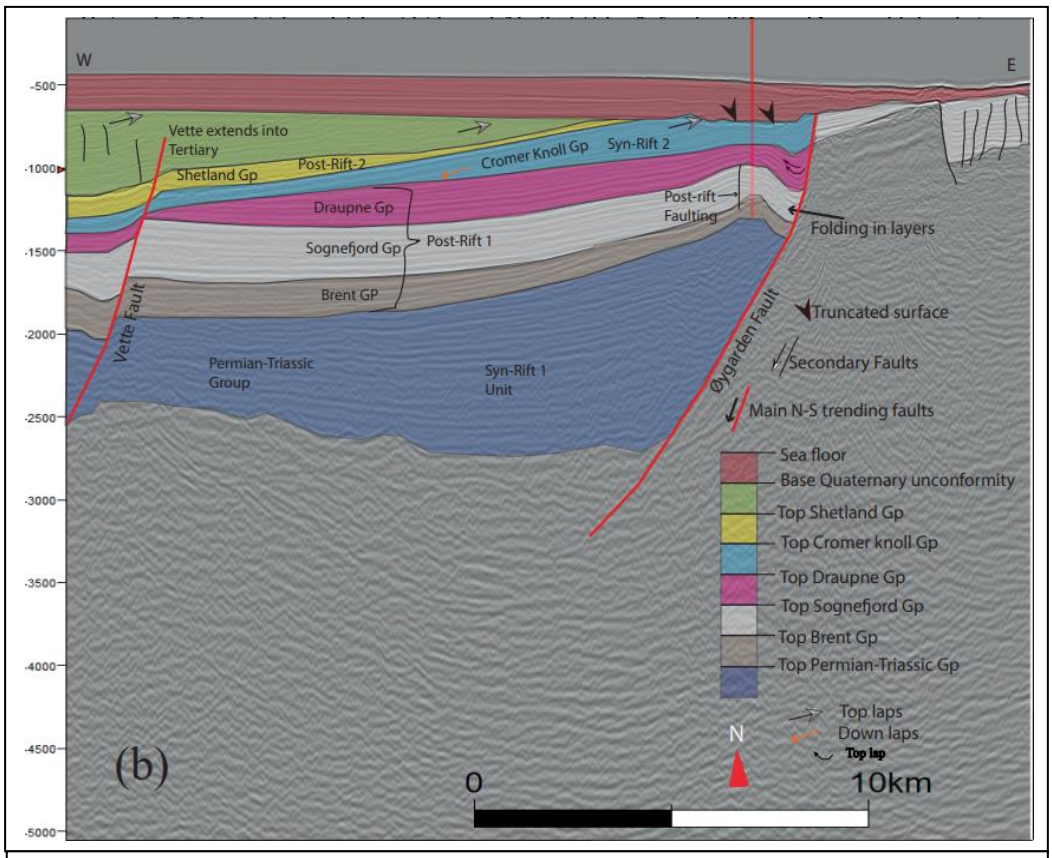

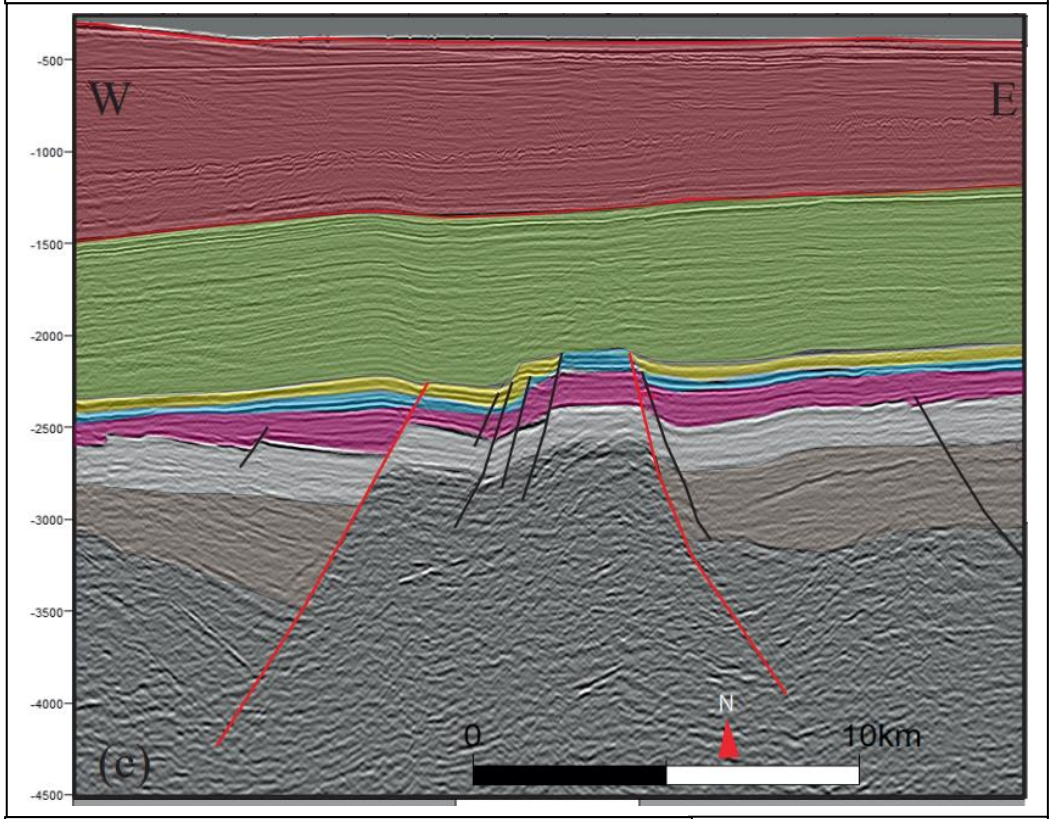

Fig 4.5: Down-stepping depocenters bounded by NE-SW trending faults. Central basins bounded by listric N-S trending large faults (b). Horst and graben system in the south (c). Note folding within the Jurassic units, near the Øygarden Fault. Downlapping and onlapping strata (see Fig 3.0, for the location of the figures)

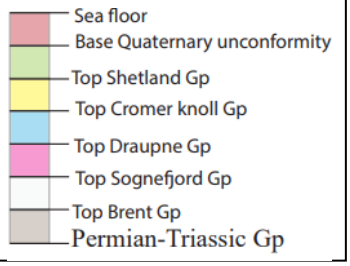

4.4.3 Fault interaction

In terms of fault interaction, the faults in the study area range from listric for the main Øygarden, although in some sections, planar rotated fault blocks are observed, and do not interact or link (Fig 4.6a). The most common interaction style is in the form of splay faults, observed bifurcating off the main Øygarden Fault, (upward propagating splays). However, where the segments tip-off and sidestep, small faults are observed associated with the relay zones (see 3D Fig 4.4b) for linking small faults to the main Øygarden fault segment. Fault interaction styles are important because these may help when interrogating the propagation of the main overall fault segment.

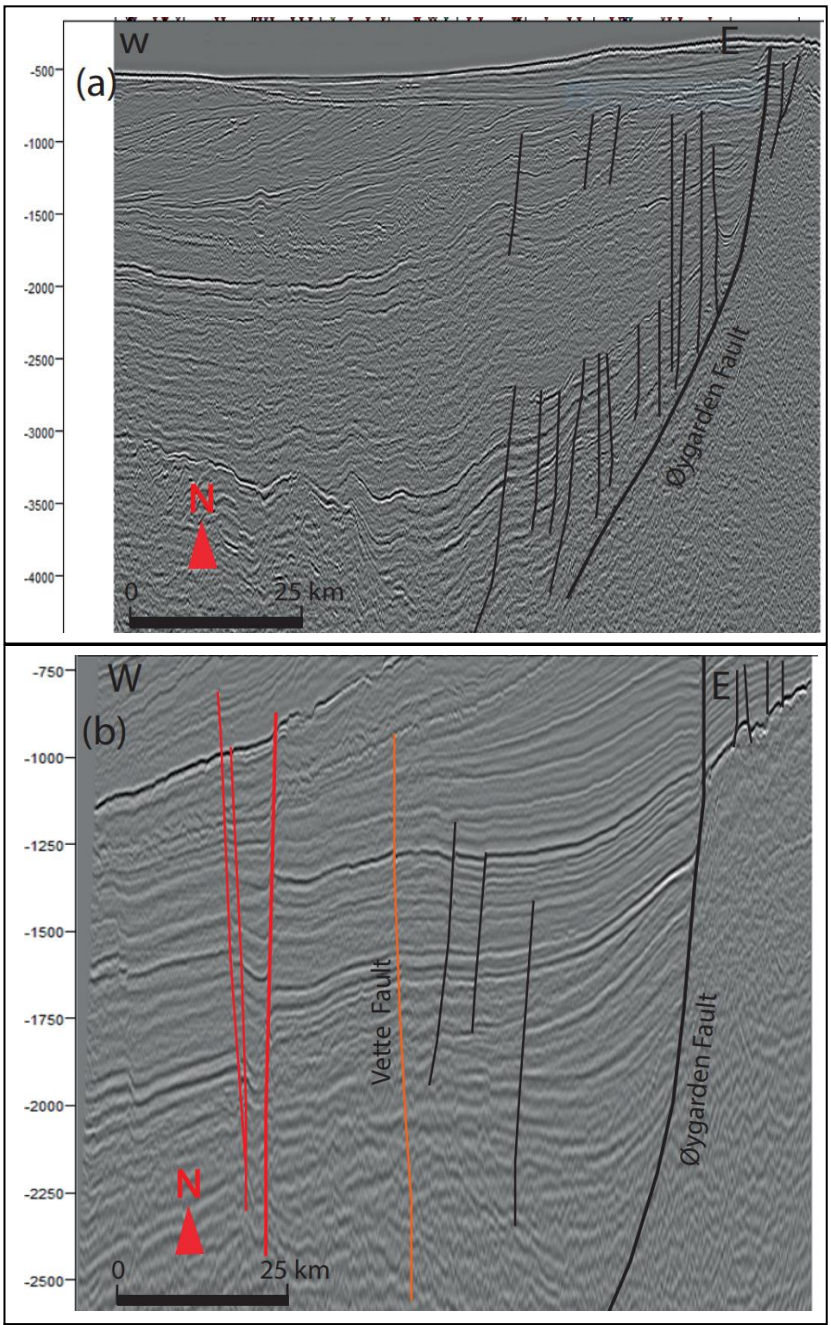

Fig 4.6: Splay fault (a) bifurction off the main Øygarden. Note the listric nature of the Øygarden, with a decrease in dip downwards into the basement. Isolated planar geometry (most prominent style).

4.4.4 Fault density

In addition to the 3 main Øygarden Fault segments, other associated faults segments are noted. Øygarden Fault segment 3 (ØFS3) shows the highest density of secondary faults, associated with it. This is followed by Øygarden Fault segment 2 (ØFS2), and finally segment 1 (ØFS1), which doesn't show many more secondary faults. The secondary faults in the North are oriented in the NW-SE direction and dip towards the east, contrary to the Øygarden (Fig 4.5b), which trends in the N-S, decreasing in throw into the basement, and dips towards the west. The change in orientation of the secondary faults and tthe kind of basins formed (see Fi 4.5a) may give information about strain change or influence of basement structures on the evolution of the Horda Platform.

Three fault interaction areas are noted to show relay zones, namely relay zones 1-3 (Fig 4.7). The 3D fault density map aids in the visualization of density and interaction of faults. At the Øygarden Fault segment 1 relay zone, we can note a possible damage zone, in which secondary faults occur (deformation zone). The density fault map gives information about possible connectivity and communication in reservoir.

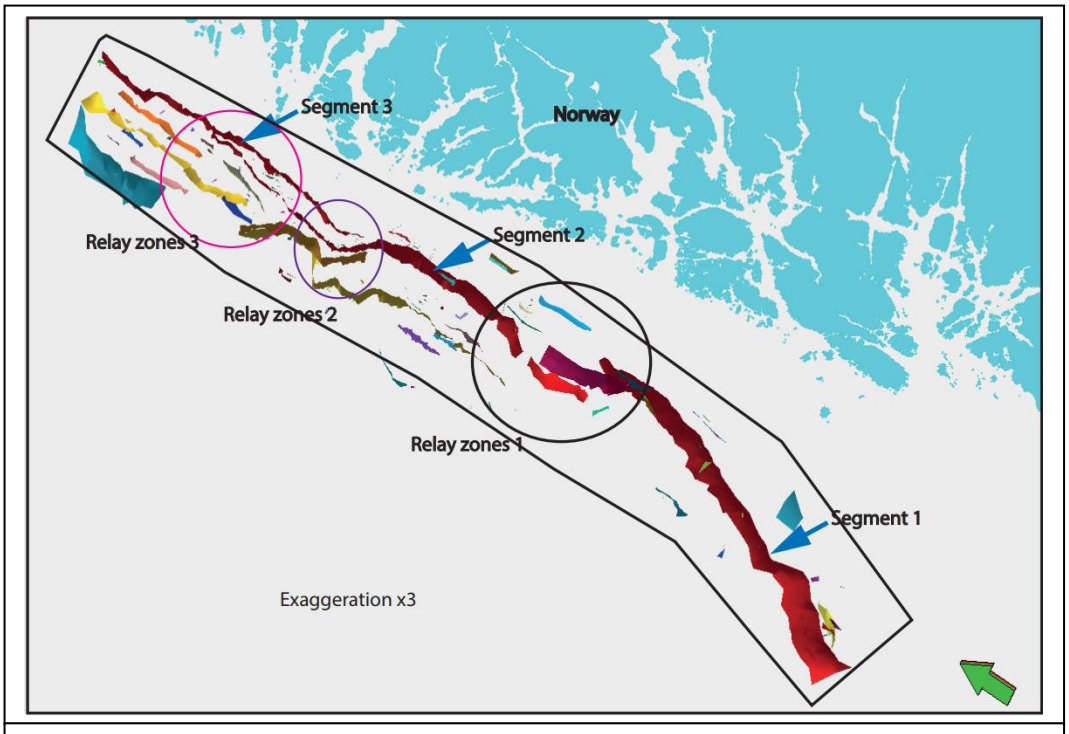

Fig 4.7: Main Øygarden Fault segments, relay zone and associated secondary faults. Note the high density of faults in the northern Horda and further north in the Måløy slope.

4.4.5 Throw-distance and Depth-Throw analysis

When working with seismic data, it is not easily possible to discern indicators of the displacement vector such as groove marks. In addition, with the difference in scale between the horizontal and vertical axes, the throw is used as a proxy for fault displacement (Whipp et al., 2014). The throw-distance plots are plotted for the main Øygarden fault segments, and the depth-throw plot is made for the Vette Fault to understand fault evolution. Fault throw for a particular horizon against the distance along the fault, are used to study the growth and linkage of fault systems (e.g., Peacock and Sanderson 1991; Deng et al., 2017).

Displacement analysis was carried out along the strike of the entire segmented Øygarden Fault (South to North to orientation). Three throw-distance plots for the Øygarden Fault segments, Fault segment 2, and, the Vette exhibit multiple variations, which depict different oscillations, in which either minima or maxima are noted.

4.4.5.1 Øygarden Fault segment 1

The displacement plot for segment ØFS1 shows 5 main maxima throws of 700 at (I), 600 at (II), 690 at (III), 900 at (IV), and 660 at (V), all in ms/(TWT) respectively. These are separated by four main minima throws, marked by star (*). Segment ØFS1, therefore, shows variations in throw with distance, although a general decrease of throw with distance is noticed.

This kind of increase to decrease and repetition of the same are interpreted to imply fault segment that initiated, and propagated through the linkage process into a fully recognized size and geometry we observe now (Fig 4.8a, blue).

4.4.5.2 Øygarden Fault Segment 2

In general, segment 2 doesn't show a large abrupt increase and decreases in throw with distance. The most notable maxima are marked with yellow squares. The maximas are about 560 at 200 km, 500 at 225, and 470 ms at 290 km (Fig 4.8b, orange curve), however, the minimas are markedly less pronounced compared to those in ØF1. Moreover, ØFS 2 doesn't show large throw values such as the observed in ØF1. The lack of large variations in a throw during propagation of this segment, therefore, indicates a proportionally same amount of strain was experienced.

4.4.5.3 Øygarden Fault segment 3

Segment 3 overlaps and starts at segment 2, an indicator that these two fault segments are in communication, possibly as splay or linking. Similar to Øygarden Fault segment 2, this

segment doesn't show big differences in throw maxima and minima and only small variations which oscillate a lot. Multiple small oscillations, minima of 289 ms (TWT) at 246 km, and maxima of 633 ms (TWT) at 246 km (Fig 4.8b) are observed.

Towards the tip end of the second ØFS2 segment, towards the East, throw decreases, forming minima. At this point, segment ØFS3 joins, and propagates. The strain within the area of linkage between ØF2 and ØFS3 was transferred through small fractures and faults or the folding of layers process.

The presence of interpreted points of maxima, also known as nucleation points (VI)-(IX), imply that this fault segment was initiated, and propagated through the linkage process, to eventually forming what we observe as segment ØFS3, which eventually accumulated the total displacement and length we observe (Fig 4.8a, green).

An abrupt decrease in throw, at the point where segment 3 joins and starts at segment 2. This abrupt decrease could be a fault branch line, and thus segment 3 is just a splay of the main segment 2

4.4.6 Depth-throw plot

To understand the timing of fault activities, depth-throw analyses were carried out. These give information about the vertical propagation history of the faults (e.g., Deng et al., 2017). The Vette fault and two Øygarden Fault segments (Fig 4.8c) were considered for depth-thow analysis. The generated T-z plot (Fig 4.8d) shows a general increase in the throw with depth in all three Faults. However, variations at different ages as the fault propagates upsection may be observed, e.g., in segment Øygarden fault, there is a decrease in throw from the basement into the Brent, which means a decrease in fault activities upsection. A slight increase in throw is then observed, for the unit between Brent and Sognefjord. This increase points to a reactivation of the fault during this unit. The reactivation, however, isn't corroborated with seismic interpretations, which, show relatively uniform, parallel, and non-wedging tabular strata (Fig 4.1b). In the Cromer-Knoll, a decrease in throw towards the surface occurs. A slight increase in throw between Cromer Knoll and Shetland is then observed. The increase between Cromer Knoll to shetland is related to sny-rifting phase 2, which has been augmented further by the thickening package in the unit (e.g.Fig 4.1b). A similar trend of throw variations on the Øygarden fault is observed for the Vette fault. However, at the Vette F3, the throw variation between the Cromer Knoll and Shetland continued to decrease, implying that within this unit, the Vette fault faut activities ceased, and did not continue, contrary to what is

observed with Øygarden. Segment F2 (Fig 4.8c) (splay off the Øygarden?), also shows a general increase in throw with depth (Fig 4.8d). However, F2 does not show the reactivations observed in the Øygarden and the Vette above.

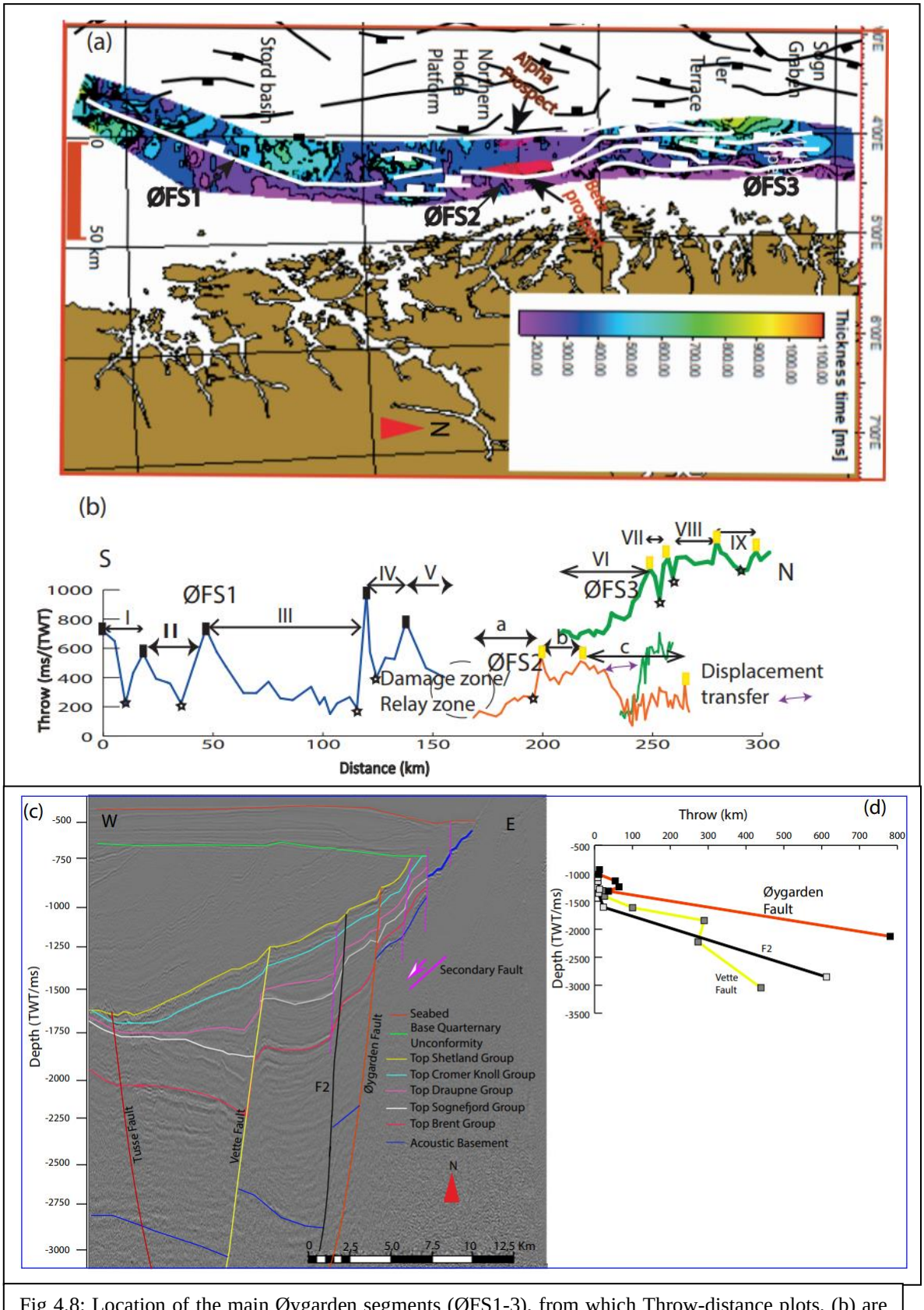

Fig 4.8: Location of the main Øygarden segments (ØFS1-3), from which Throw-distance plots, (b) are calculated. (c) The seismic section shows the location of the segments on which the Depth-throw (d) is plotted. X-IX indicates linking small segments that are linked to form the present large segments. Rectangular shapes are maxima points, and the star shapes indicate throw minima.

Chapter five

5.0 Discussion and conclusions

5.1 Evolution of the Øygarden Fault

The evolution of the Øygarden Fault is derived primarily from the patterns of growth strata and associated deformation/fault geometries. These were corroborated further with Throw-distance and Depth-throw plots (Fig 4.8b, d). The strata were divided into syn-rift 1, syn-rift 2, and post-rift phases, as shown in the interpreted seismic section (Fig 4.1b).

Using thickness maps of key intervals, it is possible to identify fault-controlled changes in sediment thickness while the absence of the across-fault thickening indicates periods of inactivity (Deng et al., 2017; Mulrooney et al., 2020; Fazlikhan et al., 2020; Wu et al., 2021; Pan et al., 2021; Wang et al., 2022). Thus, from the corresponding thickness map (Fig 4.3a), we infer that during the Permian-Triassic Period, slip on the Øygarden Fault Segment 2 (ØFS2) controlled the observed thickening in the hanging-wall of the Øygarden in the center of the study area (Fig 4.3a). This is consistent with previous interpretations that the main depocenters were in the northern Horda Platform and the Stord basin (e.g., Phillips et al., 2019; Fazlikhan et al., 2021). During the initial rifting phase, the strain was focused on the center of the north sea, i.e., the rift axis centered underneath the Horda platform and stord Basin (e.g., Færseth, 1996; Ravnås et al., 2000; Whipp et al 2014; Bell et al., 2014; Duffy et al., 2015; and Mulrooney et al., 2020). The area, therefore accommodatedated maximum strain, and the observed large depocenters are mostly related to the displacement accrued on the active faults.

The depth-throw plot (Fig 4.8d**)** agrees that the Øygarden Fault segment, and indeed the Vette, another major N-S basin bounding fault accrued maximum throws within the Permo-Triassic period. These major faults nucleated in the Permian-Triassic, during what is termed rifting phase 1, consistent with other studies (Mulrooney et al., 2020; Wu et al., 2020; Whipp et al., 2014; Bell et al., 2014; Fazlikhan et al., 2017; 2021).

During the Permian-Triassic, the thickening noted further South is localized in the hanging wall of a small fault segment (Fig 4.3a), which later became hard-linked to form the present-day ØFS1. This kind of localized fault-controlled thickening of the Øgarden Fault, developed first by linkage of isolated small segments, which eventually resulting in what we observe as the present ØFS1. In their study, Fazlikhan et al., (2021) infer that the observed thickening is

associated with displacement on their ØFS5, which in our study, corresponds to the small segment (i) (Fig 5.1).

In the north, the lack of thickness variations across the Maløy slope is related to the lack of an active Øygarden fault segment during the Permian-Triassic rifting. This is consistent with onshore studies that propose that the first phase of rifting was not significant within the Måløy slope area compared with the Horda Platform (e.g., Fossen et al., 2021; Bauck et al., 2021).

The Sognefjord and Brent units (Fig 4.3b) were deposited during the middle/Late Jurassic period. The seismic data (Fig 4.1C), shows that these units do not exhibit lateral variations in facies, neither shows growth strata towards the Øygarden Fault. The lack of variations in strata implies uniform deposition occured when there was little or no fault activity, after cessation of fault activity on the main ØFS. Thus, a post_rift phase1 is inferred for these units. This is supported by the thickness map (Fig 4.3b) which does not show much variation in the thickness of the strata across fault.

Where small thick (800-900 ms) depocenters exist, for instance in the north (Fig 4.3b), these were possibly related to small fault activities which are infered and are prominent during the Jurassic (e.g., Råvnås et al., 2000; Wu et al., 2021; Baucke et al., 2022; Fazlikhan et al., 2021). In our study, this is supported by an increase in throw on the Depth-Throw plot (Fig 4.8d).

In the central area around the Horda Platform, the thickness map does not show much variation, confirming that at this time, the segments ØFS2 and southern segment ØFS1 were not active.

In the north, the sporadic occurrence of small, localized thick depocenters is related to the various east dipping fault-bound segments that were possibly active at the time. This however is speculative.

Like the Sognefjord, the Draupne unit deposited in the Jurassic, exhibits a lack of lateral growth in strata towards the Øygarden (Fig 4.1b) in the central segment of the margin. However, the thickness map shows that the southern part is highly thickened, with values up to 550 ms compared to the central and northern area. The thickening in the south is quite laterally extensive, rather than localized and does not seem to be associated with any specific fault. The lack of indicators of fault movement imply that the observed extensive thickening was possibly driven by regional subsidence, and sediment loading, consistent with

observations by several authors (e.g., Bauck et al., 2021; Gabrielsen et al., 2001; Råvnås et al., 2000). However, since the observed thickening is localized to a small portion of ØFS1, it is possible that it related to activity on the very first segment that linked to the observed ØFS1. Thus, fault controlled subsidence was experienced, albeit locally (e.g., Fazlikhan et al., 2021). This is possible because the second phase of rifting has been reported to start in the middle Jurassic, with specific emphasis to the Draupne (Wu et al., 2021; Mulrooney et al., 2020).

The Brent, Sognefjord and Draupne units therefore form a post_rift 1 phase widely referred to by several authors (Fazlikhan et al., 2020; Råvnås et al., 2000; Whipp et al., 2014; Deng et al., 2017; Mulrooney et al., 2020), but experienced episodes of inter_rifting (e.g., Råvnås et al., 2000).

The Cromer Knoll unit was deposited during the Early Cretaceous, and, forms the center of the main second phase of rifting (e.g., Bell et al., 2014; Phillips et al., 2019; Fazlikhan et al., 2017; 2021; Mulrooney et al., 2020, Wu et al., 2021; Bauck et al., 2021; Osmond et al 2021). This augument for the second phase of rifting is supported further with observed growth strata towards the Øygarden Fault (e.g., Fig 4.1b). The thickness map (Fig 4.3D) shows a drastic thickening of the unit, both in the north (Måløy slope), in the central Horda Platform, and to the South, in the Stord Basin. Previous studies determined that during the Late Jurassic and early Cretaceous, the main thick-skinned normal faults inherited from the Permian-Triassic Phase were reactivated (e.g, Fazlikhani et al., 2021; Bell et al., 2014; Phillips et al., 2019; Osmond et al., 2021). This reactivation is responsible for the observed thickening, and the growth strata observed indicate syn-tectonic activity. One could therefore be tempted to conclude that at the time, the entire Platfrom and all the three fault segments were active.

In the Måløy Slope area to the North, far away from the segment ØFS3, the observed thickening does not appear to be related to the Øygarden segment 3 (ØFS3). Instead, the thickening is related to the activity in the Sogn Basin, which is said to have subsided with the deposition of sediments during the Cretaceous period (e.g., Bauck et al., 2021). This unit, in addition, experienced erosion on the eastern part, where the large section shows truncations and an undulating surface (Fig 4.1b). This happened when the footwall crests of tilted fault blocks were subaerially exposed (e.g., Færseth 1996; Gabrielsen et al., 2001). The erosion of such structural highs, resulted in several onlap relationships and unconformities such as Base Quaternary unconformity (BQU) (Fig 4.1b). The Base Quaternary Unconformity was formed

due to regional uplift associated with glacial rebound, when the Norwegian channel Ice Stream, eroded a significant poportion of the early Pleistocene sediments, and the older strata across the continental shelf (Batchelor et al., 2021).

Much as the Late Cretaceous units have presumed to be areas of post rift phase 2, in which case, the subsidence was mainly through thermal relaxation, some fault activy continued even after the early Cretaceous, as evidenced by thick depocenters of the shetland Group in the central area of the Horda Platform (Fig 4.3E**).** The thick depocenters are localized to portions of fault segment ØFS2, which imply that a part of this entire segment was active.

Subsidence due to thermal relation continued through the Tertiary to the Base Quaternary (Whipp et al., 2014; Mulrooney et al., 2020). During the Tertiary, most of the large displacement N-S trending faults activities had ceased or atleast the faults were burried by recent deposits. However, Polygonal faults and pockmarks on the seaflor have been mapped in the Tertiry units (e.g., Mulrooney et al., 2020; Wrona et al., 2017), and these faults were related to a second phase of rifting. Moreover, there was a change of extension direction during the deformation resulting in the polygonal faults (Mulrooney et al., 2020; Wrona et al., 2017).

Based on the evolution of depocenters, therefore, it is evident that the fault activity started in the Permian-Triassic rift phase (RP1) and continued intermittently through to the middle Jurassic to the early Cretaceous rift phase (RP2). Fault activity, in combination with further regional subsidene controlled the thickness patterns observed (Fig 5.0), and that strain localization dominated the basin development (e.g., Cowie et al., 2005).

5.2 Fault growth and propagation.

In a single rifting phase, three stage of fault growth have been proposed based on field and numerical observations. These include (a) initiation, (b) interaction and linkage and (c) through-going faults zones (e.g., Childs et al., 2003; Cowie et al., 1995; 2005; Deng et al., 2017). In stage (a), short and small displaced normal faults initiate in the earth crust. During this stage, the faults are isolated from each other without interaction. With conituned strain accumulation in stage (b), fault tips propagate radially. Stress feedback between segmenst influence their growth as faults tips grow closer to eacher. In stage (b) still, linkage may occur and deformation begins to be localized along a fem major faults. In the final stage (c) i.e., the through-going fault stage, continued strain localization alomg major faults result in depoceneter developmet. We propose that the observed fault segments ØFS1-3 underwent

same processes of initiation, linkage and eventual growth as through-going fauls. Understanding of growth, propagation, and eventual interaction of the Øygarden Fault segments are very important when assessing risks associated with the Beta structure as a potential storage site.

At present ØFS1 is as a single fault segment, but it is highly likely that this segment formed from several isolated segments, through the stages (a)-(c) described above. This assumption is corroborated by the throw distribution along fault (T-x) plot **(**Fig 4.8b**)** which shows five main throw maxima that coul dbe interpreted as nucleation points (I)-(V). Fazlikhan et al., (2021) interpreted the same Øygarden in the south (Stord basin areas) as single isolated faults, further augmenting our interpretations, and indeed in agreement with our T-x plot.

Nucleation of a fault typically starts at the central maximum point of throw and decreases towards the fault tip, which represents points of minimum throw (Peacock and Sanderson 1991; Cartwright and Huuse, 2005; Freeman et al., 2010; and Nedham et al., 1996; Lathrop et al., 2021). The step-like throw shown in the throw-distance profile (Fig 4.8b) is an indicator of the hard linkage process (e.g., Duffy et al., 2015; Peacock and Sanderson 1991; Wrona et al., 2017; McLeod et al., 2000; Wang et al., 2022).

A similar process is inferred for the second segment ØFS2, which, although shows fewer nucleation points, developed through the same linkage process. The same process again applied to the third segment ØFS3 (Fig 4.8a; Fig 4.8b).

In general, the fault growth model for the Øygarden Fault involves initially, physically isolated small segments which became linked as the segments accomodated increasing strain and propgated laterally (e.g., Jackson and Rotevatn 2013; Fossen and Rotevatn 2016; Wang et al., 2022; Jackson et al., 2017; Lathrop et al., 2021; Rotevatn et al., 2019; Tvedt et al., 2013), eventually forming the present ØFS1-3 segments. The large segments then progressively localised the strain.

Newly formed faults in general strike perpendicular or sub-perpendicular to the principal stress direction (e.g., McClay et al., 2010; Giba et al., 2012), hence, the broadly N-S trending Øygarden Fault is inferred to have formed under an E-W extension. This is consistent with several northern North Sea structural studies (e.g., Mulrooney et al, 2020; Whipp et al., 2014; Wu et al., 2021; Færseth, et al., 1995; Råvnås et al., 2000).

The interactions between different fault segments produce stress concentration areas and perturbations which affect the geometry and kinematics (e.g., Crider and Pollard 1998; Bourne and Willemse 2001). These stress concentrations and perturbation at the faults tips result in the creation of secondary fractures/faults in the damage zones (Choi et al, 2016; Bastesen and Rotevatn 2012; Crider and Pollard 1998). This is possibly true in our study where secondary faults are evident in relay zones (Figs 4.7, 5.1 relay zone 1). The secondary faults and fracture (subseismic scale) and other strained rocks are responsible for the transfer of displacement. Faults are known to influence the displacement patterns of other active faults with which they interact e.g., in the case of sub-parallel normal faults that interact, displacement can be transferred (Peacock and Sanderson, 1991; Peacock et al., 2017; Walsh et al., 1999). The transfer of the high displacement at the tips is always accommodated through strained rocks. Relict damage zones from prevously relay zones that have become hard-linked also take up some of the strain accumulated due to displacement.

The segments ØFS1-3 do not physically link, resulting in the observed relay zones (Fig 4.7; 4.8b; Fig 5.1). It is within these relay areas that strained rocks and secondary faults/ fractures may form, accommodating the high displacement.

In our case, we observe approaching tip damage zones, i.e., areas of deformation occurring between two faults that do not intersect (Fig 4.7; Fig 5.1). Because each of Øygarden Fault was made up of small segments, which linked, to finally form what we presently observe, each of the small segments had a breached relay formed. Where further displacement accrues, the consequent increase in displacement gradients may result in the breaching of the initially soft-linked relays, forming what become hard-linked structures along a breaching or cross-fault (e.g., Peacock and Sanderson 1991). This is the case with breached relay zones formed by the small segments, prior to linkage, which resulted in the individual large segments 1-3 of the Øygarden Fault. Damage zones formed of two interacting but not linked faults have been referred to as interacting damage zones, in which case, they can be approaching or intersection zones (e.g., Peacock et al., 2016; 2017) or linking damage zones (Kim et al., 2014; Rotevatn and Fossen 2011).

With regard to vertical propagation, depth-throw (T-z) plots which indicate variations in throw with depth are analysed. There is a general increase in fault throw with depth, starting from the Top Shetland Gp to the Basement. This increase indicates that all the Øygarden Fault segment originated in the Permian-Triassic period with certain section sof the fault more

active at the time. This is corroborated by the hanging-wall growth packages, which indicate syn-rift deposition during the rifting phase 1. The Øygarden segment (F1) and splay fault (F2) **(**Fig 4.8C**)**, in addition, experienced some phases of reactivation, possibly during the Jurassic and early cretaceous, as supported by slight increases in throw in the T-z plots (Fig 4.8D). Within Jurassic units, formation of seondary faults (Fig 4.1b) has been reported (e.g., Wu et al., 2021; Mulrooney et al., 2020; Råvnås et al., 2000), and evident in the present studies (Fig 4.1b) during the post-rift phase.

The faults in the Måløy slope, which change in orientation to the NW-SE did not originate in the Permian-Triassic period because at the time, the Måløy slope was inactive, and thus, little fault activity occurred (e.g, Baucke et al., 2021). The faults in Måløy slope are inferred to developed during the second phase of rifting, albeit with a change in extension direction (Fig 4..5a), consistent with other studies (e.g., Mulrooney et al., 2020; Wrona et al., 2017).

The Øygarden and Vette Fault (Fig 4.8C, F1 & F3 respectively), on the other hand, experienced slight reactivation during the Early Cretaceous (Fig 4.8D), in what is referred to as the second phase of rifting (RP2) (e.g., Mulrooney et al, 2020; Osmond et al., 2021; Bauck et al., 2021; Bell et al., 2014; Wu et al., 2021). Continued fault reactivation during the deposition of the Cromer Knoll and Shetland units is not uncommon, since the main N-S segments were still active even after the syn-rift phase 2 (RP2) (Wu et al., 2021; Mulrooney et al., 2020; Deng et al., 2017).

In the Post Cretaceous units (Tertiary units), a few faults oriented in the NW-SE direction have been mapped. Such faults have been mapped, and attributed to a second phase of faulting, and their orientation was related to a switch in extension direction to a NE-SW extension (e.g., Deng et al., 2017; Phillips et al., 2019; Mulrooney et al., 2020).

We therefore relate our faults in the Måløy slope which are oriented in the NW-SE to a second rift phase, and that there was a change on orientation, due to the influence of the basement (e.g., Fazlikhan et al., 2017).

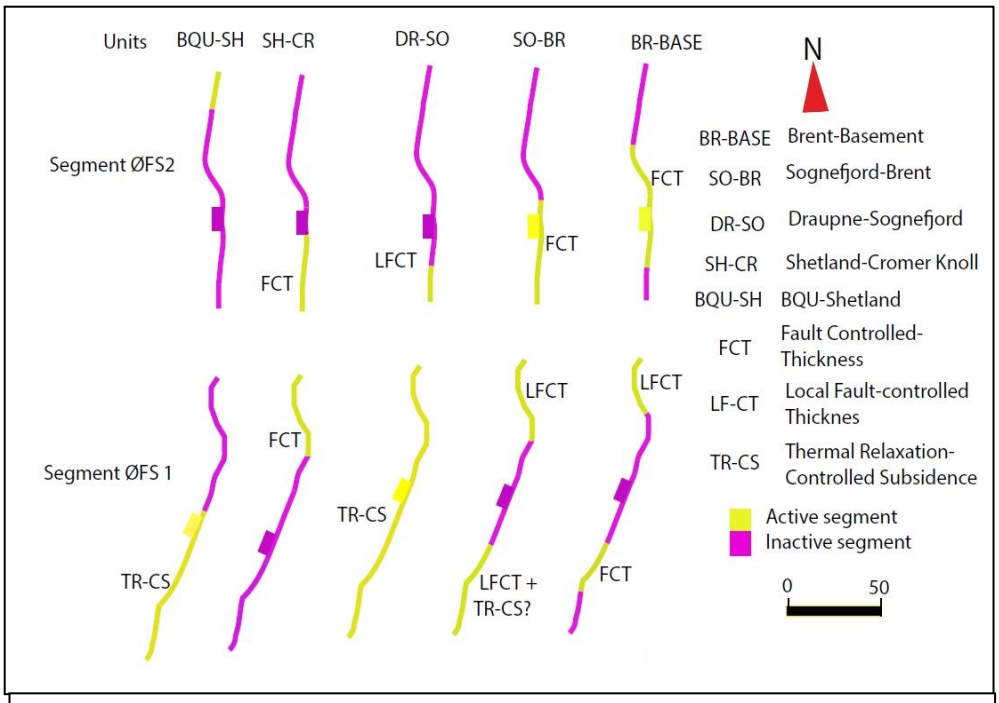

Fig 5.0: Summary of fault activities on individual Fault segments. Note, Segment 3 (not shown) in the north, (Måløy slope) does not show any fault activity.

5.3 Implications for CO2 migration

CO2 storage projects are long term, and therefore all risks that may be related to; geomtery, structural and geochemical appraisals of storage units, monitoring and caprock integrity need to need be assessed carefully (Miocic et al., 2013; Wu et al., 2021). The role of faults in trying to assess the capacity of the storage prospect was recognised (eg., Bretan et al., 2011; Yielding et al., 2011; Wu et al., 2021; Mulrooney et al., 2020). Faults not only impact projects through across-fault, across-fault reservoir pressure but also along fault CO2 migration/leakage. The latter risks occur because of variations in pressure and temperature, and CO2 exhibits unique physical properties and flow behaviour. With the bouyant nature of the CO2, the gas can easily escape updip along fault planes, if not constrained.

In trying to understand the risks involved with potential CO2 storage on the nearshore Norwegian Continental shelf, we focus the risk of leakage along faults using the geometry of the fault, the density of the faults, and the formation of damage zones. Additionaly, where porous CO2-bearing formations are juxtaposed against basement (e.g. across the basin-bounding Øygarden Fault Complex), we consider across-fault leakage risk. Previous studies have determined that on the east (onshore) and offshore to the west, the basement rocks are weathered and fractured (Torabi et al., 2018). All the above combined have quite far-reaching

effects regarding derisking of a CO2 storage site. As this is a regional-scale screening of the shelf, we do not consider the presence or absence of mebrane seals on indivudal faults.

5.3.1 Relay zones

Relay zones are areas of fault interaction where strain or displacement is transferred or relayed from one structure to another or simply put, where two master faults with fault tips interact (Fossen and Rotevatn 2016; Rotevatn and Bastesen 2012; Nixon et al, 2019; Pan et al 2021). During normal fault growth and subsequent development of relay structures, the latter act to affect reservoir distribution, stratigraphic trap geometry, and fluid migration pathways (Williams et al., 2020). Relay zones also act to affect drainage patterns, as well distribution of facies along active faults that may breach the surface (Fossen and Rotevatn 2016). Relay ramps are known zones of active fluid pathways, especially the subseismic relays, which are in commnication with reservoirs (e.g., Rotevatn et al., 2007), and, in this case, we focus on possible CO2 leakage.

In our case, the emphasis is placed on the role these structures (relay zones) play in CO2 migration. As discussed in Wu et al., (2021), the Beta prospect resides in the hanging of the Øygarden Fault, and specifically in the hanging wall of ØFS2 in the central Horda. It is the same segment that forms relays with the segment ØFS1 in the south and ØFS3 in the north (Fig 4.7). Uncertainties in the juxtaposition of Beta prospect in the Viking sandstone with the basement have been hinted at (e.g., Wu et al., 2021). Similarly, the same view is upheld herein and corroborated with the observed relay zones.

Additionally, the uncertainty is not only focused on leakage across the Øygarden, but also on leakage along the fault plane. This is premised on the bouyance of CO2, which allows it to flow updip along the fault (see introduction to this section). This implies along fault planes, CO2 can easily escape along the Øygarden Fault to the surface, if not constrained by seal membranes or mineralization on fault plane. We therefore consider faults as potential fluid pathways in this screening study.

Moreover, in the northern Horda and Måløy slope areas, high density of faults is quite visible (Fig 4.7), especially around relay zones 2 and 3. These planar, isolated faults (Fig 4.6a, b) may cause communication challenges. However, where interacting faults such as splay systems occur, these may cause additional risks.

Splay faults have been described as a system where multiple shallow faults link at depth to a form a single fault plane (e.g., Jackson and Rotevatn, 2013; Whipp et al., 2014; Walsh et al.,

2002; Giba et al., 2012). The splay faults in our study area linked with the main Øygarden, and therefore poses greater risks to CO2 migration.

5.3.2 Change in character of the Øygarden along strike.

Along strike, changes in the character of the Øygarden are observed, starting in the south, with hosts and graben systems (Fig 4.5c), basin bounded by listric and planar faults (Fig 4.5b) in the center and eventually in the north, where down-stepping small depocenters are bounded by small faults to the north (Fig 4.5a) are explaianed by the changes in strain accomodation.

Changes in stress regime could explain the changes observed along strike. In the south, the extension regime change from NW-SE (which resulted in NE-SW fault orientation), to an E-W extension in the central areas which resulted in the N-S observed major faults. In the north, the extenstion changed to NE-SW, and resulted in NW-SE fault orientation (Fig 4.5a) during the second phase of rifting, in agreement with several authors (e.g., Mulrooney et al., 2020; Phillipe et al., 2019 and Deng et al., 2017). A clockwise rotation of stress from what led to extension in the Permian-Triassic phase therefore was proposed. However, possible local stress pertubations of the main N-S trending faults have been inferred (e.g., Duffy et al, 2015; Whipp et al., 2014).

Furthermore, the changes in character may be inferred from the influence of basement structures. Using anaogue and numerical models, the influence of prexisting structures on rift basin evolution, location and their geometry have been explored (Fazlikhani et al., 2017 and references therein; Deng et al., 2017; Osagiede et al., 2020). However, the influence is considered at regional scale, focusing on first order segmentation, but less influential on individual faults and subbasins (e.g., Fazlikhani et al., 2017; Whipp et al., 2014). In the Stord and Shetland basins, for example, the basement shear zones reactivated during rifting, and locally controlled the location and geometry of depocenters (Falikhani te a., 2017). This was the case because, the NE-SW and N-S oriented shear zones were favorably oriented and therefore more prone to reactivation with respect to E-W Permian extension direction. In the Maløy slope on the other hand, the pre-existing structures were orineted in the E-W to ENE-WSW, just close to the E-W Permian-Triassic extension direction, making it difficult to reactivate. The observed changes in strike therefore were related to basement influence, which was mostly heterogeneous during the construction of the northern North Sea depoceners (e.g., Fazlikhani et al., 2017).

With regard to effects on CO2 storage, the changes in strain distribution resulted in segmentation of the fault along the strike. The segmentation resultes in varying architecture of basins. Basins showing heterogeneity in reservoirs may therefore be expected (e.g., Ward et al., 2016; Wu et al., 2016). The observed depocenters in north (Måløy slope) were compartmentalised by the basin-bounding faults, which faults (e.g., Faults in Fig 4.6 a-b), being isolated cause connectivity questions.

5.3.3 Damage zones and relays zones

When evaluating for structural risks, damages zones are important to consider. The damage zones were created to accommodate displacement, influence CO2 migration (e.g., Rotevatn et al., 2007; 2009b; Manzocchi et al., 2010) and entrapments (Rotevatn and Fossen 2011). The damage zones exhibit active and high fracturing, in which case these increase the permeability (Peacock et al., 2017; Ward et al., 2016; Curewitz and Karson 1992), faults, folds and deformation bands (e.g., Kim et al., 2014; Torabi et al., 2017). Driven by the spatial growth of fault archtecture, damage zones are defined along and across the fault, but also around fault tips (process zones) (e.g., Torabi et al., 2017; Choi et al., 2016). Depending on the distribution of deformation across the fault, we may have inner and outer damage zones (e.g., Torabi et al., 2017). The structures and damage inside the fault zones will either enhance or baffle fluid flow across and along.

In our study, with the exception of approaching tip damage and relays zones observed (Fig 5.1), other damage zones associated with the Øygarden Fault along and across the fault is speculative. This is because such zones are formed of subseismic structures, such as fractures, faults and disformation bands that are not easily observed on seismic section. Such small structures and damage zones are best gathered from outcrops. However, using seismic attributes attempts at mapping and visualizing of fault damage zones has been carried-out (e.g., Dutzer et al., 2010; Iacopini et al., 2016; Torabi et al., 2017; Alaei and Torabi 2017; Botter and Champion 2022). Torabi e al., (2017) applied Discrete frequencies to generate coherence attributes to map spatial and temporal variations of fault damage zones, laterally and vertically at various depths along strike.

Sigmoidal and horsetail structures were mapped using enhanced attributes from broadband sesimic data (Jorgensen and Alaei., 2015), whereas using fault distortion zone (FDZ) concept, Dutzer et al., (2010) mapped inner and outer damage zones which are characterised distortion on seismic data in the case of inner zone, and by drag and folds in the case of outer zones.

Postive correlation of displacement with damage zone width, especially for high displacement faults such as the Øygarden Fault, has been carried out, albeit with scatter in data, brought about by dificulties in defining damage zones (e.g., Choi et al., 2016; Torabi et al., 2017; Kim et al., 2014). This means most high displacement fault tend to form wide damage zones, which have effects on the fluid flow properties within the fault.

Based on the above studies, we speculate that damage zones along and across fault segments and process zones can be extended to the Øygarden Fault, which is a high displacement fault, and therefore such fault zones are possible.

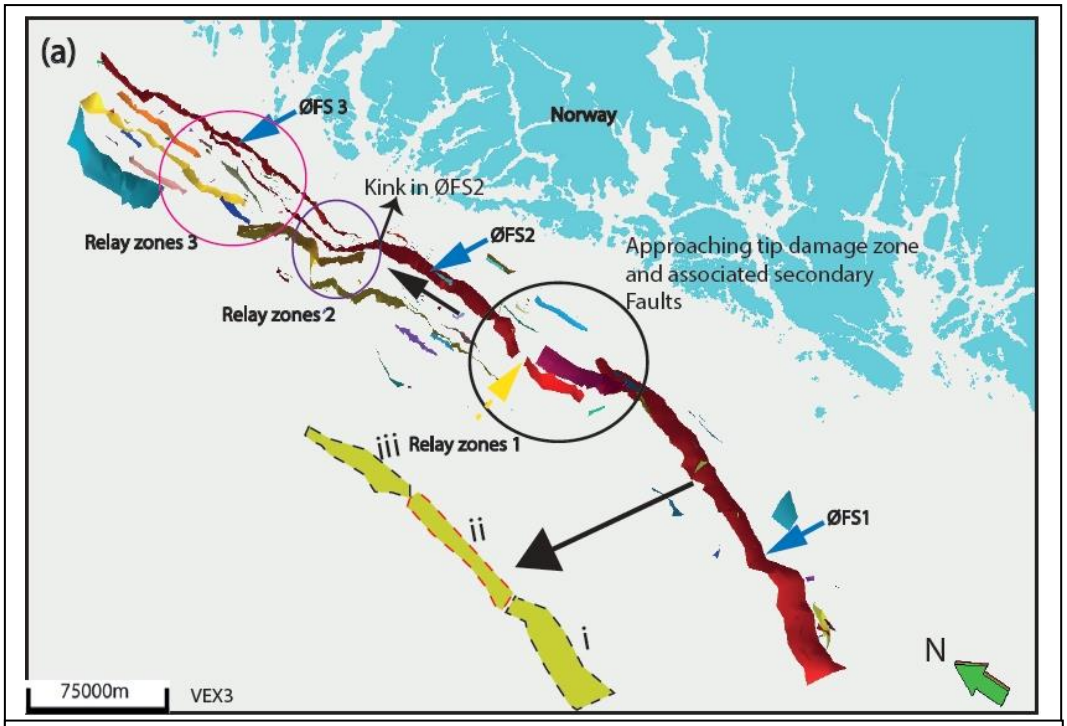

Fig 5.1: Approaching damage zone, circled black (cf. Peacock el., 2016; 2017). The yellow segment, (dashed), indicates possible earlier separate segments prior to linking to form ØFS1 (cf. Fazlikhan et al., 2021). Small segment (i) is what Fazlikhan et al., (2021) name ØFS5, which was active, resulting in thickening observed.

5.3.4 Weathered and fractured basement

In stiff, low basement rocks, deformation and alteration processes drastically affect mechanical strenght and alter permeability by developing secondary porosity (e.g., Stanek and Geraud 2019; Cecato et al., 2020). With interests in exploration and production of georesources, therefore, there has been need to understand the basement rocks and proceses which cause alterations. Weathering of the basement rocks in the Utsira has been well

documented (Ceccato et al., 2020). The Top-Basement weathering profile indicates a decrease in alteration intensity with depth, and that structural discontinuities are catalysts in the alteration. We speculate that similar processes observed in Ceccato et al., (2020) are applicable to the Øygarden Fault rocks, which have quite similar composition.

With regard to CO2 de-risking, Bjørnstad (2022) carried out direct shear tests on the natural basement rocks from the Øygarden Fault. With varying angles (weak an strong rocks) of friction betwen 16.8 to 31.1), coupled with average coefficient of friction of 0.50, it was concluded that Øygarden Fault gouge rocks transist between stable to unstable slip regimes. Bjørstad (2022) concluded that some rocks in the Øygarden that are mature and with weak fault gouges, and follow E-W to NE-SW extension are likely to undergo reactivation by stable sliding (coeffiecint of internal friction less that 0.5). Similar observations were made onshore by Ksienzyk et al., (2016), in which fault gouge were observed to be prone to reactivation. In the northern parts of the Øygarden Fault Complex, it was also observed that the fault is still active (e.g. Olsen et al., 2013; Bell et al., 2014; Mulrooney et al., 2020; Wu et al., 2021). All these observations point to risks that are associated with Øygarden Fault which have consequences for the Beta prospect.

6.0 Summary, Conclusions and future works

Variations in tectonic activity of the Øygarden Fault have been observed; dependant on when the fault segments were active, thick depocenters are have been observed. In the Permian-Triassic, thick depocenters have been observed within the central areas on segment ØF2, an indicator of active faulting on the same segment. We observe no fault activity in the north, around the Maløy slope, in which case, we conclude that at the time, the Måløy slope was not tectonically active. These observations and interpretations are similar to several regional studies in the northern North Sea.

We also observe relative quietness during the Jurassic units, which show relatively uniform, continous and tabular seismic reflectors. These are indicators of sediment deposition during a time of relative quietness. However, locally, small thick depocenters have been observed, implying local tectonic activity during the Jurassic. This has been referred to as a phase of post-rifting phase 1, that locally experienced some tectonic activity, in agreement with a number of studies on northern North Sea (e.g., Råvnas et al., 2000; Mulrooney et al., 2020; Wu et al., 2021). In the early Cretaceous, we observe growth strata in the Cromer-Knoll unit; it is this unit that experienced much of the second rifting phase (RP2).

We observe changes in strain accomodation through changes in type of basin arrangment along strike (Fig 4.5). In the south, Stord Basin, we observe horst and graben system (Fig 4.5c), followed by large basin bounding large basins in the central (Fig 4.5b), and finally in the north, downstepping mini-depocenters (Fig 4.5a). We speculate that the basement had a large influence on the formation of these basins and the changes in orientation of the faults were as a result of the basement structure, similar to preditions in Fazlikhan et al., (2017).

The CCS is the most in-demand technology for directly reducing CO2 emissions, but the project requires continued search for new storage facilities in the subsurface. In our study, we do not predict any new sites, beause we do not observe any trapping mechanisms, other than those already determined. In the study therefore, Beta prospect has been considered however, its' location in the hanging-wall of the Øygarden Fault which is juxtaposed with fractured basement, this requires more detailed investigations of risks that are associated with the Øygarden Fault.

Our regional structural study on the nearshore Norwegian Continetal shelf, focus has been put on the leakage along faults. We used fault geometry, density of the fault and formation of

damage zones in order to a contribution to derisking of the Beta reservoir. We map and assess and map damage zones between the tips of the soft-linking segments, what we refer to as the approaching tip damage zones. We also speculate that the individual faults segments have wide damage zones, especially for such large displacement faults. These zones have serious consenquences for CO2 migration into the fractured basement, and yet the CCS requires storage sites where reservoirs must be in position to retain almost 99% of the CO2 after 100 years post-injection.

We observe relatively high fault density of isolated faults in the northern Horda and within the Måløy slope areas. These play a big role in assessing for connectivity and flow rates. In addition, the high denity of faults are critical for placement of injectors and producers. The geometry of Øygarden Fault which is made of listric, planar faults and consists of segmented fault-bound depocenters, may have communication/connectivity implications.

We also speculate, based on previous studies else where that, the basement being fractured and weathered, risks in the Beta prospect may arise due to the fractured and weathered rocks of the Øygarden Fault. Additionally, the possibility for the Øygarden fault to reactivate exist, based on the recent works in Bjørnstad (2022).

The above consideration when put in persepective, therefore, the study findings have far reaching implications for the Beta prospect as a candidate for CO2 storage. The along fault investigations are paramount considering the Gaseous and bouyant state of CO2 in shallow reservoirs. The damage and relays zones are known areas for fluid migration, and the same is concluded in ths study. The CCS projects being very long term, therefore, every risk must be evaluated.

In order to have a good understanding of the risks herein, and therefore an assessment of the Beta prospect, future works need to focus on mapping the damage zones with advanced seismic attribute methods to map fault zones (e.g.,Torabi et al., 2017), and compare with the groundtruthed data from outcrops, onshore.

We also speculate that fault-bound mini depocenters need detailed modeling to evaluate for CO2 communication and placememt of injectors, especially in areas with isolated, but high density faults in the north.

References

Akhurst, M., et al. (2015). "Risk assessment-led characterisation of the SiteChar UK North Sea site for the geological storage of CO2." Oil & Gas Science and Technology–Revue d'IFP Energies nouvelles 70(4): 567-586.

Anders, M. H. and R. W. Schlische (1994). "Overlapping faults, intrabasin highs, and the growth of normal faults." The Journal of Geology 102(2): 165-179.

Bastesen, E. and A. Rotevatn (2012). "Evolution and structural style of relay zones in layered limestone–shale sequences: insights from the Hammam Faraun Fault Block, Suez rift, Egypt." Journal of the Geological Society 169(4): 477-488.

Bauck, M. S., et al. (2021). "Late Jurassic to Late Cretaceous canyons on the Måløy Slope: Source to sink fingerprints on the northernmost North Sea rift margin, Norway."

Bell, R. E., et al. (2014). "Strain migration during multiphase extension: Observations from the northern North Sea." Tectonics 33(10): 1936-1963.

Bell, R. E., et al. (2014). "Strain migration during multiphase extension: Observations from the northern North Sea." Tectonics 33(10): 1936-1963.

Bense, V., et al. (2013). "Fault zone hydrogeology." Earth-Science Reviews 127: 171-192.

Billi, A., et al. (2003). "The damage zone-fault core transition in carbonate rocks: implications for fault growth, structure and permeability." Journal of Structural Geology 25(11): 1779-1794.

Bjørnstad, A. (2022). Fault Gouge Characterization in the Øygarden Complex in SW Norway-Relevance for offshore CO2 storage, The University of Bergen.

Bolle, L. (1992). "Troll Field: Norway's Giant Offshore Gas Field: Chapter 28."

Botter, C., & Champion, A. (2022). Seismic attribute analysis of a fault zone in the Thebe field, Northwest shelf, Australia. *Interpretation*, *10*(2), T325-T340.

Bourne, S. J. and E. J. Willemse (2001). "Elastic stress control on the pattern of tensile fracturing around a small fault network at Nash Point, UK." Journal of Structural Geology 23(11): 1753-1770.

Braathen, A., et al. (2000). "Devonian, orogen-parallel, opposed extension in the Central Norwegian Caledonides." Geology 28(7): 615-618.

Caine, J. S., et al. (1996). "Fault zone architecture and permeability structure." Geology 24(11): 1025-1028.

Ceccato, A., et al. (2021). "In–situ quantification of mechanical and permeability properties on outcrop analogues of offshore fractured and weathered crystalline basement: Examples from the Rolvsnes granodiorite, Bømlo, Norway." Marine and Petroleum Geology 124: 104859.

Chadwick, R. (2013). Offshore CO2 storage: Sleipner natural gas field beneath the North Sea. Geological Storage of Carbon Dioxide (CO2), Elsevier: 227-253e.

Childs, C., et al. (2017). "Introduction to the geometry and growth of normal faults." Geological Society, London, Special Publications 439(1): 1-9.

Childs, C., et al. (2012). Fault Core/damage Zone; an Unhelpful Description of Fault Zone Structure? 3rd EAGE International Conference on Fault and Top Seals, European Association of Geoscientists & Engineers.

Childs, C., et al. (1995). "Fault overlap zones within developing normal fault systems." Journal of the Geological Society 152(3): 535-549.

Choi, J. H., et al. (2012). "Rupture propagation inferred from damage patterns, slip distribution, and segmentation of the 1957 MW8. 1 Gobi-Altay earthquake rupture along the Bogd fault, Mongolia." Journal of Geophysical Research: Solid Earth 117(B12).

Choi, J.-H., et al. (2016). "Definition and classification of fault damage zones: A review and a new methodological approach." Earth-Science Reviews 152: 70-87.

Christiansson, P., et al. (2000). "Crustal structure in the northern North Sea: an integrated geophysical study." Geological Society, London, Special Publications 167(1): 15-40.

Corfu, F., et al. (2014). "The Scandinavian Caledonides: main features, conceptual advances and critical questions." Geological Society, London, Special Publications 390(1): 9-43.

Cowie, P. A. and C. H. Scholz (1992). "Displacement-length scaling relationship for faults: data synthesis and discussion." Journal of Structural Geology 14(10): 1149-1156.

Cowie, P. A. and C. H. Scholz (1992). "Growth of faults by accumulation of seismic slip." Journal of Geophysical Research: Solid Earth 97(B7): 11085-11095.

Crider, J. G. and D. D. Pollard (1998). "Fault linkage: Three-dimensional mechanical interaction between echelon normal faults." Journal of Geophysical Research: Solid Earth 103(B10): 24373-24391.

Curewitz, D. and J. A. Karson (1997). "Structural settings of hydrothermal outflow: Fracture permeability maintained by fault propagation and interaction." Journal of Volcanology and Geothermal Research 79(3-4): 149-168.

Davies, R. J., et al. (2001). "Sequential dip-slip fault movement during rifting: a new model for the evolution of the Jurassic trilete North Sea rift system." Petroleum Geoscience 7(4): 371-388.

Davies, R. J., et al. (2001). "Sequential dip-slip fault movement during rifting: a new model for the evolution of the Jurassic trilete North Sea rift system." Petroleum Geoscience 7(4): 371-388.

Deng, C., et al. (2017). "Influence of fault reactivation during multiphase rifting: The Oseberg area, northern North Sea rift." Marine and Petroleum Geology 86: 1252-1272.

Deng, H., et al. (2020). "3D structure and evolution of an extensional fault network of the eastern Dampier Sub-basin, North West Shelf of Australia." Journal of Structural Geology 132: 103972.

Duffy, O. B., et al. (2015). "Fault growth and interactions in a multiphase rift fault network: Horda Platform, Norwegian North Sea." Journal of Structural Geology 80: 99-119.

Dupuy, B., et al. (2018). Norwegian large-scale CO2 storage project (Smeaheia): baseline geophysical models. 14th Greenhouse Gas Control Technologies Conference Melbourne.

Dutzer, J. F., Basford, H., & Purves, S. (2010, January). Investigating fault-sealing potential through fault relative seismic volume analysis. In *Geological Society, London, Petroleum Geology Conference series* (Vol. 7, No. 1, pp. 509-515). Geological Society of London.

Eiken, O., et al. (2011). "Lessons learned from 14 years of CCS operations: Sleipner, In Salah and Snøhvit." Energy procedia 4: 5541-5548.

Fazli Khani, H., et al. (2017). "Basement structure and its influence on the structural configuration of the northern North Sea."

Fazlikhani, H., et al. (2021). "Strain migration during multiphase extension, Stord Basin, northern North Sea rift." Basin Research 33(2): 1474-1496.

Fossen, H. (2010). "Extensional tectonics in the North Atlantic Caledonides: a regional view." Geological Society, London, Special Publications 335(1): 767-793.

Fossen, H., et al. (2017). "Post-Caledonian extension in the West Norway–northern North Sea region: the role of structural inheritance." Geological Society, London, Special Publications 439(1): 465-486.

Fossen, H., et al. (2000). "Detachments and low-angle faults in the northern North Sea rift system." Special Publication-Geological Society Of London 167: 105-132.

Fossen, H. and A. Rotevatn (2016). "Fault linkage and relay structures in extensional settings—A review." Earth-Science Reviews 154: 14-28.

Fossen, H., Mangerud, G., Hesthammer, J., Bugge, T., & Gabrielsen, R. H. (1997). The Bjorøy Formation: a newly discovered occurrence of Jurassic sediments in the Bergen Arc System. *Norsk Geologisk Tidsskrift*, *77*(4), 269-287.

Færseth, R. (1996). "Interaction of Permo-Triassic and Jurassic extensional fault-blocks during the development of the northern North Sea." Journal of the Geological Society 153(6): 931-944.

Færseth, R. B., et al. (1995). "Influence of basement in structuring of the North Sea basin, offshore southwest Norway." Norsk Geologisk Tidsskrift 75(2-3): 105-119.

Gabrielsen, R., et al. (1999). "Structuring of the Northern Viking Graben and the Møre Basin; the influence of basement structural grain, and the particular role of the Møre-Trøndelag Fault Complex." Marine and Petroleum Geology 16(5): 443-465.

Gabrielsen, R. H., et al. (2001). "The Cretaceous post-rift basin configuration of the northern North Sea." Petroleum Geoscience 7(2): 137-154.

Ganerød, G. V., et al. (2008). "Predictive permeability model of extensional faults in crystalline and metamorphic rocks; verification by pre-grouting in two sub-sea tunnels, Norway." Journal of Structural Geology 30(8): 993-1004.

Gee, D. G., et al. (2008). "From the early Paleozoic platforms of Baltica and Laurentia to the Caledonide Orogen of Scandinavia and Greenland." Episodes Journal of International Geoscience 31(1): 44-51.

Giba, M., et al. (2012). "Segmentation and growth of an obliquely reactivated normal fault." Journal of Structural Geology 39: 253-267.

Helland-Hansen, W., et al. (1992). "Advance and retreat of the Brent delta: recent contributions to the depositional model." Geological Society, London, Special Publications 61(1): 109-127.

Iacopini, D., Butler, R. W. H., Purves, S., McArdle, N., & De Freslon, N. (2016). Exploring the seismic expression of fault zones in 3D seismic volumes. *Journal of Structural Geology*, *89*, 54-73.

Jackson, C. A.-L., et al. (2017). "Techniques to determine the kinematics of synsedimentary normal faults and implications for fault growth models." Geological Society, London, Special Publications 439(1): 187-217.

Jackson, C. A.-L. and A. Rotevatn (2013). "3D seismic analysis of the structure and evolution of a salt-influenced normal fault zone: a test of competing fault growth models." Journal of Structural Geology 54: 215-234.

Kaldi, J., et al. (2013). "Containment of CO2 in CCS: Role of Caprocks and Faults." Energy procedia 37: 5403-5410.

Kim, Y.-S., et al. (2004). "Fault damage zones." Journal of Structural Geology 26(3): 503-517.

Lathrop, B. A., et al. (2021). "Normal fault kinematics and the role of lateral tip retreat: An example from offshore NW Australia." Tectonics 40(5): e2020TC006631.

Lauritsen, H., et al. (2018). Assessing potential influence of nearby hydrocarbon production on CO2 storage at Smeaheia. Fifth CO2 Geological Storage Workshop, European Association of Geoscientists & Engineers.

Lenhart, A., et al. (2019). "Structural architecture and composition of crystalline basement offshore west Norway." Lithosphere 11(2): 273-293.

Lervik, K. (2006). "Triassic lithostratigraphy of the northern North Sea Basin." Norsk Geologisk Tidsskrift 86(2): 93.

Lloyd, C., et al. (2021). "A regional CO2 containment assessment of the northern Utsira Formation seal and overburden, northern North Sea." Basin Research 33(3): 1985-2017.

Lonergan, L., et al. (2007). "Fractured reservoirs."

Lothe, A. E., et al. (2019). "Storage resources for future European CCS deployment; A roadmap for a Horda CO2 storage hub, offshore Norway."

Loveless, S., et al. (2011). "Fault architecture and deformation processes within poorly lithified rift sediments, Central Greece." Journal of Structural Geology 33(11): 1554-1568.

Lu, P., et al. (2012). Reducing uncertainties in model predictions via history matching of CO2 plume migration at the Sleipner Project, Norwegian North Sea. AGU Fall Meeting Abstracts.

Maldal, T. and I. Tappel (2004). "CO2 underground storage for Snøhvit gas field development." Energy 29(9-10): 1403-1411.

Manzocchi, T., et al. (2010). "Faults and fault properties in hydrocarbon flow models." Geofluids 10(1-2): 94-113.

Mayolle, S., et al. (2019). "Scaling of fault damage zones in carbonate rocks." Journal of Structural Geology 124: 35-50.

Miocic, J. M., Johnson, G., & Gilfillan, S. M. (2014). Fault seal analysis of a natural CO2 reservoir in the Southern North Sea. *Energy Procedia*, *63*, 3364-3370.

Miocic, J. M., et al. (2016). "Controls on CO2 storage security in natural reservoirs and implications for CO2 storage site selection." International Journal of Greenhouse Gas Control 51: 118-125.

Miocic, J. M., et al. (2019). "Uncertainty in fault seal parameters: implications for CO 2 column height retention and storage capacity in geological CO 2 storage projects." Solid earth 10(3): 951-967.

Mondol, N. H., et al. (2018). Petrophysical analysis and rock physics diagnostics of Sognefjord Formation in the Smeaheia area, Northern North Sea. Fifth CO2 Geological Storage Workshop, European Association of Geoscientists & Engineers.

Mulrooney, M., et al. (2018). Smeaheia, a potential northern north sea CO2 storage site: structural description and de-risking strategies. Fifth CO2 Geological Storage Workshop, European Association of Geoscientists & Engineers.

Mulrooney, M. J., et al. (2020). "Structural analysis of the Smeaheia fault block, a potential CO2 storage site, northern Horda Platform, North Sea." Marine and Petroleum Geology 121: 104598.

Nazarian, B., et al. (2018). Storing CO2 in a reservoir under continuous pressure depletion; A simulation study. 14th greenhouse gas control technologies conference Melbourne.

Nicol, A. and R. Van Dissen (2002). "Up-dip partitioning of displacement components on the oblique-slip Clarence Fault, New Zealand." Journal of Structural Geology 24(9): 1521-1535.

Nipen, H. (2020). Permo-Triassic basin development on the Horda Platform and Stord Basin–Pre-rift architecture and rift phase 1 evolution (Master's thesis).

Osagiede, E. E., et al. (2020). "Pre-existing intra-basement shear zones influence growth and geometry of non-colinear normal faults, western Utsira High–Heimdal Terrace, North Sea." Journal of Structural Geology 130: 103908.

Osmond, J. L., et al. (2022). "Structural traps and seals for expanding CO2 storage in the northern Horda platform, North Sea." AAPG Bulletin(20,220,404).

Osmundsen, P. and T. Andersen (2001). "The middle Devonian basins of western Norway: sedimentary response to large-scale transtensional tectonics?" Tectonophysics 332(1-2): 51-68.

Pan, S., et al. (2022). "Evolution of normal fault displacement and length as continental lithosphere stretches." Basin Research 34(1): 121-140.

Peacock, D. (2002). "Propagation, interaction and linkage in normal fault systems." Earth-Science Reviews 58(1-2): 121-142.

Peacock, D., et al. (2017). "Interacting faults." Journal of Structural Geology 97: 1-22.

Peacock, D. and D. Sanderson (1991). "Displacements, segment linkage and relay ramps in normal fault zones." Journal of Structural Geology 13(6): 721-733.

Phillips, T. B., et al. (2019). "The influence of structural inheritance and multiphase extension on rift development, the NorthernNorth Sea." Tectonics 38(12): 4099-4126.

Quirie, A. K., et al. (2019). "The Rattray Volcanics: Mid-Jurassic fissure volcanism in the UK Central North Sea." Journal of the Geological Society 176(3): 462-481.

Ravnås, R., et al. (2000). "Syn-rift sedimentary architectures in the Northern North Sea." Geological Society, London, Special Publications 167(1): 133-177.

Richards, F. L., et al. (2015). "Interpretational variability of structural traps: implications for exploration risk and volume uncertainty." Geological Society, London, Special Publications 421(1): 7-27.

Roche, V., et al. (2021). "Variability in the three-dimensional geometry of segmented normal fault surfaces." Earth-Science Reviews 216: 103523.

Rotevatn, A. and E. Bastesen (2014). "Fault linkage and damage zone architecture in tight carbonate rocks in the Suez Rift (Egypt): implications for permeability structure along segmented normal faults." Geological Society, London, Special Publications 374(1): 79-95.

Rotevatn, A., et al. (2009). "Overlapping faults and their effect on fluid flow in different reservoir types: A LIDAR-based outcrop modeling and flow simulation study." AAPG Bulletin 93(3): 407-427.

Rotevatn, A. and H. Fossen (2011). "Simulating the effect of subseismic fault tails and process zones in a siliciclastic reservoir analogue: Implications for aquifer support and trap definition." Marine and Petroleum Geology 28(9): 1648-1662.

Rotevatn, A., et al. (2007). "Are relay ramps conduits for fluid flow? Structural analysis of a relay ramp in Arches National Park, Utah." Geological Society, London, Special Publications 270(1): 55-71.

Rotevatn, A., et al. (2019). "How do normal faults grow?" Journal of Structural Geology 125: 174-184.

Sacco, T. (2018). CO2 trapping in the Smeaheia reservoir–time mass estimation using geochemical models.

Sanderson, D. J. and Y.-S. Kim (2005). "The relationship between displacement and length of faults." Earth-Science Reviews 68(3-4): 317-334.

Serck, C. S. and A. Braathen (2019). "Extensional fault and fold growth: Impact on accommodation evolution and sedimentary infill." Basin Research 31(5): 967-990.

Song, G., et al. (2021). "Along-strike structural linkage and interaction in an active thrust fault system: A case study from the western Sichuan foreland basin, China." Basin Research 33(1): 210-226.

Torabi, A., et al. (2018). "Faults and fractures in basement rocks, their architecture, petrophysical and mechanical properties." Journal of Structural Geology 117: 256-263.

TRUDGILL, B. and J. CARTWRIGHT (1994). "Relay-ramp forms and normal-fault linkages, Canyonlands National Park, Utah." Geological Society of America Bulletin 106(9): 1143-1157.

Tucker, R. D., et al. (2004). "Thrusting and extension in the Scandian hinterland, Norway: New U-Pb ages and tectonostratigraphic evidence." American Journal of Science 304(6): 477-532.

Underhill, J. R. and M. Partington (1993). Jurassic thermal doming and deflation in the North Sea: implications of the sequence stratigraphic evidence. Geological Society, London, Petroleum Geology Conference Series, Geological Society of London.

Vetti, V. V. and H. Fossen (2012). "Origin of contrasting Devonian supradetachment basin types in the Scandinavian Caledonides." Geology 40(6): 571-574.

Walsh, J., et al. (2003). "Formation of segmented normal faults: a 3-D perspective." Journal of Structural Geology 25(8): 1251-1262.

Walsh, J. J. and J. Watterson (1991). "Geometric and kinematic coherence and scale effects in normal fault systems." Geological Society, London, Special Publications 56(1): 193-203.

Wang, S., et al. (2022). "Growth and linkage of normal faults experiencing multiple non-coaxial extension: A case from the Qikou Sag, Bohai Bay Basin, East China." Basin Research 34(2): 748-770.

Ward, N. I., et al. (2016). "Reservoir leakage along concentric faults in the Southern North Sea: Implications for the deployment of CCS and EOR techniques." Tectonophysics 690: 97-116.

Whipp, P., et al. (2014). "Normal fault array evolution above a reactivated rift fabric; a subsurface example from the northern Horda Platform, Norwegian North Sea." Basin Research 26(4): 523-549.

Wrona, T., et al. (2017). "Kinematics of polygonal fault systems: Observations from the northern North Sea." Frontiers in Earth Science 5: 101.

Wu, G., et al. (2016). "Effects of structural segmentation and faulting on carbonate reservoir properties: A case study from the Central Uplift of the Tarim Basin, China." Marine and Petroleum Geology 71: 183-197.

Wu, L., et al. (2021). "Significance of fault seal in assessing CO2 storage capacity and containment risks–an example from the Horda Platform, northern North Sea." Petroleum Geoscience 27(3): petgeo2020-2102.

Ziegler, P. (1992). "North Sea rift system." Tectonophysics 208(1-3): 55-75.

Ziegler, P. A. (1990). Geological atlas of western and central Europe, Geological Society of London.